Politecnico di Torino

ScuDo
Scuola di Dottorato ~ Doctoral School
WHAT YOU ARE, TAKES YOU FAR

Doctoral Dissertation
Doctoral Program in Energetics (36^{th}cycle)

Unlocking district cooling potential by means of design optimization

By

Manfredi Neri

******

Supervisor(s):
Prof. Vittorio Verda, Supervisor
Prof. Elisa Guelpa, Supervisor

Doctoral Examination Committee:
Prof. Anna Volkova , Referee, Tallinn University of Technology
Prof. Aldo Bischi, Referee, Università di Pisa
Prof. Marco Cavana, Politecnico di Torino
PhD Marco Cozzini, Eurac Research
Prof. Matteo Fasano, Politecnico di Torino

Politecnico di Torino
2024

Declaration

I hereby declare that, the contents and organization of this dissertation constitute my own original work and does not compromise in any way the rights of third parties, including those relating to the security of personal data.

Manfredi Neri
2024

* This dissertation is presented in partial fulfillment of the requirements for **Ph.D. degree** in the Graduate School of Politecnico di Torino (ScuDo).

Acknowledgements

I would like to express my deepest gratitude to my supervisors, Vittorio Verda and Elisa Guelpa. I couldn't have wished for better mentors. They provided invaluable technical advice that helped me overcome significant challenges in my research, but more importantly, they offered human support during difficult times. Additionally, they cultivated a united and close-knit research group, where we always enjoyed a warm atmosphere.

I extend my thanks to my colleagues Martina, Giulia, Umberto, Azad, and Jesus, who contributed to creating such a positive office environment. I already miss our old habits like having lunch together outside, our afternoon teas, and our whiteboard discussions about technical doubts.

I am also grateful to all my friends, who helped me rest my mind from the research work when I needed it.

I would like to thank my parents for their constant support throughout my PhD journey. They believed in me even when I doubted myself and supported me in every possible way.

Last, but not least, I want to thank Rossella for always being by my side both during good and challenging times, even when we were 10.000 km apart with a six-hour time zone difference.

Thank you all for being part of this journey with me.

Abstract

The increasing demand for space cooling presents a pressing challenge in achieving sustainability goals, particularly the target of net-zero emissions by 2050. In this context, district cooling represents a feasible alternative to conventional cooling technologies, especially in densely populated areas. Larger industrial chillers used in district cooling networks are indeed characterised by better performances, compared to the smaller residential ones. Moreover, the non-contemporaneity of demand peaks makes the load of district cooling networks more homogenous than the one of a single building. As a consequence, if on one hand residential chillers are usually oversized and tend to work at lower loads with worse performances, on the other hand the centralized chillers of a district cooling network are properly sized and operate more uniformly with better performances. In addition, further energy savings can be achieved by integrating this technology with renewable energy technologies or waste heat from industrial plants. Moreover, the integration with thermal energy storage in the context of power-to-cool strategies can reduce the pressure on the grid while lowering the operation costs, thanks to lower electricity tariffs during off-peak hours. On the other hand, the diffusion of this technology is strongly affected by the higher pumping and piping costs, due to the large mass flow rates required. Optimization tools are therefore necessary to fully exploit the potential of district cooling. This thesis hence focuses on the development and implementation of novel optimization models for the design and operation of district cooling networks, with the goal of enhancing the potential of this technology. Initially, a simplified optimization problem is defined, which is gradually made more complex in the rest of the thesis, with the goal of taking more aspects into account. The initial problem consists in optimizing the network layout, building connections, and pipe diameters for a single-plant network, minimizing the sum of operation and capital costs while considering pressure drops and pumping costs. A Mixed Integer Linear

Programming (MILP) model and a genetic algorithm have been implemented to tackle this problem.

The first additional complexity consists in considering the uncertainty of cooling demand and cost parameters, optimizing both the initial network design and possible future expansion by means of a two-stage stochastic programming model. The second problem complexity involves considering thermal energy storage and multiple plants, optimizing their positions and the buildings connected to the network. A genetic algorithm was implemented to address a simplified version of this problem with a fixed storage strategy, while a Mixed Integer Quadratic Programming (MIQP) model was implemented to optimize the cooling power dispatch, fixing the building connections. The two models were also compared to evaluate the impact of optimizing simultaneously both design and operation.

The final problem formulation includes additional decision variables such as the storage technology to be installed and the network supply temperature, considering its impact on chiller efficiency, piping, and pumping costs. A hierarchical model integrating a genetic algorithm with MILP models has been developed for this purpose. All the implemented models have been applied to real or realistic case studies to evaluate the potential of district cooling and determine the conditions for economic viability in Mediterranean and tropical urban contexts.

Contents

List of Figures

List of Tables

Chapter 1

Introduction

1.1 The rise of cooling demand

The demand for building space cooling has more than tripled in the last three decades [1] and a further increase is expected in the upcoming years, making it one of the fastest increasing demands in the energy sector. By 2050 two thirds of residential buildings will be equipped with air conditioning [2, 3].

The reasons behind this increase of demand are mainly attributed to the general rise of the temperatures, due to global warming, the major accessibility of cooling technologies in emerging economies and the demographic growth in the warmest countries [4]. Indeed, climate is certainly the first factor influencing cooling demand, but the higher incomes and the improvement of living standards, linked to the cost reduction of AC units, are pushing residents to install cooling systems. While in the past air conditioning was a privilege of few countries, in the recent years it has been becoming more accessible also in developing countries. Hence, building space cooling is a social-economic challenge and it should be made more accessible, as it provides significant benefits in terms of health conditions, well-being and productivity [5].

On the other hand, space cooling has a strong impact on the overall energy consumption and on the power grid stability. On average, it is responsible for 16% of electricity demand peaks, reaching 70% in warmer regions like Middle East or different areas of the United States [2]. Grid overcharging is also common during

heat waves and can cause severe complications, including power outages that can put at risk the energy system of an entire country [6].

Without proper actions aiming at maximising the energy efficiency of air conditioning systems, the electricity demand for building space cooling will continue to increase with a rate between 4 and 6% every year [2]. This means that by 2050, the demand and the carbon footprint could more than double with respect to nowadays levels. Major generation capacity will be therefore required to manage the higher peaks, contributing to a general increase of electricity costs, since expensive flexible power generation plants will have to be installed [7]. As a consequence, more actions need to be taken by the governments to increase the efficiency of cooling units to be installed or to promote measures aiming at improving energy performance of buildings.

1.2 District cooling

In this context, district cooling (DC) is a promising technology especially in densely populated areas [8]. Figure 1.1 shows a scheme of a district cooling network. The general principle of this technology is similar to district heating, as district cooling systems (DCS) are characterised by one or multiple chillers, where chilled water is produced and distributed through a piping system to the buildings energy transfer stations. There, the network chilled water is used to feed the air conditioning systems of the buildings. Consequently, it is heated up and circulates back to the chiller plants, completing a loop [9].

The connection of a building to the network can be either direct or indirect. In direct connections, network chilled water circulates directly in the building cooling system, while in indirect connections, intermediate heat exchangers are present to separate the district cooling chilled water from the fluid circulating in the building cooling system. The second option is the most frequent, as operation is easier and network pressure requirements do not depend on the pressure drops occurring in the building internal piping systems. On the other hand, the presence of intermediate heat exchangers is inevitably a cause of exergy destruction.

In general, district cooling is more efficient than individual cooling systems, thanks to the installation of larger centralized chillers which have better performances than

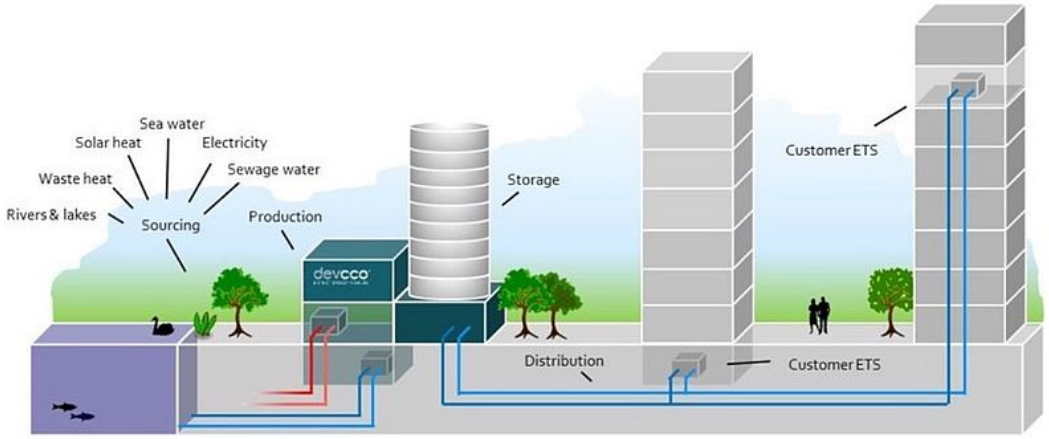

Fig. 1.1 Scheme of district cooling technology (Courtesy of DEVCCO District Energy Venture)

smaller residential ones [10]. In addition, lower capacity is required, since building demand peaks are not simultaneous, but rather phased out over time [11]. For the same reason, chillers in a district cooling network operate also more homogeneously and closer to design conditions with better performances. In addition, further reduction of demand peaks can be achieved, thanks to the integration of district cooling networks with thermal energy storage [12]. Moreover, district cooling networks can be coupled with renewable energy sources, unlocking additional energy savings and reduction of carbon emissions.

1.2.1 History of district cooling

District cooling technology has been evolving since its birth. Ostergaard et al. [13] applied the concept of network generations, very popular in district heating, to district cooling. They described the history and evolution of this technology identifying four main generations, represented in in Figure 1.2.

The first generation took place between the end of the 19th and the beginning of the 20th century. In these networks the refrigerant fluid, mainly ammonia or brine, flowed directly in the pipelines. They were characterised by a centralized condenser, multiple decentralized evaporators and refrigerant fluid flowing directly in the pipelines. The technology was realized mainly to substitute ice storage in

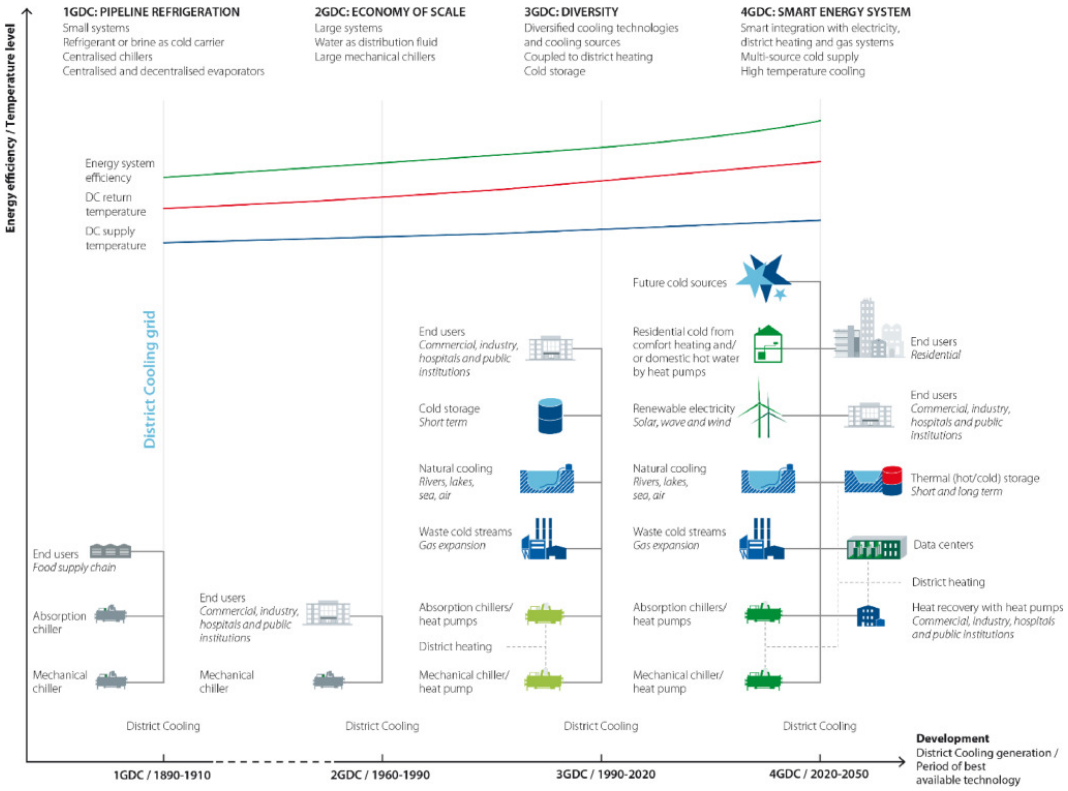

Fig. 1.2 Four generations of district cooling [13]

the food supply chain industry. The first documented examples are the networks of Denver [14] and New York [15].

The second generation of district cooling took place in the second half of 20th century. The main difference with the first generation is the exploitation of economies of scale, using chilled water as heat transfer medium in the underground pipes and large mechanical chillers. The weight of cooling generation was therefore entirely moved towards the utility suppliers, allowing a simplification of the systems thanks to the removal of decentralized evaporators. Moreover, the systems became safer thanks to the change from refrigerant pipelines to chilled water ones. These networks were installed in large districts to exploit economies of scale, employing large compression and absorption chillers instead of decentralized smaller ones. The target of district cooling networks was not anymore only the food industry, but included also residential and commercial buildings with space cooling demand for thermal comfort purposes. The first system of this kind was realized in Hartford(USA) [16] in 1962, employing both absorption and compression chillers. Other district cooling networks were realized also in the 60's in Germany and France. Large scale systems

were installed also in China [10, 17] and Middle East [18, 19], with cooling capacity ranging from few tens to hundreds of MW.

The third generation of district cooling arrived in the 1990s. The main driver for the technology change was the ban to chlorofluorocarbons and hydrochlorofluorocarbon refrigerants, as a result of the Montreal protocol [20]. Third generation district cooling networks were characterised by the use of large variety of cooling technologies or resources, including compression chillers, natural cooling from large water basins, short or long term storages, absorption chillers that use waste heat from industrial processes, and cold recovery from heat pumps. One of the first networks, part of the new generation is the one realized by Climespace in Paris in 1991 [21]. This network, apart from relying on multiple chiller plants and cold storages uses also the Seine river to provide free-cooling [22]. In Northern Europe, networks like the ones of Helsinki or Stockholm utilize seawater free cooling [23] and waste cooling from large heat pumps [24–26]. In general third generation district cooling networks exploit local resources with benefits in terms of economic feasibility, energy efficiency and carbon footprint.

The fourth generation of district cooling networks represents a concept of the latest years and is parallel to the fourth/fifth generation of district heating systems [27]. Indeed, these technologies are going towards the same direction, exploiting the synergies of combined heat and cooling. Waste cooling from heat pumps is therefore used to supply users requiring cooling demand, while waste heat is used to satisfy heating demand. This means that cooling and heating demands shall be balanced in order to fully exploit these synergies. However, one demand is always prevailing on the other. In this context, seasonal storages are used to store the excess heat during the summer to release it during the winter, when the heating demand is larger[28]. At the same time, during the winter months, waste cooling is stored. Networks that exploit these synergies have been realized in the 2010s especially in University campuses as demonstration plants [29]. In the ETH campus, in Zurich, the "anergy grid" [30, 31] is operating since 2013. It consists in a system characterised by geothermal energy storage, two anular networks, with temperatures between 8° C and 23° C. The system, during the winter, uses the thermal energy stored in the summer and waste heat from data centres to satisfy the heating demand of different buildings. During the summer, the cooling energy stored in the winter is instead used to cool the buildings and the data centres. Another example of combined heat and cooling synergy is the network installed in Saclay University in Paris [32, 33].

The system, realized in 2017 is characterised by two low temperature networks and integrates different sources including geothermal wells, heat pumps and back-up gas boilers.

1.2.2 Integration with renewable energy sources

Among the benefits of district cooling there is the possible integration with other energy systems, including renewable energy technologies. This allows to further reduce the electricity consumption and the carbon footprint of cooling.

Natural cooling or free cooling is one of the most popular ways of integrating renewable energy sources with district cooling networks. It consists in exploiting cold water reservoirs, such as rivers, lakes or seas. This cooling energy can be used either directly or, in case the temperature level is not sufficiently low, it can be used to increase the efficiency of water-cooled chillers [34]. Different networks in Europe integrate cold energy from rivers or seawater to satisfy part of the cooling demand. An example is the Gothenburg district cooling network which uses cold water from the river Göta älv [35]. It is estimated that district cooling systems that exploit these resources can be up to 10 times more efficient than alternative cooling solutions [36].

Thermal energy from renewable energy sources, like solar, geothermal, biomasses can be used to produce cooling energy and to satisfy the demand of a district cooling network. This is possible by means of absorption chillers, which convert heat to cooling energy by means of thermochemical processes to drive vapor compression cycles [37]. The ParcBit solar district [38], located in Mallorca island, is an example of a district heating and cooling network partially fed by solar energy. The system includes flat plate solar collectors, diesel generators and a biomass boiler. During the winter, the system satisfies the heating demand of a university and other public buildings. During the summer, cooling energy is produced both by electric and absorption chillers that use the heat produced by the solar collectors. The Munich district cooling utility SWM has planned to use geothermal energy to increase the cooling capacity of an existing 20 km network and to enhance it by 5 km, connecting new buildings [39].

Solar energy can be integrated also by coupling district cooling networks with photovoltaic plants. In this case, the solar energy is transformed into electricity and used to supply electrical chillers. One of the main benefits of this solution is the high

synergy, since cooling demand and the power generated have simultaneous peaks [40].

Waste heat from industrial processes or data centers can be used to feed district cooling networks. For instance, in Vienna [41] waste heat from incineration plants is used to feed the local district cooling network run by Wien Energy. Compared to conventional cooling systems, this solution consumes from 4 to 10 times less primary energy.

1.2.3 Thermal energy storage integration

Additional benefits can be achieved by coupling district cooling networks with cold energy storages. In particular, the main advantages are:

- Reduction of the required chiller capacity.
- Chillers operate with more homogenous loads and with better performances.
- Power-to-cool strategies can be adopted, reducing the cooling load during peak hours, hence stabilizing the electrical grid. At the same time, savings in terms of operation expenditures can be achieved by operating the chillers during off-peak periods, when the electricity tariffs are lower.

The most frequent types of cold storage in district cooling applications are sensible and latent heat storages. The firsts are characterised by chilled water tanks, while latent heat storages are represented by ice or other commercial phase change materials, such as paraffins, fatty acids or salt hydrates. The benefits of chilled water tanks are their low price and flexible operating temperatures. On the contrary, their volumetric capacity is lower, due to the absence of latent heat and the low temperature range. As a consequence, these storages are not feasible in cities with larger space occupancy costs or with surface shortage. Ice thermal storage is also characterised by lower capital costs, but the production of ice involves lower chiller efficiency. However, thanks to the latent heat, the volumetric capacity is larger, compared to chilled water tanks and lower spaces are required. Phase change materials are commercially available with almost any melting temperature. Indeed, any existing PCM can be modified by adding other compounds that change the melting point. On the other hand, they are characterised by higher costs and have shorter life-cycles [12].

1.2.4 Challenges and opportunities

Although the different benefits of district cooling compared to conventional cooling, this technology is less developed and diffused than district heating. District cooling is, indeed, characterised by different challenges that contribute to obstruct its diffusion.

Large initial costs and design uncertainty

The higher initial capital costs are one of the main challenges of this technology. Contrarily to district heating networks, where the temperature difference between supply and return is between 50 and 60°C [42], in district cooling networks the temperature difference is between 6 and 11° C [43, 44]. As a consequence, at least five times larger mass flow rates are required to transfer an equivalent amount of thermal power. This therefore has an effect on both piping and pumping costs.

In addition, the design of these systems should take into account the evolution of cooling demand and the possible future network expansions. In that case, the initial network design must be sufficiently robust, to allow further installations in the future. Moreover, the uncertainty of energy prices and cooling demand makes district cooling investments particularly risky. Indeed, cooling demand depends on the weather conditions and on the thermophysical properties of the buildings. In addition, the thermal comfort and cooling habits varies among the users. It is therefore difficult to predict the cooling demand and its evolution with time. The risks related to these uncertainties may affect the potential of district cooling. As an example, plants may result more expensive compared to the estimated cost. Chiller plants could be undersized or oversized, due to a discrepancy between the estimated cooling loads and the real ones.

In addition, the uncertainty relative to the alternative cooling solutions also affects the diffusion of district cooling, as the evaluation of the savings and the benefits of district cooling compared to other technologies may not be accurate. For instance, underestimating the efficiency of individual chillers may lead to overestimate the operation savings of district cooling, making it appearing more convenient than it is in reality.

All these aspects represent therefore a challenge for decision makers when designing district cooling networks. As a consequence, if not properly designed, the potential

of these systems may be lower than expected and the benefits may be limited or even absent. Design optimization tools are therefore necessary to fully exploit and enhance the potential of district cooling systems.

Minimization of operation expenditures

In order to maximize the advantages of district cooling, operation expenditures shall be minimized as well. Since a district cooling system is made by multiple components, it should be optimised as a whole, exploiting also the potential synergies with other energy systems. As a consequence, when operating a district cooling network, the performances of one or more components could be sacrificed with the goal of maximising the overall system efficiency.

One critical aspect of optimization is determining the supply temperature of the network. While a higher supply temperature can increase chiller efficiency, reducing both electricity consumption and carbon footprint, it also leads to increased pumping costs due to reduced temperature differences across energy transfer stations. Striking a balance and selecting an optimal supply temperature is, therefore, crucial in minimizing the combined costs of chillers and pumps.

Additional opportunities regarding the operation optimization of district cooling networks involve the exploitation of the synergy with other energy technologies, in the context of multi-energy systems [45]. For instance, district cooling networks can be used to stabilize the electrical grid by means of power-to-cool strategies, encouraging a major penetration of renewable energy sources. Further savings can be obtained by optimizing the integration with district heating systems, especially when cooling is produced by trigeneration plants. Exploiting the synergies between these systems can indeed reduce CO2 emissions by up to 90% and increase energy efficiency by more than 50% [46].

Increase of supply temperatures

District cooling networks are usually fed with low supply temperatures in the range of 5-8°C [44] and return temperatures in the range of 12-16°C.

These temperature levels make more difficult the integration of natural resources, like free cooling from water basins. In tropical humid countries, lower temperatures

are however needed for de-humification requirements. Indeed, to remove moisture, air must be cooled down below the dew temperature. On the other hand, different types of buildings, like data centers, have mainly sensible cooling demand and lower dehumidification needs. These buildings could be therefore supplied with higher chilled water temperatures up to 17° C [47]. These temperature levels could reduce the electricity consumption and the carbon footprint of district cooling, thanks to higher efficiencies and major use of free cooling resources [48].

Increasing district cooling supply temperature is challenging also for the low delta-T syndrome. This problem is due to a decrease in the return temperature from the energy transfer stations, causing a further increase of the mass flow rates and of the energy demand.

Different solutions have been studied in literature [49], including the correct sizing of control valves or controlling the mass flow rate through heat exchangers, instead of the set-points. However there is not a common approach that can work for all buildings and finding the solution for every single energy transfer station requires a large quantity of resources [50].

1.3 Objectives and structure of the thesis

This thesis aims at providing new methods and models for the optimal design and operation of district cooling networks with the final goal of providing general design guidelines.

Firstly, the previous works regarding the simulation and optimization of district heating and cooling networks have been analysed in *chapter 2*, in the form of a literature review. The identified research gaps allowed to define the aspects that needed further consideration when optimizing district cooling networks and which have been addressed in the thesis.

The work starts by first defining a simplified optimization problem, which is gradually complicated and generalized, by introducing additional variables or considering other aspects according to specific requirements, as shown in Figure 1.3. The initial problem, addressed in *chapter 3*, regards the optimization of the network layout and the buildings to be connected. To solve this optimization problem, a MILP model was initially implemented. Due to its computational cost, a genetic algorithm has

been implemented to solve the reformulated version of the problem, characterised by a reduced search space. The latter was also improved by integrating it with a clustering approach with the goal of easing the convergence to the optimum. These models allow to exploit the potential of district cooling in a particular urban context by properly selecting the network topology and the buildings to be connected.

In *chapter 4*, additional complexity is added to the model by taking into account the parameters uncertainty and the possible evolution of cooling demand during the years. The objective consists therefore in optimizing the initial network layout and the possible future enhancements on the base of the conditions that may arise. The goal is to select a sufficiently robust initial design that works well for the whole combination of possible scenarios. To solve this optimization problem the MILP model implemented in *chapter 3* has been improved and transformed into a two-stage stochastic programming model. The impact of uncertainty was assessed, by comparing the model with deterministic approaches.

In *chapter 5*, the initial problem defined in *chapter 3* is generalized. In particular, networks with multiple chiller plants and thermal storages are considered. The objective consists therefore in optimizing not only the set of buildings to connect and the topology, but also the positions of chillers and storages within the network, as they influence both piping and pumping costs. For this purpose, the heuristic approach implemented in *chapter 3* has been adapted and improved.

Another complication of the initial problem regards optimizing simultaneously the design and storage strategy of a district cooling network in order to determine the trade-off between equipment capacity and operation. Indeed, theoretically, increasing the capacity of chillers and storages, could unlock power-to-cool opportunities at the cost of larger capital expenses. The impact of combinedly optimizing these two aspects is studied in *chapter 6* under different scenarios. For this scope, a Mixed Integer Quadratic model has been implemented and compared with the heuristic approach developed in *chapter 5*.

In *chapter 7* the problem is further complicated by introducing additional decision variables. In particular, the problem consists in optimizing also the supply temperature and the storage technology to be installed. The problem has been addressed by considering a Singapore case study under different scenarios and has been solved by implementing a hierarchical approach that combines a genetic algorithm and

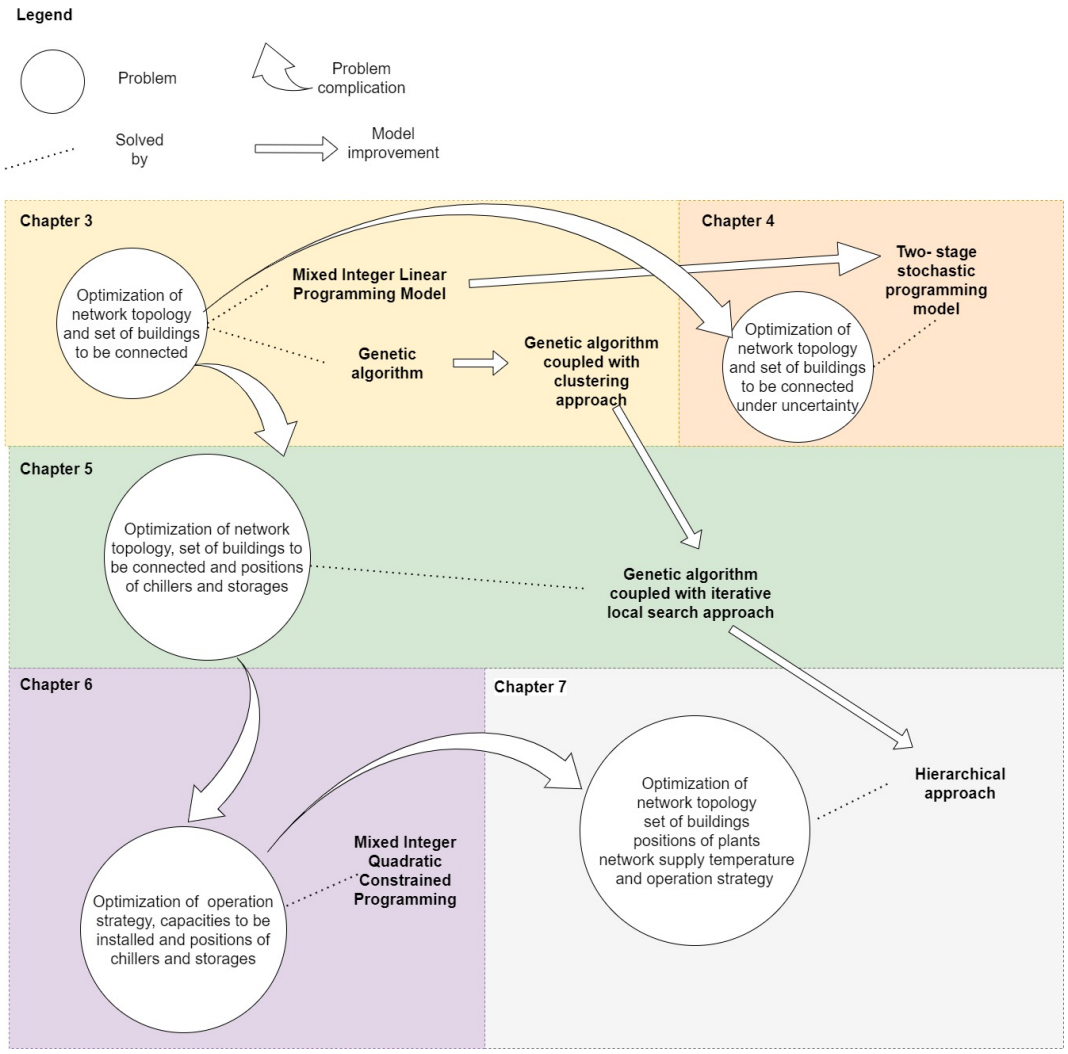

Fig. 1.3 Summary of models described in the thesis

different MILP models. This last model therefore represents a further improvement of the heuristic approach developed in *chapter 3* .

The results obtained by solving these problems allowed to provide guidelines, summarized in the concluding Chapter, regarding the optimization and the design of district cooling networks in the European and Singaporean contexts.

Chapter 2

Numerical models for the simulation and optimization of DHC networks

Different numerical models of district heating and cooling networks exist already in literature. These can be classified in simulation and optimization models, depending on their main purpose. In this chapter the existing numerical models for the simulation and optimization of district heating and cooling networks are analysed, with particular focus on the optimization models.

2.1 Simulation models

Two different categories of simulation models can be identified: physical and black-box models. The main difference is that the firsts directly model the physical equations of heat transfer and fluid dynamics phenomena, while black box models do not.

2.1.1 Physical models

Physical models for the simulation of district heating and cooling networks are mainly characterised by one-dimensional thermal fluid dynamic models. Different authors implemented nodal models that combine graph theory concepts and computational fluid dynamics methods.

Sciacovelli et al. [51–56] developed a nodal model able to solve Navier-Stokes and energy equations to evaluate the mass flow rates flowing in each pipe, the pressure drops and the thermal profile of district heating and cooling networks. The approach is based on 1D finite volumes and on the Backward Euler schemes for space and time discretization, respectively. In case of tree-shaped networks, continuity equations alone are sufficient to compute the mass flow rates. On the other hand, in case of looped networks momentum equations and continuity equations are solved together. The non linearity of momentum equations is handled by means of the SIMPLE method, which consists in assuming initial values of mass flow-rates and pressures and correcting them iteratively until they satisfy all mass balance and momentum equations. Since finite volumes scheme is characterised by diffusion errors, the network pipes need to be highly discretized, making this method highly computationally expensive, especially in the case of wide networks.

Another common method consists in using a Lagrangian approach, in which the observer travels through the network pipes with a moving fluid particle [57–59]. This method allows to accurately predict the temperature propagation, also in the case of fast changing boundary conditions, avoiding numerical diffusion [60].

2.1.2 Black box models

Black box models are less computationally expensive than physical models, but their accuracy is limited, especially for conditions outside of the training datasets.

These methods do not model the physical phenomena, contrarily to physical models, which are based on the equations that describe heat transfer and fluid dynamic phenomena. In black box models, instead, the district heating and cooling network is modelled by creating a function or a combination of functions by using statistical methods on the available data, such as linear interpolation. The non-linearities which cannot be modeled by linear interpolation are instead described using artificial neural networks or standard transfer functions [61–63].

With the objective of reducing the computational time of a physical model based on finite volumes scheme, Guelpa et al. [64] implemented a reduced order model by using radial basis functions and orthogonal decomposition. This approach allowed to reduce the computational time by 80% compared to the physical model and to obtain only 2% less accurate results in the tested conditions.

Other authors instead developed black-box models to simulate specific components of district heating and cooling networks, such as the performance of production plants. With this regard, Cox et al [65] developed a neural network model to predict the electricity consumed by a chiller plant of a large district cooling network feeding a university campus.

2.2 Optimization models

Different numerical models have been developed for the optimization of design and operation of district heating and cooling networks. Design optimization regards the aspects related with design decisions to be taken in the early stages of a project. These can include the network topology, the pipe sizes and the capacity of the equipment to be installed. Operation optimization includes the power dispatch from the different plants or storages, but also the optimal choice of set-point parameters, such as temperatures, pressures or mass flow rates. Optimization models are mainly based on Mixed Integer Linear Programming or heuristic approaches. Some authors also considered non-linearities in the constraints and objective function, using different linearization methods, including reformulation linearization technique (RLT) and the cutting plane method [66, 67].

2.2.1 Design optimization

Concerning the design optimization of district heating and cooling networks, different authors developed models to find the optimal layout, pipe sizes and location of pumps, chillers or storages.

In district cooling networks, pumping cost can be detrimental for the feasibility of the technology. As a consequence, a correct pumping configuration is necessary to minimize pumping costs and increase the potential of this technology. Lo et al. [68] developed different mathematical models to select the optimal pumping configuration in a district cooling network, choosing between multiple pumping stations and a single station with multiple pumps. The results showed that the optimal solution allows to reduce by 23% the electricity consumed by the pumps. Guelpa et al. [69] optimized the position of heat pumps in a district cooling network, with the goal of reducing the sum of piping and pumping costs.

Other studies focused on the topology optimization of district cooling networks. In particular, different authors proposed approaches for the layout optimization and for the selection of the diameters [70]. Chan et al. [71] developed a genetic algorithm coupled with a local search approach for the layout optimization of a district cooling network. They considered an input graph where there is a branch for every couple of nodes and found the optimal tree network that minimized the piping and pumping costs. Dobersek and Goricanec [72], starting from a looped network and taking into account the real limitations of an urban district, through a non-linear optimization method found the optimal layout of a tree-shaped district heating network minimizing the pumping and piping costs. Al-Noaimi, Khir and Haouari [73, 74] developed a tool for the optimization of both design and operation of district cooling systems. They modelled the problem as a MINLP that minimizes the total cost taking into account both capital and operation costs. In their case study, they considered a starting looped graph with several sources and storages. The objective of their optimization was to find the optimal tree-shaped network, the optimal diameter for every pipe and the optimal location and size of storages and plants. The authors handled the non-linearities through reformulation linearization techniques. Soderman [75] developed a Mixed Integer Linear Programming to combinedly optimize the design and the operation of district cooling networks. His tool is able to optimize the network layout, the position of chillers and the cold storages. In addition the model optimizes also the capacity of chillers and storages and their operation schedules, with the goal of minimizing total costs. The tool, however was tested only on simpler networks. Other authors optimized the topology of district heating and cooling networks by using heuristic assumptions based on typical graph theory concepts, such as the minimum spanning tree or the shortest path tree [76–79].

Some studies also proposed some methodologies that take into account the progressive enhancement of the networks within the years. Wirtz et al. [80] developed two multiperiod optimization models for the design of fifth generation district heating and cooling systems(5GDHC). The results showed that multi-period models, compared to single period ones, allow to reduce by 17% the total cost savings.

2.2.2 Operation optimization

Concerning the operation optimization, the existing studies in literature mainly focus on:

- daily schedule of chillers and storages
- chilled water supply temperature and mass flow rates
- chiller systems operating parameters such as the condenser supply temperature and mass flow rates
- optimal pumping operation

Powell et al. [81] optimized the cooling power dispatch in the case of multiple chillers and cold energy storage. They implemented a dynamic programming algorithm to optimize the charge and discharge of the storage and a quadratic-programming model to select the optimal load for each chiller.

The schedule of chillers and storages was optimized also by Cox et al [65], who implemented a model predictive control based on an artificial neural network and coupled it with a genetic algorithm.

Zaw et al. [82] implemented a framework for the optimal dispatch of cooling power characterised by three modules: an artificial neural network for the prediction of cooling demand, an optimization module to optimize the supply temperatures and mass flow rates of chilled water from each chiller, and the second optimization module to optimize the temperature and mass flow rate of the condenser water.

Wang et al [83] optimized the operation of chiller plants, implementing a hybrid model. In addition, in order to keep the computational time low, they proposed variable search bounds in the constraints of the genetic algorithm limiting the fluctuations of the variables with minor impact on the optimization.

Concerning the optimization of the network supply temperature, Zhang et al. [84] handled this problem in the context of a multi-cold source district cooling system. The model they implemented allows to vary the supply temperature following the changes in the outdoor conditions. Compared to a baseline scenario, where the supply temperature is constant, this approach allows to reduce the energy consumption by about 20%.

Guelpa and Verda [85] proposed a method for the optimization of pumping operation in district heating networks during malfunctions. The approach is general and could be used also in district cooling systems. It consists in a genetic algorithm which selects the pressure rises in each pump and the mass flow rates inserted into the network from the power plants, minimizing the primary energy consumption and maximizing the flexibility.

Chiam et al [86] implemented a hierarchical approach to optimize simultaneously the operation of all the components of a district cooling networks. The framework is characterized by a genetic algorithm at a master level, whose variables are the parameters for a MILP at inferior level. This method allows the optimization of the whole system, without strong assumptions on the single components, such as constant efficiencies. Moreover, compared to the optimization limited to chillers, it guarantees major savings, thanks to the consideration of the whole system.

2.2.3 Optimization under uncertainty

Most of the optimization models available in literature are based on deterministic assumptions. However, in the real world, uncertainties exist and affect the solution, if the real parameters are distant from the estimated ones used as input.

In the context of district cooling networks, cooling demand is uncertain as it changes every year and depends on the weather conditions, on the building properties and on the users habits. Moreover, the economic parameters are also uncertain, as the cost of electricity varies due to market changes and geopolitical factors. In addition, the capital costs are also subject to some degree of uncertainty. These uncertainties should therefore be considered when optimizing either the design or the operation of district heating and cooling networks. Only few authors handled uncertainty when optimizing these systems.

Gang et al. [87] developed a method for the robust optimal design of district cooling networks, taking into account equipment reliability and the uncertainty of cooling load.

Mavromatidis et al. [88] implemented a two-stage stochastic programming model for the design of a district energy system. They considered different sources of uncertainty, such as heat and electricity demands, energy prices and weather conditions. The model optimizes the size and technologies to be installed (1st stage variables)

and optimizes the operation (2nd stage variables) on the base of the scenario that occurs.

Lambert et al [89] proposed a multistage stochastic programming model to optimize the design phases and the expansion of district heating systems, while taking into account the uncertainties related to costs and interest rates.

Zhou et al. [90] developed a two-stage stochastic programming model for the optimal design of distributed energy systems. They optimized the first stage variables by means of a genetic algorithm, while the second stage decisions are taken through a Monte Carlo method.

Lastly, Bratseh et al. [91] proposed a stochastic programming model to optimize the operation of a district heating system with seasonal storage and local waste heat re-utilisation, while taking into account the demand uncertainty.

2.3 Commercial tools

Different commercial software tools are widely available in the market. Termis and Leanheat, owned respectively by Schneider Electric and Danfoss, allow to simulate district heating and cooling networks and also have modules for the operation optimization. Apros, developed by Fortum and VTT [92], is a multipurpose tool, initially used mainly for nuclear applications, but nowadays allows also to simulate the dynamic behaviour and to optimize the operation of district energy systems. In the latest years, also different startups started to explore this area, developing simulation and optimization tools for district heating and cooling networks. Among these, Gradyent developed a real time digital twin able to simulate the network dynamics. Npro [93], a spin-off company of RWTH Aachen University, realised a tool for the planning, design and simulation of district energy systems. In particular, the tool offers also functionalities for 5GDHC networks.

2.4 Research gaps

Further effort is needed in the optimization of district cooling networks. From the literature review, the following research gaps have been identified:

- The topology optimization plays a fundamental role in the reduction of total life-cycle costs. However, very few studies focused on the optimization of the buildings to be connected to a district energy network. On the other hand, choosing the right buildings to connect to a network is fundamental to fully exploit the potential of district cooling and to carry out fair comparisons with other technologies.
- Most of the existing models are based on the logic “now or never" and are purely deterministic. Very few considered the impact of the uncertainty and the possibility to split the district cooling networks design in multiple phases. However, deterministic approaches tend to work well only in conditions close to the assumed ones.
- The existing models tend to optimize only few specific aspects, due to their large computational costs. On the other hand, additional benefits can be obtained by optimizing a wider range of variables.

The work starts by addressing the first research gap. In particular, a MILP and a genetic algorithm coupled with a clustering approach have been implemented to optimize the network layout and the buildings to be connected. The rest of the work focuses on the gradual improvement of these two models with the goal of solving more complex problems and addressing the other research gaps.

The first improvement represents therefore the inclusion of uncertainty in the optimization problem. In particular, it was implemented a two-stage stochastic programming model to optimize the initial network design and the possible future expansions, while taking into account the uncertainty of the cost parameters and of the evolution of cooling demand in the upcoming years. The goal of this model is to select a robust initial network that works well for the whole combination of possible scenarios that can arise.

The second evolution direction has the objective of addressing the third identified research gap and solving a more generalized version of the initial problem. It is characterised by multiple steps with the ultimate goal of implementing of a tool able to optimize not only the topology and the set of buildings to be connected, but also the plant positions, the storage technology to be installed, the network supply temperature, the equipment capacity and the operation strategy.

Chapter 3

Topology and connections optimization of district cooling networks

The content of this chapter has been previously published in the following paper [67]:
Manfredi Neri, Elisa Guelpa and Vittorio Verda. "Design and connection optimization of a district cooling network: Mixed integer programming and heuristic approach." Applied Energy 306 (2022): 117994

3.1 Introduction

In this chapter are presented two novel models: a mixed integer programming and a heuristic approach, for the design optimization of district cooling networks. They optimize simultaneously:

- the network layout;
- the pipe diameters;
- the set of buildings to be connected.

The objective of both models is to minimize the sum of capital and operation expenditures.

Particular attention is also paid to the evaluation of pumping costs, which are highly non-linear and need to be treated rigorously. These, indeed, are non-negligible, due to the large mass flow-rates flowing in district cooling networks.

The models have been applied to three different case studies. The first is characterised by a simple neighbourhood with a limited number of branches and nodes. The other two case studies, instead represent two typical Italian residential districts.

The first model is described in Section 3.2 and is characterised by a MILP, where non-linearities are handled by means of different linearization techniques.

The second approach, described in Section 3.3, is a genetic algorithm, based on the assumption that the optimal layout is a minimum spanning tree. For more complex cases, this algorithm is coupled with a clustering approach, with the goal of reducing the number of variables and easing the convergence to the optimum.

The two models have been then compared, analysing their advantages, disadvantages and applicability.

3.2 Mixed Integer Linear Programming model

In this section, the mathematical model, based on the MILP approach is presented. This model receives as input a graph that represents a neighbourhood, with a set of user nodes (the buildings) with a known cooling demand, a plant node and a set of internal nodes, called Steiner nodes. The goal of the model is to determine (a) the optimal set of buildings to connect to a district cooling network; (b) the optimal tree-shaped network layout; (c) the optimal diameter for every pipe of the network. In Tables 3.1 and 3.2 the main parameters of the model, the sets and the indices are reported, while the decision variables are reported in Table 3.3. Since the flow direction in each pipe is not known a priori, the input graph is modelled as bi-directional. As a consequence, each network branch is considered twice: one for each possible flow direction. Figure 3.1 shows a scheme regarding the concepts of bi-directional graph, user nodes, production node and Steiner nodes.

M	Set of possible diameters, indexed by m
E	Set of all edges, indexed by (i, j)
V	Set of all nodes, indexed by i or j
S	Set of Steiner nodes, indexed by i or j
Ut	Set of user node, indexed by i or j
$centr$	Index referring to plant node
Θ	Set of time steps, indexed by t
V_j^+	Set of successor nodes of generic node j
V_j^+	Set of predecessor nodes of generic node j

Table 3.1 Sets and indices used in the mathematical formulation of the models

G^m_{max}	Maximum mass flow rate for the diameter m [kg/s]
L_{ij}	Length of the edge (i,j) [m]
$c_{op,chill,DC}$	Operational cost of the central chiller [€/kWhe]
$c_{op,chill,ind}$	Operational cost of independent chillers [€/kWhe]
$c_{chiller,DC}$	Investment cost of central chiller [EUR/kW]
$c_{chiller,ind}$	Investment cost of independent chillers [€/kW]
c_{ETS}	Investment cost of energy transfer station [€/kW]
EER_{DC}	Energy efficiency ratio of the central chiller
EER_{ind}	Energy efficiency ratio of performance of independent chillers
c^m	Cost of installation for pipes having the diameter m [€/m]
η_{pump}	Efficiency of pump [%]
ΔT	Temperature difference between supply and return [°C]
β_{ij}	Sum of local head drop coefficients for edge (i, j)
f^m	Friction coefficient of pipes with diameter m
Δt	Time-step [s]
$G^t_{ext,j}$	Mass flow requested from user j at time t [kg/s]
Q_j	Thermal demand requested by user j at time t [kW]
c_p	Specific heat [kJ/kg/K]
r	Interest rate [%]
n_y	Life-time [y]
n_d	Length of cooling season [d]

Table 3.2 List of model parameters

z_{ij}	Binary variable equal to 1 if edge (i, j) is selected
y_j	Binary variable equal to 1 if the user node j is independent
x_{ij}^m	Binary variable equal to 1 if m diameter is selected for pipe (i, j)
G_{ij}^t	Mass flow rate flowing in pipe (i, j) at time t
G_{centr}^t	Mass flow rate entering from plant node at time t
Y_{ij}	Inverse of fluid dynamic resistance of pipe (i,j) per unit of mass flow rate
p_s^t	Pressure on node s at time t
Δp_{ij}^t	Pressure drop on pipe (i, j) at time t

Table 3.3 List of model variables

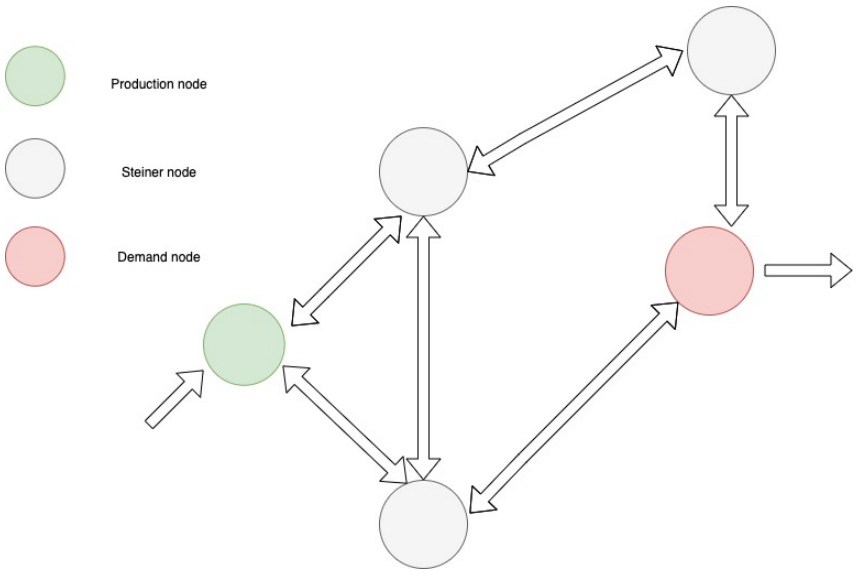

Fig. 3.1 Scheme of bi-directional graph

3.2.1 Assumptions

The model is based on the following assumptions:

- every time-instance is considered as an independent steady state (quasi steady-state);
- heat gains are neglected due to the low temperature difference between the chilled water flowing in the pipes and the ground;
- the final network must have a tree-shaped layout;
- centralized chillers are more efficient than individual ones and their specific cost per unit of installed cooling capacity is lower;
- the network has a single production plant (centralized chiller) with known position.

Since heat gains are neglected, the temperatures on the supply and return lines are considered constant and equal to 7°C and 12 °C, respectively. Consequently, the temperature difference between supply and return across energy transfer stations is always equal to 5°C. For this reason, only the fluid dynamic behaviour of the network is considered, while the thermal one is neglected. As a consequence, the cooling demands are converted in terms of mass flow rate demands, dividing them by specific heat and the temperature difference between supply and return as specified in eq. (3.1).

$$G^t_{ext,j} = \frac{Q^t_j}{c_p * \Delta T} \qquad \forall j \in Ut, t \in \Theta \tag{3.1}$$

3.2.2 Objective function

The objective function is characterised by the following terms:

- Capital cost of centralized $Cost^{cap}_{chill,DC}$ and individual chillers $Cost^{cap}_{chill,ind}$;
- Capital cost of piping $Cost_{pipe}$ and energy transfer stations $Cost_{ETS}$;
- Operation cost of centralized $Cost^{op}_{chill,DC}$ and individual chillers $Cost^{op}_{chill,ind}$;

- Operation cost of pumps

Operation expenditures are actualized considering a life-time period of 30 years. The optimization problem consists therefore in the minimization of the sum of these costs as shown in (3.2):

$$\begin{aligned} min(O.F. =& Cost_{pipe} + Cost_{ETS} + Cost^{cap}_{chill,DC} \\ &+ Cost^{cap}_{chill,ind} + Cost^{op}_{chill,DC} \\ &+ Cost^{op}_{chill,ind} + Cost_{pump}) \end{aligned} \tag{3.2}$$

Piping cost

The piping cost depends on the selected branches and pipe diameters, as defined in (3.3).

$$Cost_{pipe} = \sum_{ij}^{E} \sum_{m}^{M} x^m_{ij} * c^m_{pipe} * L_{ij} \tag{3.3}$$

Energy transfer stations cost

The cost of the energy transfer stations is defined in (3.4):

$$Cost_{ETS} = \sum_{j}^{Ut} c_{ETS,j} * (1 - y_j) \tag{3.4}$$

This is equal to the sum of the cost of the single energy transfer stations installed in every building connected to the district cooling network. The term $(1 - y_j)$ indicates that in this sum are not considered the buildings with individual cooling systems, for which $y_j = 1$.

Capital cost of chillers

The model considers two categories of chillers: centralized ones that supply the district cooling network and individual ones installed in the buildings not connected to the network. The firsts are more efficient and their specific cost per unit of capacity is lower, due to economies of scale. Equations (3.5) and (3.6) report the capital cost

of centralized and individual chillers.

$$Cost^{cap}_{chill,DC} = Q_{centr} * c_{chill,DC} \tag{3.5}$$

$$Cost^{cap}_{chill,ind} = \sum_{j}^{Ut} \max_{t \in \Theta} Q^{t}_{j} * c_{chill,ind} * y_{j} \tag{3.6}$$

Operation costs of chillers

The operation costs of centralized and individual chillers depend on the cost of electricity and on the energy efficiency ratio. In addition, these costs must be multiplied by an actualization coefficient, which depends on the discount rate and on the lifetime of the investment. The operation costs for centralized and individual chillers are defined in equations (3.7) and (3.8), respectively.

$$Cost^{op}_{chill,DC} = \sum_{t}^{\Theta} \frac{G^{t}_{centr} * c_{p} * \Delta T}{EER_{DC}} * c_{el} * n_{d} * \Delta t * \sum_{n=1}^{n_{y}} \frac{1}{(1+r)^{n}} \tag{3.7}$$

$$Cost^{op}_{chill,ind} = \sum_{j}^{C} \sum_{t}^{\Theta} \frac{Q^{t}_{j} * y_{j}}{EER_{ind}} * c_{el} * n_{d} * \Delta t * \sum_{n=1}^{n_{y}} \frac{1}{(1+r)^{n}} \tag{3.8}$$

Pumping costs

The cost of pumping is defined in equation (3.9). Since supply and return line are modelled together, the pressure drops of the return line are taken into account, by incorporating them with the pressure drops of the supply line using the method presented by Sciacovelli et al. [52]. As a consequence, the pressure node variables refer to relative pressure between supply and return line on these nodes, rather than to absolute values. The pumping power which depends therefore on the product between mass flow rate and the pressure difference between supply and return on the plant node is redefined as the product between mass flow rate and plant node pressure in the equivalent network model. A simple quantitative example is shown in Figure 3.2 to better explain how this method works. The example presents a network with three nodes, where the pressure drops on all the branches is set to 1 bar. The absolute pressure supplied by the first node is 8 bar, while the return pressure on the same node is 6 bar. By converting the network to the equivalent one, where the

return line pressure drops are summed to the supply line ones, it can be observed that the new node pressure values correspond to the pressure differences between supply and return line on the same nodes.

$$cost_{pump} = \sum_{t}^{\Theta} \frac{G^{t}_{centr} * p^{t}_{centr}}{\rho * \eta_{pump}} * c_{el} * \sum_{n=1}^{n_y} \frac{1}{(1+r)^n} \tag{3.9}$$

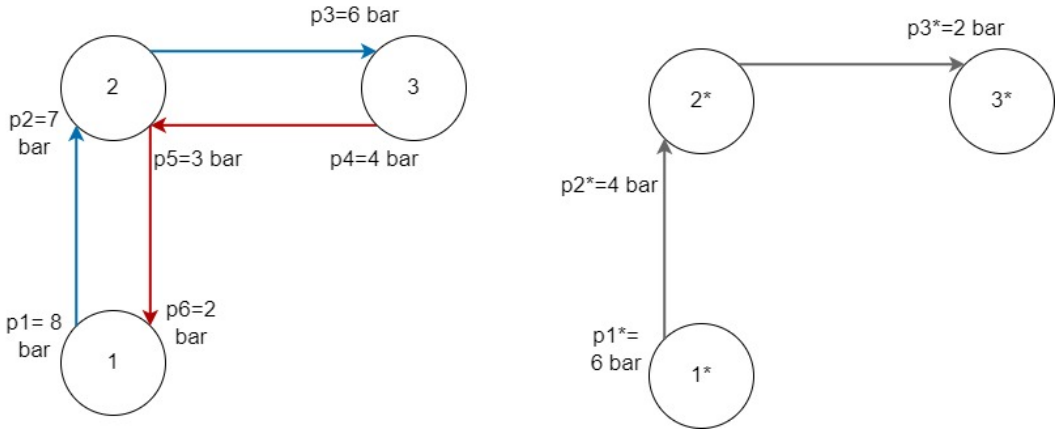

Fig. 3.2 Quantitative example on the equivalent network method

3.2.3 Constraints

The model is characterised by different constraints classifiable as: i) topology constraints, ii) mass balances, iii) pressure balances.

Topology constraints

Topology constraints are required in to ensure that the final network layout is feasible, connected and tree-shaped. The tree-shaped condition is guaranteed by constraint (3.10), which indicates that a Steiner node must be connected by one predecessor node, at most.

$$\sum_{i}^{V_j^-} z_{ij} \leq 1 \qquad \forall j \in S \tag{3.10}$$

Constraint (3.11) indicates that if a demand node is not connected to the network, no incoming edges shall be selected. At the same time, the constraint ensures that if a demand node is connected, only one incoming edge must be selected, in order to guarantee the tree-shape of the final network.

$$\sum_{i}^{V_j^-} z_{ij} + y_j = 1 \qquad \forall j \in Ut \tag{3.11}$$

Constraint (3.12) guarantees that two nodes can be connected by one edge, at most. This is equivalent to say that only one flow direction can be chosen for each pipe.

$$z_{ij} + z_{ji} \leq 1 \qquad \forall (i,j) \in E \tag{3.12}$$

Constraint (3.13) ensures that only one diameter is selected for each pipe.

$$\sum_{m}^{M} x_{ij}^{m} \leq 1 \qquad \forall (i,j) \in E \tag{3.13}$$

Constraint (3.14) ensures that Steiner nodes not connected to any predecessor nodes, are not connected to any nodes.

$$z_{jk} \leq \sum_{i}^{V_j^-} z_{ij} \qquad \forall j \in S, k \in V_j^+ \tag{3.14}$$

Constraint (3.15) indicates that if a Steiner node has a predecessor node, at least an outgoing edge must be selected.

$$\sum_{k}^{V_j^+} z_{jk} \geq \sum_{i}^{V_j^-} z_{ij} \qquad \forall j \in S \tag{3.15}$$

Mass flow constraints

Mass flow constraints are needed to ensure that mass balances are respected and that the pipes have sufficient capacities. Constraint (3.16) ensures that the mass flow rate

flowing in a pipe does not exceed the admissible one for the selected pipe diameter.

$$G_{ij}^{t} \leq \sum_{m}^{M} Gmax^{m} * x_{ij}^{m} \qquad \forall (i,j) \in E, t \in \Theta \tag{3.16}$$

Constraints (3.17)-(3.19) are mass balances on Steiner, users and plant nodes, respectively. On user nodes there is a net extracted mass flow rate, on plant node mass flow rate is injected into the network, while on Steiner nodes there is neither entering nor exiting mass flow rate.

$$\sum_{i}^{V_j^-} G_{ij}^{t} - \sum_{k}^{V_j^+} G_{jk}^{t} = 0 \qquad \forall j \in S, t \in \Theta \tag{3.17}$$

$$\sum_{i}^{V_j-} G_{ij}^{t} - \sum_{k}^{V_j^+} G_{jk}^{t} + G_{ext,j}^{t} * (1 - y_j) = 0 \qquad \forall j \in Ut, t \in \Theta \tag{3.18}$$

$$\sum_{k}^{V_{centr}^+} G_{centr,k}^{t} - G_{centr}^{t} = 0 \qquad \forall t \in \Theta \tag{3.19}$$

Constraints (3.20) and (3.21) indicate that the mass flow rates are non-negative.

$$G_{ij}^{t} \geq 0 \qquad \forall (i,j) \in E, t \in \Theta \tag{3.20}$$

$$G_{centr}^{t} \geq 0 \qquad \forall t \in \Theta \tag{3.21}$$

Constraint (3.22) limits the mass flow rate that can be inserted into the network, based on the installed chiller capacity.

$$G_{centr}^{t} * c_p * \Delta t \leq Q_{centr} \qquad \forall t \in \Theta \tag{3.22}$$

Pressure constraints

Pressure constraints are needed to take into account the pressure drops in the network. Constraint (3.23) forces, for every selected edge, the pressure difference between the

entry and the exit node to be equal to the pressure drop. For the non selected edges, the equation is identically null.

$$p^t_j * z_{ij} - p^t_i * z_{ij} + \Delta P^t_{ij} = 0 \qquad \forall (i,j) \in E, t \in \Theta \tag{3.23}$$

Constraints (3.24)-(3.25) ensure that the pressure of a connected node is within the defined bounds. At the same time, if the node is not connected to the network the constraints force its pressure to be null.

$$p_{min} * \sum_{i}^{V_j^-} z_{ij} \leq p^t_j \qquad \forall t \in \Theta, j \in Ut \cup S \tag{3.24}$$

$$p^t_j \leq p_{max} * \sum_{i}^{V_j^-} z_{ij} \qquad \forall t \in \Theta, j \in Ut \cup S \tag{3.25}$$

Constraint (3.26) defines the inverse of the fluid dynamic resistance per unit of mass flow rate as a function of the selected diameter. Since the pressure drops of the supply and return line are modelled together, the inverse of fluid dynamic resistance is considered halved on each edge.

$$Y_{ij} - \sum_{m}^{M} x^m_{ij} \frac{\rho * \pi^2 * D^{m4}/16}{f^m * L_{ij}/D^m + \beta_{ij}} = 0 \qquad \forall (i,j) \in E \tag{3.26}$$

Constraint (3.27) defines the non-linear relation between mass flow rates and pressure drops.

$$\Delta P^t_{ij} = {G^t_{ij}}^2 / Y_{ij} \qquad \forall (i,j) \in E \tag{3.27}$$

3.2.4 Linearization

The model as it is defined is non-linear, since both cost function and some constraints are non-linear. In particular, the non linear terms are:

- the pumping costs defined in (3.9);
- the products between pressure and binary variables in (3.23);

- the relation between pressure drop, fluid dynamic resistance and mass flow rate in (3.27).

Linearization of pressure balance equation

To linearize the products between pressure and binary variables it is used the method based on reformulation linearization technique (RLT), developed by Khir, Al-Noaimi and Haouari [73, 74]. The first step consists in introducing additional variables called o^t_{ij}, which represent the pressure on the entry node of a generic edge, if that edge is selected.

$$o^t_{ij} = p^t_i * z_{ij} \qquad \forall (i,j) \in E, t \in \Theta \tag{3.28}$$

In addition, the following constraints are also added to linearize (3.28) and to reformulate the equation (3.23).

$$\sum_i^{V_j^-} o^t_{ij} - p^t_j - \sum_i^{V_j^-} \Delta p_{ij} = 0 \qquad \forall j \in Ut, t \in \Theta \tag{3.29}$$

$$\sum_i^{V_j^-} o^t_{ij} - p^t_j - \sum_i^{V_j^-} \Delta p_{ij} \leq 0 \qquad \forall j \in S, t \in \Theta \tag{3.30}$$

$$o^t_{ij} + o^t_{ji} - p^t_j - \sum_i^{V_j^-} \Delta p^t_{ij} \leq 0 \qquad \forall (i,j) \in E, t \in \Theta \tag{3.31}$$

$$o^t_{ij} + o^t_{ji} - p^t_j - \sum_i^{V_j^-} \Delta p^t_{ij} - p_{max} * z_{ij} - p_{max} * z_{ji} \leq -p_{max} \qquad \forall (i,j) \in E, t \in \Theta \tag{3.32}$$

$$o^t_{jk} - o^t_{ij} - \sum_i^{V_j^-} \Delta p^t_{ij} \geq 0 \qquad \forall j \in Ut \cup S, k \in V_j^+, t \in \Theta \tag{3.33}$$

$$o_{ij}^t + \sum_{i}^{V_j^-} \Delta p_{ij}^t - \sum_{k}^{V_j^+} o_{jk}^t \leq 0 \qquad \forall (i,j) \in E, t \in \Theta \tag{3.34}$$

$$o_{ij}^t \leq p_{max} * z_{ij} \qquad \forall (i,j) \in E, t \in \Theta \tag{3.35}$$

$$o_{ij}^t \geq p_{min} * z_{ij} \qquad \forall (i,j) \in E, t \in \Theta \tag{3.36}$$

Moreover, constraints (3.37)-(3.40) are introduced to linearize the product between p_{centr}^t and $z_{centr,k}$ variables. If $z_{centr,k}$ is equal to zero, $o_{centr,k}^t$ would result equal to zero, due to constraints (3.37) and (3.39). On the other hand, if $z_{centr,k}$ is equal to one, $o_{centr,k}^t$ would be equal to p_{centr}^t, due to constraints (3.38) and (3.40).

$$o_{centr,k}^t \geq p_{min} * z_{centr,k} \qquad \forall k \in V_{centr}^+, t \in \Theta \tag{3.37}$$

$$o_{centr,k}^t \geq p_{max} * z_{centr,k} + p_{centr}^t - p_{max} \qquad \forall k \in V_{centr}^+, t \in \Theta \tag{3.38}$$

$$o_{centr,k}^t \leq p_{max} * z_{centr,k} \qquad \forall k \in V_{centr}^+, t \in \Theta \tag{3.39}$$

$$o_{centr,k}^t \leq p_{min} * z_{centr,k} + p_{centr}^t - p_{min} \qquad \forall k \in V_{centr}^+, t \in \Theta \tag{3.40}$$

Linearization of pumping cost

The pumping cost depends on the product of two variables: the pressure on the plant site and the mass flow rate entering into the network. To linearize this term, the reformulation linearization technique has been applied to the mass balance equations. In particular, the following equation is the linear combination of the mass balance constraints, which holds true if those constraints are not violated. The equation indeed indicates that the mass flow rate inserted into the network from the central plant is equal to the sum of the mass flow rates required by the users connected to the network. This is equal to the difference between the sum of the mass flow rates required by all users and the sum of the mass flow rates required by the buildings not

connected to the network.

$$G^t_{centr} + \sum_j^{Ut} y_j * G^t_{ext,j} = \sum_j^{Ut} G^t_{ext,j} \qquad \forall t \in \Theta \tag{3.41}$$

By multiplying all terms of the equation (3.41) by the pressure at the plant node, it is obtained the following equation, which is not violated if the mass balances are respected.

$$G^t_{centr} * p^t_{centr} + \sum_j^{Ut} y_j * G^t_{ext,j} * p^t_{centr} - \sum_j^{Ut} G^t_{ext,j} * p^t_{centr} = 0 \qquad \forall t \in \Theta \tag{3.42}$$

This equation includes two non-linearities: the products $G^t_{centr} * p^t_{centr}$ and $y_j * p^t_{centr}$. The first is also the term needed to compute the pumping cost in (3.9). Two new sets of variables are therefore introduced in the model to linearize these terms.

$$Gp^t_{centr} = G^t_{centr} * p^t_{centr} \qquad \forall t \in \Theta \tag{3.43}$$

$$p^t_{centr,j} = y_j * p^t_{centr} \qquad \forall j \in Ut, t \in \Theta \tag{3.44}$$

To guarantee that (3.44) holds true, additional McCormick constraints (3.45)- (3.48) shall be introduced to linearize the product between binary and continuous variables.

$$p^t_{centr,j} \geq p_{min} * y_j \qquad \forall j \in Ut, t \in \Theta \tag{3.45}$$

$$p^t_{centr,j} \geq p_{max} * y_j + p^t_{centr} - p_{max} \qquad \forall j \in Ut, t \in \Theta \tag{3.46}$$

$$p^t_{centr,j} \leq p_{max} * y_j \qquad \forall j \in Ut, t \in \Theta \tag{3.47}$$

$$p^t_{centr,j} \leq p_{min} * y_j + p^t_{centr} - p_{min} \qquad \forall j \in Ut, t \in \Theta \tag{3.48}$$

By ensuring that eq. (3.44) holds true, it is also guaranteed the validity of eq. (3.43), thanks to constraint (3.42), which is reformulated using the new auxiliary variables in eq. (3.49)

$$Gp^t_{centr} + \sum_j^{C} G_{ext} * p^t_{centr,j} - \sum_j^{C} G_{ext,j} * p^t_{centr} = 0 \qquad \forall t \in \Theta \tag{3.49}$$

Linearization of pressure drops

The pressure drop on network branches depend on the square of mass flow rates and on the inverse of fluid dynamic resistance. The non linearity has therefore the form $x1^2/x2$, which is convex for $x2 > 0$. As a consequence, it can be linearized using the cutting plane method [94]. It consists in solving the problem iteratively as a MILP and to add new constraints after each iteration. The method takes advantage of the property of convex functions of being always larger than their first order Taylor series approximations. The new constraints, introduced after each iteration, ensure that the function is greater or equal to its Taylor series approximation, based on the results of the last iteration. The convergence is reached, when the difference between the effective pressure drops and the ones found by the solver is below a certain tolerance. A flow-chart of the method is shown in Figure 3.3. Eq. (3.50) shows the constraints that are introduced after each iteration. The right hand side represents the Taylor series approximation of ${G_{ij}^t}^2/Y_{ij}$ where the upscript $'$ refers to the solution of the last iteration.

$$\Delta p_{ij}^t \geq 2 * G_{ij}^t * \frac{G_{ij}^{t'}}{Y_{ij}'} - \frac{{G_{ij}^{t'}}^2}{{Y_{ij}'}^2} * Y_{ij} \qquad \forall (i,j) \in E, t \in \Theta \tag{3.50}$$

3.2.5 Fixed velocity MILP formulation

A modified version of this model has also been implemented and assessed. The original MILP model as it is defined can be characterized by thousands of variables, depending on the size of the problem. Consequently, in the case of more complex networks the problem may become intractable under the computational point of view.

It was therefore decided to limit the freedom in the choices of some variables using some common rules of thumbs in the field of district heating and cooling.

In the original model the only constraint that limits the choice of the diameters is that the mass flow rate, hence the velocity, should not exceed a certain value. Therefore for a certain peak mass flow rate, there is only a lower boundary for the choice of the diameter. In the modified version of the MILP new constraints have been therefore

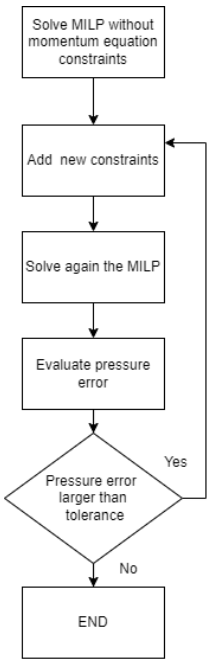

Fig. 3.3 Flow-chart of cutting plane method

introduced in order to automatically fix the choice of diameter for every selected peak mass flow rate.

This was done by imposing a fixed range of peak velocity for every diameter. This means that the maximum velocity in each diameter should be as much as possible close to a chosen value. In particular, in district heating and cooling applications, common practice and pipes constructors suggest as a trade-off between installation costs, pipe corrosion and pumping costs, peak velocities of about 1.5 m/s for diameters smaller than 250 mm and 2.5 m/s for larger diameters. Therefore these reference values have been considered in the modified version of the MILP.

Fixing a range of maximum velocity is equivalent to fix an interval of peak mass flow rate for every diameter, which means that for every peak mass flow rate, only one pipe size is feasible. Therefore the decision variables are dependant on each other and the feasibility domain is reduced, guaranteeing a faster convergence to the solution. On the other hand, due to this assumption, the solution might be slightly worse than in the original case.

3.3 Heuristic approach

The model previously defined is accurate in the search of the optimum, but it is highly expensive under the computational point of view. Since piping cost is among the most relevant in a district cooling network, the minimum spanning tree (MST) heuristic [76, 77] can be a valid alternative to Mixed Integer Programming for larger networks.

The minimum spanning tree is a subset of edges that connects all the nodes, without any loops and with the minimum total length.

The approach here proposed is a combination of the MST heuristic and a genetic algorithm. The decision variables of the genetic algorithm are the y_j variables of the MILP model, hence binary variables that tell whether the users are connected or not to the network. The minimum spanning tree that connects the selected users is evaluated inside the fitness function of the genetic algorithm. Given the network topology it is possible to directly compute the mass flow rates by solving the system of continuity equations (3.51).

$$A * G^t + G^t_{ext} = 0 \qquad \forall t \in \Theta \tag{3.51}$$

where A represents the incidence matrix of the graph, G^t is the vector of mass flow rates flowing in each pipe at time t and G^t_{ext} is the vector of inserted/extracted mass flow rates. For convention, it is assumed that inserted mass flow rates have negative values.

The pipe diameters are determined after the evaluation of the mass flow rates, by fixing a maximum velocity v_{max} through the following formula:

$$D_{ij} = \sqrt{\frac{\max_{t\in\Theta} G^t_{ij} * 4}{v_{max} * \pi * \rho}} \qquad \forall (i,j) \in E \tag{3.52}$$

It is then selected the closest commercial diameter to the one found with eq. (3.52).

3.3.1 Graph clustering

The implemented heuristic model may be suitable for networks with few users, but in case of more complex networks it could converge to suboptimal solutions. In

addition, the genetic algorithm changes the values of the variables in a stochastic way, without taking into account the distances between the users.

One would presume that two users close to each other are either both independent or both connected to the network. The method has been therefore modified for larger networks by clustering the users in function of their position in the graph. The k-minimum spanning tree algorithm [95] has been implemented for this scope. This method is based on the following steps, also shown in Figure 3.4:

- Evaluation of the minimum spanning tree
- elimination of the k-1 longest edges
- extraction of the k disconnected subgraphs, which represent the clusters

In the improved heuristic approach, the users are firstly grouped in clusters and the genetic algorithm is applied considering the whole clusters as the variables instead of the single users. The solution obtained is used as a member of the initial population of the algorithm where the variables are not clustered. By using this approach the clustered algorithm is used to explore the space of the optimum search, while the non-clustered algorithm is used for local search. The steps of the improved heuristic approach are summarized in 3.5.

3.4 Basic approach

In order to estimate the impact of the optimization provided by the two approaches a basic one has also been defined. The procedure has a computational cost almost null. It is based on the following steps:

- the objective function is computed when all nodes are connected to the network
- the objective function is re-evaluated continuously by gradually disconnecting the users, starting from the most distant from the central
- the solution with the lowest objective function is selected.

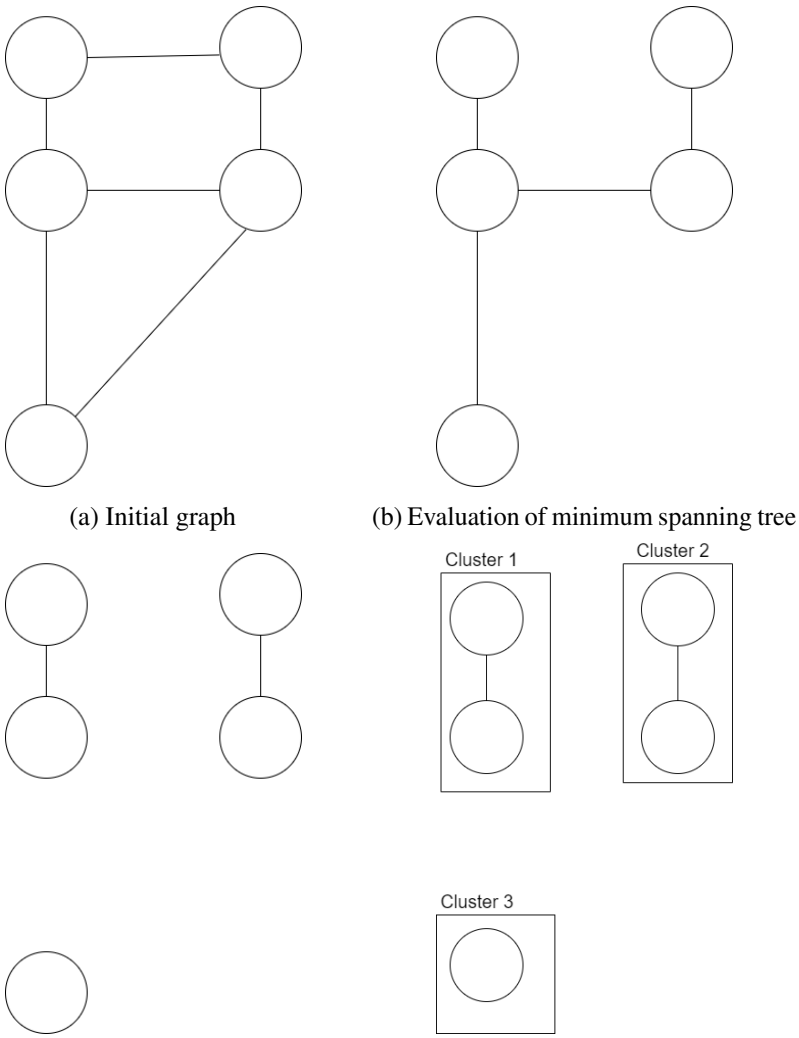

(a) Initial graph (b) Evaluation of minimum spanning tree

(c) Elimination of k-1 longest edges (d) Extraction of k clusters

Fig. 3.4 Representation of k-minimum spanning tree algorithm for k=3

3.5 Case studies

The models have been applied to three different case studies: a small network with few potential users and two larger networks with many potential users. Some of the parameters are common, while others depend on the specific case study. Table 3.4 shows the values of the parameters that the cases have in common, while Table 3.5 reports the set of commercial diameters and their relative investment costs, which are also the same for both case studies. Lastly, the costs for different sizes of energy transfer stations are reported in Table 3.6.

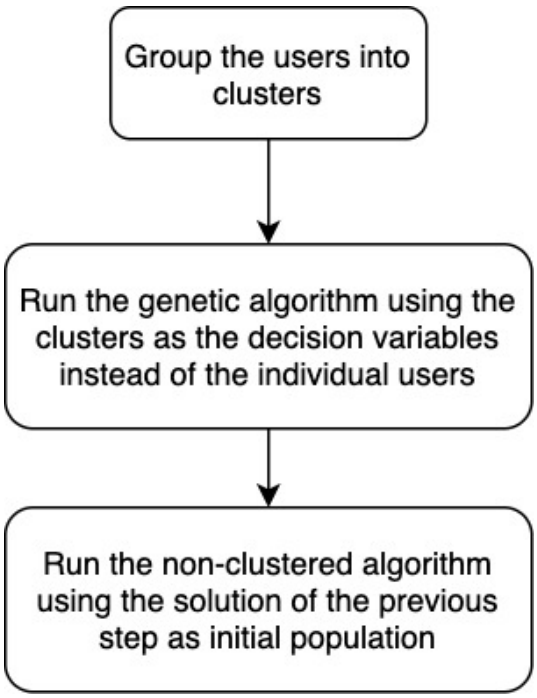

Fig. 3.5 Flowchart of the improved heuristic approach

ΔT	5°C
η_{pump}	80%
EER_{DC}	4.5
EER_{ind}	2.7
$c_{op,chill,DC}$	0.07 €/kWh
$c_{op,chill,ind}$	0.05 €/kWh
r	5%
N	30 y
p_{min}	$2 * 10^5$ Pa
p_{max}	$2 * 10^6$ Pa

Table 3.4 Values of main parameters equal for all the three case studies

3.5.1 Case study A: Small network case study

The first case study is characterised by a graph of 29 edges and 27 nodes, where 14 are user nodes, one is a production node and the other 12 are Steiner nodes (Figure 3.6). Every user node has a defined peak demand and the profile depends on the building category. There are 3 schools, 4 residential buildings, 3 industries and 4

D^m [mm]	Cost [€/m]
25	53.28
32	55.92
40	56.2
50	60.00
65	64.88
80	72.39
100	83.58
125	95.55
150	106.02
200	136.47
250	176.78
300	213.65
350	253.68
400	294.09
450	333.98
500	426.65
600	536.68
700	661.10
800	766.31

Table 3.5 Set of commercial diameters and costs per unit of length

Size [kW]	10	100	200	300	500	1000
Cost [k€]	5.4	44	55	65	79	108

Table 3.6 Cost for different sizes of energy transfer stations

shops. The profiles of the different building categories are shown in Figure 3.7, while their demand peaks are shown in Table 3.7.

3.5.2 Case study B: large network

The second case study is a distribution network of an Italian district heating system, where the heating demand is assumed as reference for the cooling load. The original subnetwork is tree-shaped, but four additional edges have been added in order to consider an initial graph with four loops. The graph is represented in Figure 3.8 and has 189 nodes, 58 users, 192 edges and one central plant. Three time steps are considered, assuming the demand as the mean value every eight hours. This assumption is based on the idea that the demand profile can be grouped in three time

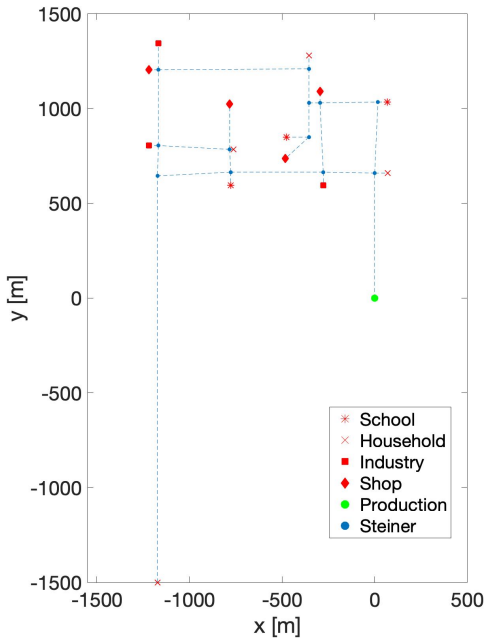

Fig. 3.6 Initial layout of the Case Study A

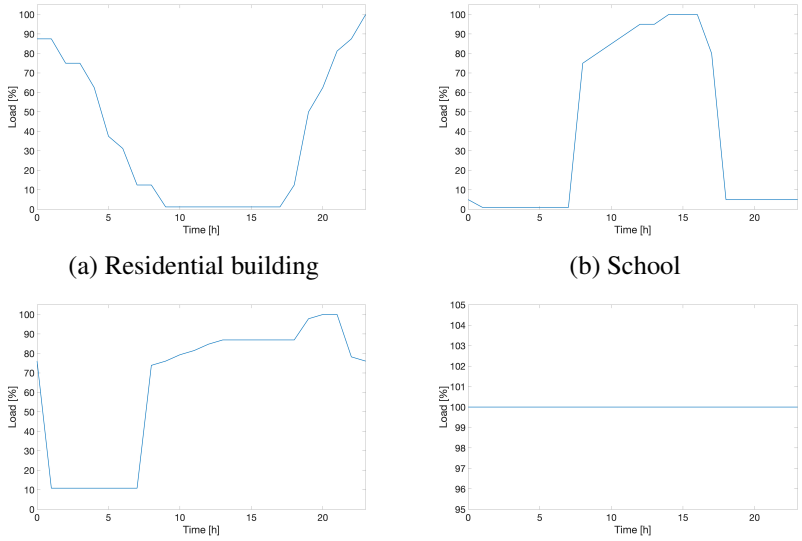

(a) Residential building

(b) School

(c) Shop

(d) Industry

Fig. 3.7 Case Study A: Load profile of the different building categories [96, 10]

slots: morning, afternoon and night. The demand is therefore considered constant along each of these time slots. For case study A, solving the standard MILP model proved to be at least 5 times more computationally expensive, providing results less than 1% more accurate compared to the other models. As a consequence, to solve

Node	Building category	Coordinates (x [m], y [m])	Peak load [kW]
8	Industry	(-1167.5, 1345)	550
13	Shop	(-481.9, 736.9)	640
14	School	(-475, 850)	750
15	Household	(-1172.5, -1500)	720
17	Shop	(-782.5, 1025)	1830
19	Household	(70, 660)	360
20	Industry	(-277.5, 595)	1320
21	Shop	(-295, 1090)	840
22	School	(-777.5, 595)	90
23	Household	(-762.5, 785)	1350
24	Industry	(-1217.5, 804)	1640
25	Shop	(-1217.5, 1205)	710
26	School	(67.5, 1035)	440
27	Household	(-355, 1280)	660

Table 3.7 Peak load and category of the buildings for case study A

case study B only the fixed-velocity MILP and the heuristic approaches have been used.

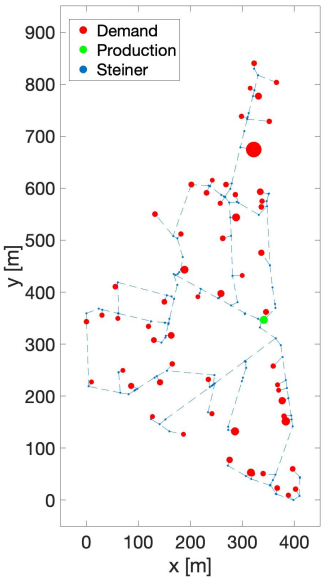

Fig. 3.8 Initial layout of the Case Study B

3.5.3 Case study C: network with multiple loops

The third case study is also a distribution network of an Italian district heating system. In this case, the original structure is completely different from the first two case studies. The topology of the network follows a Roman plant route and there are multiple loops, that can make the topology optimization more complex. The graph is shown in Fig. 3.9 and it is characterized by 99 branches and 92 nodes, whose 40 are users, 58 are Steiner nodes and one is a production node. The peaks of demand requested by the users range between 127 and 320 kW. Also in this case three time instances are considered and the problem is solved by means of the fixed-velocity MILP, the heuristic and the improved heuristic approaches

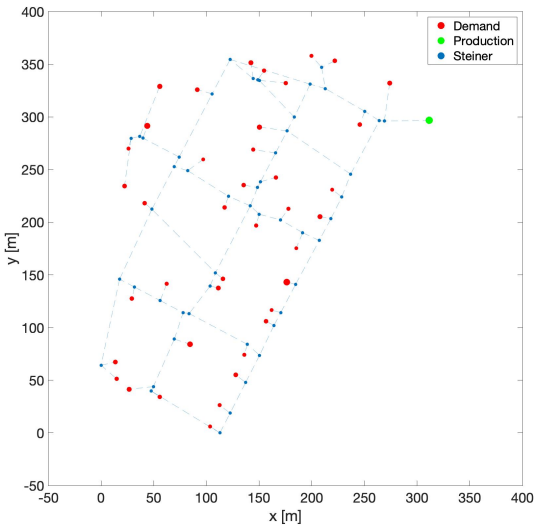

Fig. 3.9 Initial network layout of the Case Study C

3.6 Results

3.6.1 Case study A

The first case study has been solved by using three models: the standard MILP, the fixed- velocity MILP and the heuristic approach.

Standard MILP

The standard MILP model applied to the case study A is characterised by 6441 variables, of which 1174 are binary. It has been solved using the solver Gurobi, taking 20 minutes to converge with the CPU Intel i7 2.2 GHz Quad-Core.

In Figure 3.10a the resulting optimal layout is shown. Dashed lines represent pipes not connected to the network, while the continuous ones are the selected pipelines. Moreover the thickness of the branches is proportional to the pipes diameters. As it could be expected, the users far from the central chiller should not be connected to the network, because the pumping and investment costs would be too large. On these nodes, conventional technologies are therefore preferred even if they are characterised by lower performances.

Furthermore, the figure reports the maximum velocity reached on each pipe. Pipes closer to the plant have a higher maximum velocity, while in the peripherical pipes far from the production site the maximum velocity is lower. The reason is that the diameters should be large enough so that the mass flow rate can be supplied downstream. In the pipes farther from the station, larger diameters are needed, while in the closer pipes, lower diameters can be installed. Consequently on these pipes, smaller diameter sizes are chosen in order to minimize the investment costs, achieving larger velocities.

Figure 3.11 shows the scatter plot of pipe maximum velocity and the relative diameters. There is no clear correlation between diameters and maximum velocity. In fact, the optimal choice of the diameters depends on other factors such as the demand profiles and the distances from the production node.

Fixed velocity MILP

In Figure 3.10b the resulting optimal layout is shown with the relative maximum velocities and pipe sizes. The layout does not differ from the one obtained with the first model, although the selected diameters are different. In this case, the solver took less than 400 s to converge. The computational time is therefore about one third of the one of the original model. Moreover the differences in terms of cost function are less than 1%, as shown in Figure 3.12.

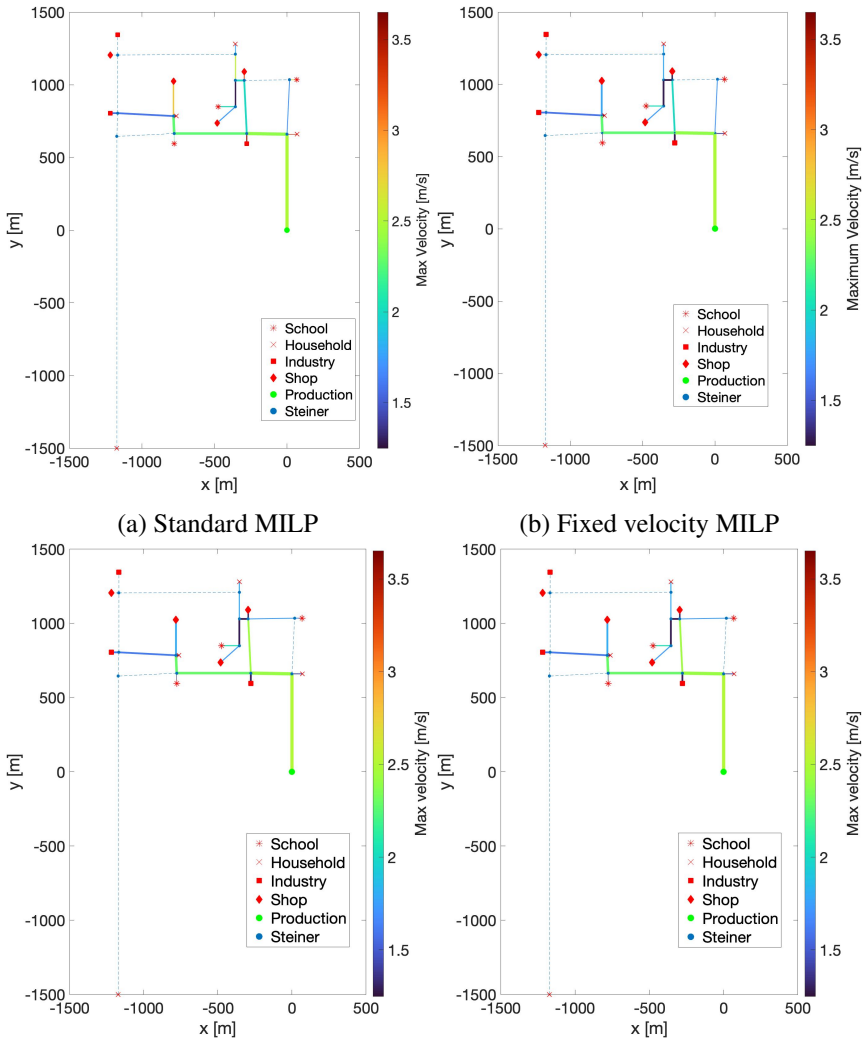

(a) Standard MILP

(b) Fixed velocity MILP

(c) Heuristic

(d) Basic approach

Fig. 3.10 Case Study A: Optimal layout according to the different approaches

In Figure 3.11 the maximum velocities and the relative diameters are plotted. The velocity, for the modified model tends to be smaller, especially for the small diameters.

Heuristic

The problem was solved using the genetic algorithm function of Matlab® and it took 36 seconds to converge. However, the resulting layout shown in Figure 3.10c is slightly different from the one of the two previous solutions, due to the use of the minimum spanning tree heuristic.

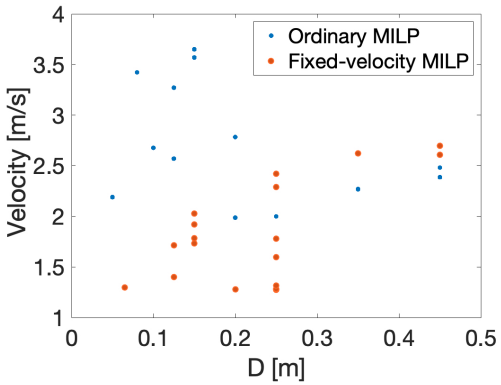

Fig. 3.11 Case study A: scatter plot reporting the relation between pipe diameter and maximum velocity

Basic approach

Figure 3.10d reports the resulting network obtained with the *basic approach*. This solution is equal to the one found by the heuristic method.

Comparison and discussion

Figure 3.12 shows a comparison of the results obtained with the different models. The standard MILP proved to be the most accurate model, since the value of objective function is the smallest one. The topology of the networks found by the two MILP and the heuristic solvers differ by how the school with coordinates (67.5,1035) is connected. This is due to the minimum spanning tree assumption present in the heuristic solver, which selects the topology by just minimizing the total length of the network. On the other hand, the MILP solver optimizes the topology and users to be connected simultaneously, without the minimum spanning tree assumption.

Concerning the fixed-velocity MILP, the topology structure is the same of the standard MILP, while only the diameters are different. The costs obtained with the fixed velocity MILP and the heuristic model are only less than 1% larger than the standard MILP. On the other hand, the differences among the models are quite evident in terms of computational time, since the standard MILP took about 20 minutes to converge, while the fixed- velocity MILP took about 4 minutes and the heuristic took only 36 seconds. The computational time therefore decreased by 82% and 97% in the two cases, respectively.

The solution obtained with the *basic approach* is equal to the one achieved with the heuristic, therefore the savings associated with the optimization are null for this case study. However, if the standard MILP model is used, it could be possible to save 0.66% of the total life-cycle cost.

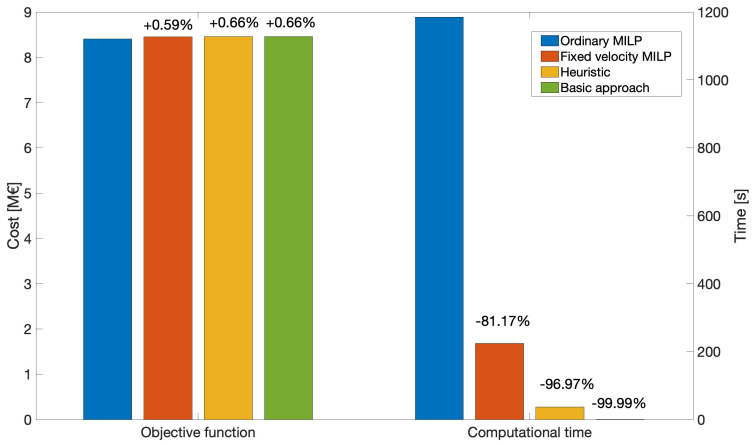

Fig. 3.12 Case Study A: Comparison of the results obtained by the different approaches in terms of objective value and computational time

3.6.2 Case study B

Due to the dimension of the network and the large number of nodes and edges, solving the case study B with the standard MILP would have been infeasible under the computational point of view. Therefore the second case study has been solved only with the fixed velocity MILP, the heuristic and improved heuristic approaches.

Fixed velocity MILP

The model is characterised by 13862 variables, of which 8890 are binary and 4972 are continuous. The solver took 2h 36' to find the optimal solution. The results are shown in Figure 3.13a. According to the solution, only 33 users should be connected to the network, while for the remaining 25, it would be more convenient to install independent chillers.

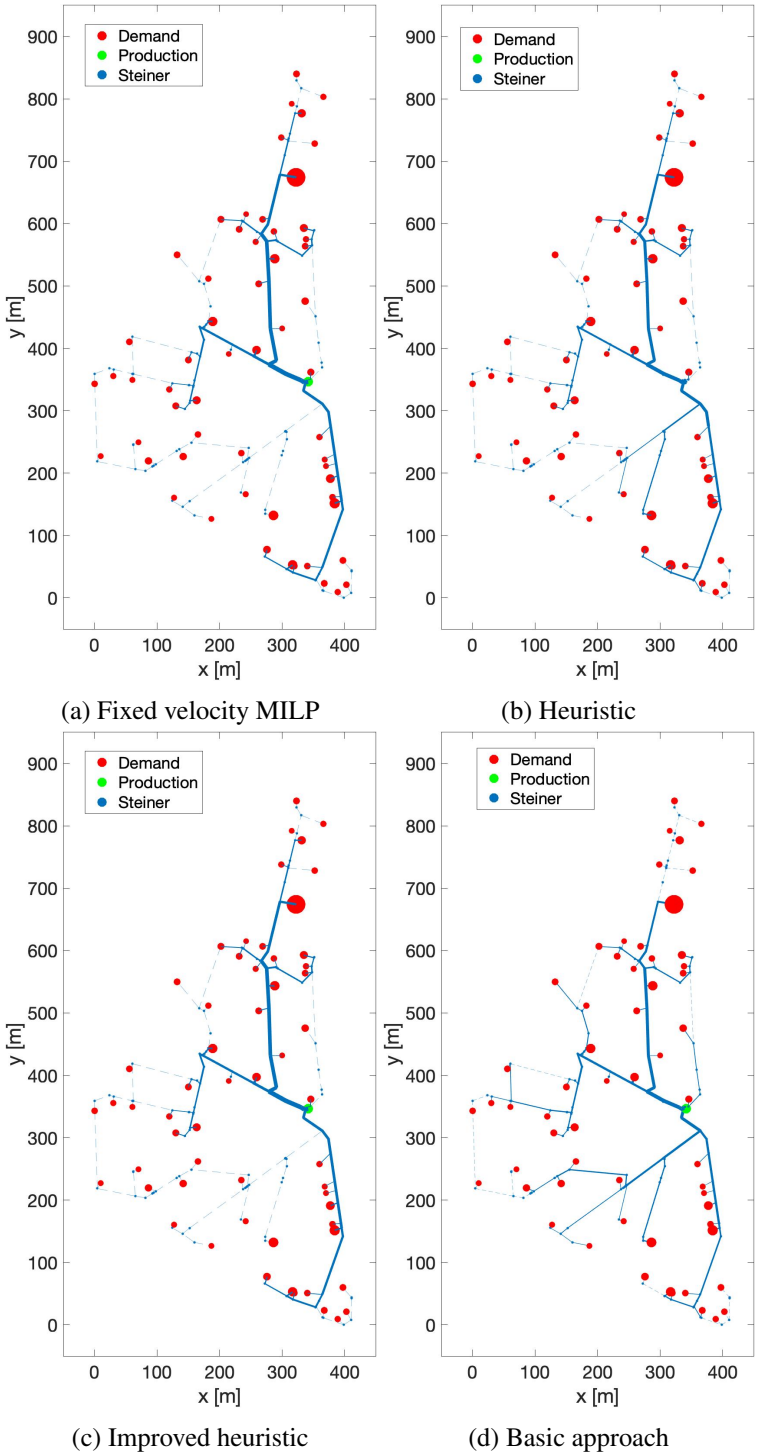

(a) Fixed velocity MILP

(b) Heuristic

(c) Improved heuristic

(d) Basic approach

Fig. 3.13 Case Study B: Optimal layout obtained by the different approaches

Heuristic

The genetic algorithm took only 60 s to converge and the resulting topology is shown in Figure 3.13b. In this case the number of users connected to the network is 37. The

solution is indeed slightly different from the one obtained by the MILP, since the genetic algorithm reached a local optimum and therefore converged to a suboptimal solution.

Improved heuristic

The improved heuristic approach was implemented to facilitate the convergence of the genetic algorithm to the global optimum. The users have been grouped in 30 different clusters (Figure 3.14) using the k-minimum spanning tree method. The

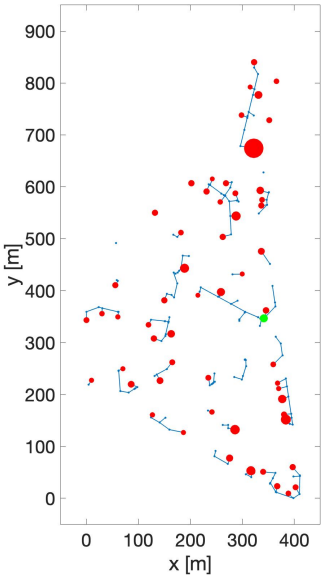

Fig. 3.14 Resulting clusters obtained through the k-spanning tree algorithm

optimal layout found by the improved heuristic approach is shown in Figure 3.13c. The model took a total of 257 s to converge. In particular, the first part, where the genetic algorithm is applied considering the clusters as the decision variables, took 54 seconds. The second part, where the genetic algorithm is solved considering the single users as the decision variables, took 203 seconds.

Basic approach

In Figure 3.13d it is shown the network that would be designed using the *basic approach*. The number of users connected would be 45, hence much larger with respect to the two optimization models.

Model	Users connected	Cost [M€]	Time [s]
Fixed-velocity MILP	33	2.8527	9410
Heuristic	37	2.8756	60
Improved heuristic	33	2.8527	257
Basic approach	45	2.9429	0.39

Table 3.8 Results for Case Study B

Comparison and discussion

In Figure 3.15 and in Table 3.8 the main results obtained by the three models for the Case Study B are reported in terms of number of connected users, objective function and computational time. Moreover they are compared with the layout obtained through the *basic approach*.

The solutions of the MILP and the improved heuristic approaches coincide, since the results in terms of users connected and value of the objective function are equal. On the other hand, the MILP took more than two hours and half to converge. The improved heuristic approach therefore proved to be as accurate as the MILP in this specific case, but much less computationally expensive.

The smallest computational time is observed in the standard heuristic, but it converges to a suboptimal solution. The difference in terms of objective function with the improved heuristic is only about 0.8%, but the users connected to the network are about 12% more. Since the demand of these additional users is small compared to the network, the objective function is only slightly affected. This proves that an heuristic approach as the minimum spanning tree coupled with a genetic algorithm can be a feasible alternative to a MILP if there is a large number of variables, but it can lead to a local optimum, as in this case. The clustering approach solved the problem of early convergence, since the solution found by improved heuristic approach is equal to the one found by the MILP model, hence the global optimum.

Consequently for complex networks with a large number of users, the improved heuristic approach is the most indicated for the good compromise between precision and computational cost. The solution suggested by the *basic approach* is different from the ones found by the solvers and the relative objective function is equal to 2.94 M€. As a consequence, by adopting a *basic approach* instead of an optimization tool, the total life-time cost would be 3.16% larger.

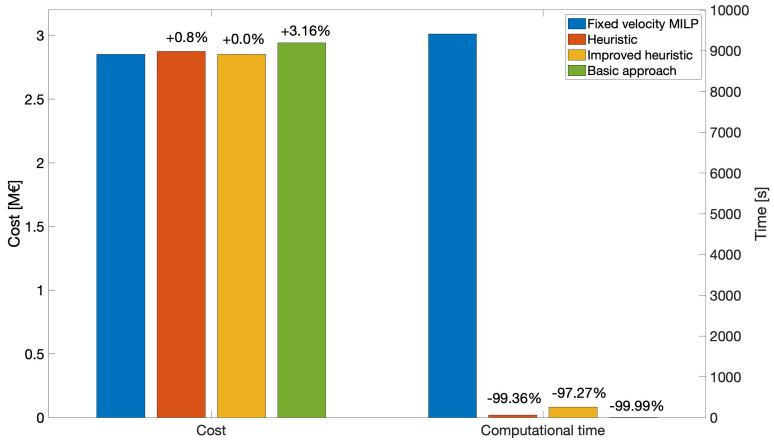

Fig. 3.15 Case study B: Comparison of the results obtained by the different approaches in terms of objective value and computational time

3.6.3 Case Study C

This case study has been solved with the fixed velocity MILP and the heuristic approaches and the results have been compared with the ones obtained through the basic approach.

Fixed velocity MILP

The model is characterised by 7175 variables, of which 4594 are binary and 2581 continuous. The solver took 37 minutes to converge. The results are shown in Figure 3.16a. According to the solution, all the potential users should be connected to the network.

Heuristic

The heuristic approach took 39 seconds to converge to the optimal solution. The relative optimal solution is shown in Figure 3.16b. In this case the users connected are 37, therefore only three users are disconnected from the network.

Improved heuristic

The improved heuristic took 73 seconds to converge and the optimal network is shown in Figure 3.16c. The solution is the same of the standard heuristic model.

Basic approach

Figure 3.16d shows the solution that would be selected with the basic approach is shown. The number of connected users would be 38/40, therefore only two users would be disconnected.

Comparison and discussion

In Figure 3.17 the results obtained by the different models have been compared in terms of objective function and computational time. The optimal network obtained with the heuristic model is slightly different from the one found by the MILP model. This is due to the fact that in the heuristic model the topology of the network is selected by considering only minimum spanning trees, while in the MILP algorithm more possibilities are taken into account. Moreover, in the heuristic approach, the minimum spanning tree is evaluated by connecting all the nodes, except from the excluded users. However, this means that the Steiner nodes should be connected, even if they are not necessary. They are excluded from the network only after the mass flow rates in every pipe are evaluated. If the pipes connecting a Steiner node are characterised by a null peak mass flow rate, the pipes and the nodes are eliminated from the network. This optimization scheme may have an impact on the solution, depending on how Steiner nodes are displaced in the original network. In this case, the optimal solution found by the MILP is not a minimum spanning tree and the optimum found by the heuristic algorithm is characterised by a cost 1.29% larger.

This result highlights the impact of simultaneously optimizing the network topology and the users to be connected. On the other hand, the heuristic approach took about 98% less time to converge. As a consequence, due to the lower computational cost, for large-scale problems the heuristic approach should be preferred.

Clustering the users in this case study do not provide any improvement to the solution, since the standard heuristic algorithm converged to the same solution of the improved

heuristic algorithm. In fact, the number of users is modest in this case and the genetic algorithm does not need any particular improvement to reach the convergence.

Concerning the basic approach, in this case the solution differs by 0.43% and 1.69% compared with the heuristic and the MILP, respectively. Therefore, the impact would be significantly larger if the MILP model is used.

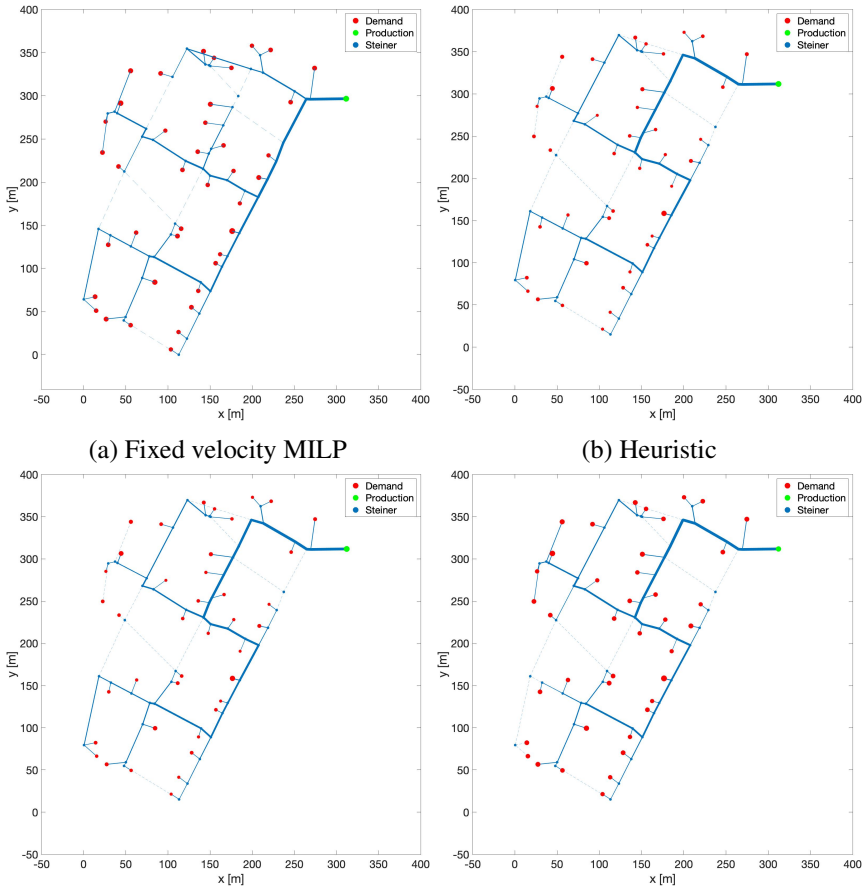

(a) Fixed velocity MILP

(b) Heuristic

(c) Improved heuristic

(d) Basic approach

Fig. 3.16 Case Study C: Optimal layout according to the approaches

3.7 Discussion and concluding remarks

The two methodologies presented in this chapter proved to effectively optimize the network layout and set of buildings to be connected, providing savings up to 3.16% compared to basic approaches that do not apply optimization tools. They therefore

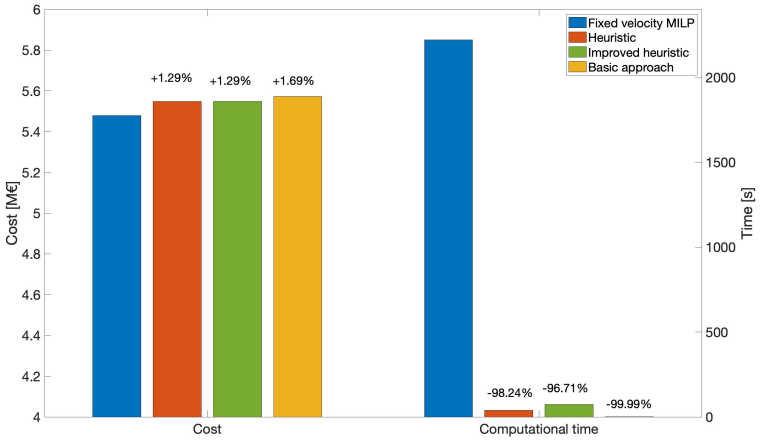

Fig. 3.17 Case Study C: Comparison of the results obtained by the different approaches in terms of objective value and computational time

Model	Users connected	Cost [M€]	Time [s]
Fixed-velocity MILP	40	5.4784	2208
Heuristic	37	5.5488	39
Improved heuristic	37	5.5488	73
Basic approach	38	5.5727	0.3

Table 3.9 Case Study C: Results in terms of number of users connected to the network, objective value and computational time

could be used by decision makers to design district cooling systems and to evaluate their potential in different urban contexts.

As expected, the MILP approach is more accurate than the heuristic one. The differences between the two approaches are visible especially in the third case study, where the heuristic provides a solution 1.16% more expensive than the one provided by the MILP model. On the other hand, the heuristic proved to be more than 90% faster.

In addition, the integration with the clustering approach proved to facilitate the convergence to the optimum. Indeed, grouping the users in clusters and considering these as the decision variables of the genetic algorithm allowed to smartly reduce the dimension of the problem.

The MILP approach shall be therefore preferred when the scale of the problem is limited, since it guarantees more precision, while the heuristic shall be adopted for large scale optimizations or multi-case simulations.

Chapter 4

Design optimization of district cooling networks under uncertainty

The content of this paper has been previously published in the following paper [97]: *Manfredi Neri, Elisa Guelpa and Vittorio Verda. "Two-stage stochastic programming for the design optimization of district cooling networks under demand and cost uncertainty" Applied Thermal Engineering 236(2024): 121594*

4.1 Introduction

The models implemented in the previous chapter allow to optimize the design of district cooling networks and the buildings to be connected, but they are based on assumptions that can be affected by uncertainty, such as the cooling demand or the cost parameters. Moreover, the literature review highlighted the lack of studies regarding the optimal planning of district cooling networks under uncertainty. In this chapter, it is therefore proposed a two-stage stochastic programming model for the design optimization of district cooling networks under demand and cost uncertainty. The goal of this model is to select the optimal initial set of buildings to connect to a district cooling network, taking into account the uncertainty of the economic parameters and the possible evolution of cooling demand. This model therefore optimizes the initial design of a district cooling network, selecting the buildings to connect and the pipe diameters, considering also the possibility to enhance the network at a second stage.

The model manages the risk of installing an oversized network, which would be economically unfeasible, in case of scenarios with lower potential of district cooling (i.e. low cooling demand or low electricity cost). At the same time, the model, considers the effect of a possible increase of district cooling potential in the future. The objective is therefore to provide a network design that can work well for the whole combination of scenarios, as a function of their probability to occur, and expand it in a second stage, if conditions are sufficiently convenient.

4.2 Two-stage stochastic programming model

The model is formulated as a two-stage stochastic programming [98]. This method treats the uncertainty in a deterministic way, by assuming that the number of possible scenarios is finite and that their probability of occurrence is known in advance. On the other hand, the values of the uncertain parameters that define the different scenarios are only revealed at a second instance in the future.

The goal of a stochastic programming algorithm is to optimize the first stage and second stage variables, minimizing the expected value of the cost function, which in this case is characterised by the sum of capital and operational expenditures. As a consequence, the stochastic programming solution is not optimal for every scenario, but it is the one that works better for the scenarios combination. The first stage variables are selected in order to guarantee robustness to the solution, while the second stage variables give flexibility to the solution. The latter, indeed also called recourse variables, remediate on the base of the scenario that occurred.

In this case, the first stage variables refer to the design decisions to be taken immediately, hence the buildings to be connected and the pipes to be installed from the beginning. On the other hand, the second stage variables refer to the future design decisions to be taken depending on the scenario that will occur. The second stage decisions therefore define how the district cooling network is expanded in each scenario.

4.2.1 General assumptions

The model has been built under the following assumptions:

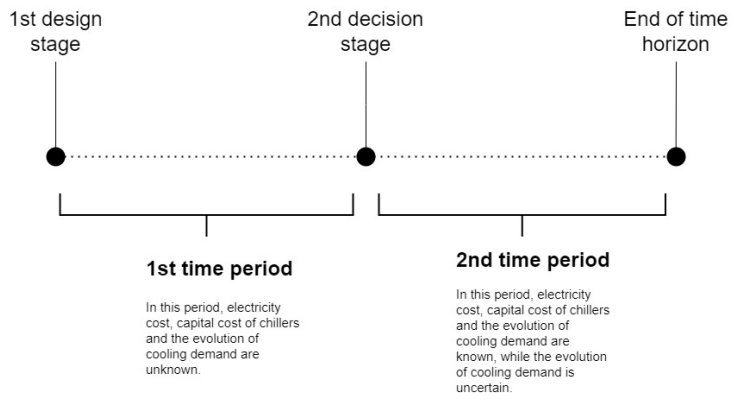

Fig. 4.1 Time horizon

- Thermal losses are neglected, due to the limited temperature difference between chilled water and the ground. Hence the difference between supply and return temperature is assumed to be constant.
- The electricity cost and the capital costs for chillers are uncertain in the first stage, but they are revealed in the second decision stage. Indeed when designing a district cooling network the capital costs for equipment are uncertain. From literature, only the ranges of these costs are known. Concerning electricity cost, this is uncertain due to the long-period considered.
- The time horizon is divided in two time periods. The first time period ranges between the first and the second decision stage, while the second time period ranges from the second decision stage to the end of the whole time horizon, as shown also in Figure 4.1
- In each time period, the cooling demand increases every year by an uncertain rate.
- In the second stage, at the end of the 1^{st} time period, the cost of chillers, the electricity price and the increase rate of cooling demand over the 1^{st} time period are known. However, the increase rate of cooling demand in the next time period is still uncertain.

As a consequence, in the first design stage, it is decided the initial network to be installed and the buildings to be connected immediately. At the second decision stage, the scenario of the 1st time period is revealed and new decisions are taken on

the basis of the conditions of this scenario. On the other hand, at the second decision stage, the second period scenario is still unknown. Hence, the decisions taken at the second stage should exploit the knowledge of what happened in the previous time period, but should also work well for the combination of new scenarios that can arise from then on.

4.2.2 Parameters uncertainty

The problem is characterised by different uncertain parameters. The scenarios are therefore generated by combining all possible values of all parameters. The uncertainty is present in the cost of electricity, the capital cost of chillers and the yearly increase rate of cooling demand.

Since the time horizon is divided into two periods, separated by the second decision stage, two levels of scenarios are defined, depending on when they are revealed. The first period scenarios are generated by properly combining all possible values that can be assumed by the parameters that are uncertain in the first stage.

Similarly, the second period scenarios are generated by properly combining the possible values that can be assumed by the parameters that are uncertain in the second design stage. The costs of electricity and for the installation of centralized and individual chillers are uncertain in the first stage, but they are revealed in the second stage. The increase rate of cooling demand in the first time period is also unknown and revealed in the second decision stage. On the other hand, in the second design stage it is still uncertain how the cooling demand will change within the second time period.

Cost of electricity

The cost of electricity can sensibly vary due to economical or geopolitical reasons, as observed in 2022 [99]. In this model it is assumed that it varies between 100 €/MWh and 500 €/MWh, with an average of 300 €/MWh. The motivation for these choices is that 100 €/MWh was the average price in 2021, while, the maximum monthly price observed in 2022 was 543 €/MWh [100]. Three possible values were hence considered for scenario generation, representing the average and the lower and upper bounds, as shown in Table 4.1.

Parameter	Value	Probability
Electricity cost [€/kWh]	[0.1 , 0.3 , 0.5]	[33.3%,33.3%,33.3%]
Demand increase rate [%]	[0, 3, 4]	[25%, 50%, 25%]
Capital cost of centralized chillers [€/kW]	[250 , 415 , 600]	[33.3%,33.3%,33.3%]
Capital cost of individual chillers [€/kW]	[400 , 600]	[50%, 50%]

Table 4.1 Values and probabilities for different parameters

Capital cost of chillers

The capital cost for the installation of chillers is affected by uncertainty, as it can range from 250 to 600 €/kW [101]. Moreover, the cost of manpower influences the installation cost, which therefore is dependent on the country. The model distinguishes two types of chillers: centralized and individual ones. For the first type the cost can vary between 250 and 600 €/kW, while the cost for the second type varies between 400 and 600 €/kW [101], as shown also in Table 4.1.

Yearly increase rate of cooling demand

The life-time of the system is assumed to be 30 years. This time horizon has been split in two parts in order to be able to enhance the network after the first period, depending on the scenario that shows up. Moreover, the life-time of an individual chiller is typically around 15 years, hence splitting the time horizon in two equal parts results to be a reasonable choice. In this way, if a building is equipped with an individual cooling system, the model decides whether to connect it to a district cooling system only at the end of chiller life-time.

In this model it is considered that in each of the two time periods the cooling demand increases with a fixed yearly rate, which, however, can vary from the first to the second period. The second stage decisions are taken after the scenario relative to the first period is revealed. However, the conditions of the second period are still uncertain when these decisions are taken. In particular, after the second stage decisions are taken, different scenarios may appear, depending on if and how cooling demand increases in the second time period.

For both time periods, three different increase rates were chosen with different probabilities, as shown in Table 4.1. The probability of having a yearly increase rate equal to 3% was set as the highest one. This decision was taken after having

evaluated the cooling demand in 2020 and in 2050 in residential buildings. The latter was evaluated using a tool [102] that predicts the variation of the typical meteorological year (TMY), due to climate change. From the analysis it emerged that cooling demand is expected to more than double in the next 30 years. If this demand increase follows an exponential behaviour with a fixed yearly rate, this would be about 3%. The two other values of yearly increase rate(0% and 4%) were added to take into account the uncertain nature of demand increase. It is assumed that in each time period the cooling demand increases with a constant yearly rate. However, this rate could vary between the two time periods. As an example, at first, the cooling demand could increase with a 4% ratio, but in the second time period it could remain stable. All possible evolutions of cooling demand in the two periods are reported in Figure 4.2. In thirty years the demand can therefore either remain constant or increase up to more than two times.

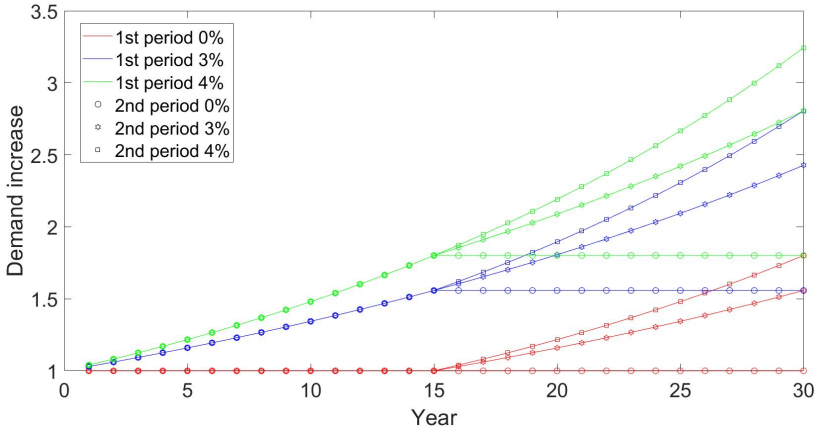

Fig. 4.2 Possible demand evolutions in the first and second time periods

Scenario generation

By combining all the possible parameter values, it results that there are 54 possible scenarios for the first time period, as shown in Figure 4.3. In the second decision stage, the only unknown parameters is the rate of increase of cooling demand. Hence, since three possible values have been considered for this parameter, each of the 54 first period scenarios can evolve in three different scenarios in the second time period. As a consequence, a total of 162 scenarios can be identified for the entire time horizon, as shown in Figure 4.4.

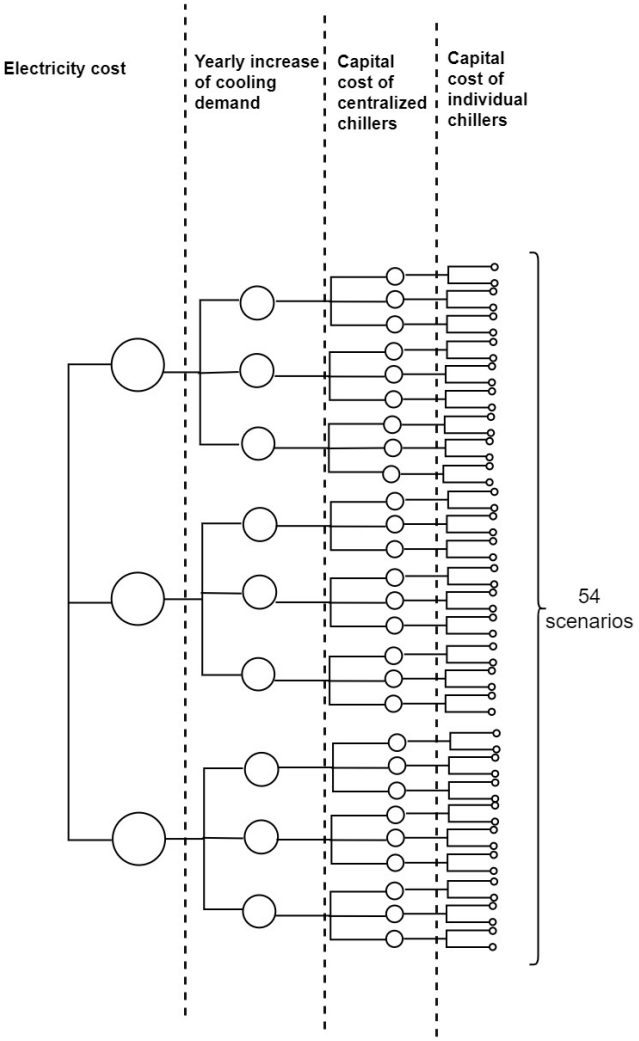

Fig. 4.3 Definition of 1st period scenarios

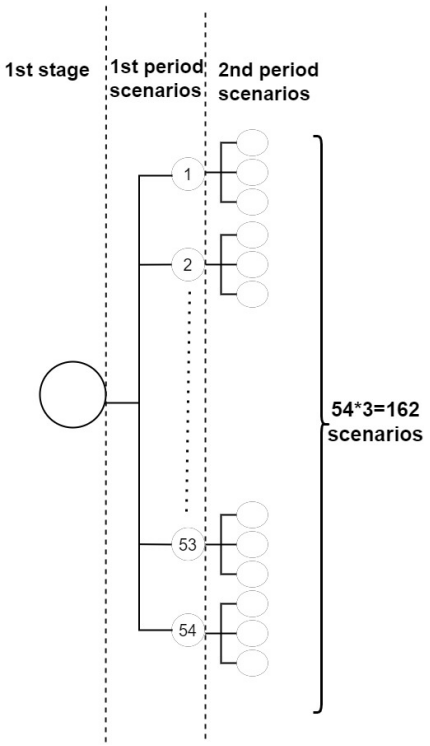

Fig. 4.4 Generation of 2^{nd} period scenarios

4.2.3 Model variables and parameters

The variables and parameters of the model are defined in Tables 4.2 and 4.3. The sets and indices used in the model equations and variables are defined in Table 4.4. The values of the input parameters used in the model are defined in Table 4.5.

4.2.4 Cost function

In a stochastic programming model the objective is to minimize the expected value of the cost function under all possible scenarios. In this case, the objective function is therefore defined as the sum of investment and operation costs in all possible scenarios, weighted by the probability of scenario occurrence.

$$Obj = Inv^{t1} + \sum_{s1}^{S1} Op^{s1} * \pi^{s1} + \sum_{s1} Inv^{t2,s1} * \pi^{s1} + \sum_{s1}^{S1}\sum_{s2}^{S2} Op^{s1,s2} * \pi^{s1} * \pi^{s2} - Assets_{value} \tag{4.1}$$

Variable	Description	Unit
G_j^{t1}	Peak mass flow rates flowing in branch j in time period $t1$	kg/s
$G_j^{t2,s1}$	Peak mass flow rates flowing in branch j in time period $t2$ after revelation of scenario $s1$	kg/s
$x_j^{m,t1}$	Binary variable that indicates if the diameter m is selected for branch j in the first time period	/
$x_j^{m,t2,s1}$	Binary variable that indicates if the diameter m is selected for branch j in the second stage for scenario $s1$	/
Y_j^{t1}	Inverse of fluid dynamic resistance per unit of mass flow rate in pipe installed in the first stage in branch j	kg*m
$Y_j^{t2,s1}$	Inverse of fluid dynamic resistance per unit of mass flow rate in pipe installed in branch j in the second stage for scenario $s1$	kg*m
$Gcentr^{t1}$	Mass flow rate flowing from centralized chiller in the first time period	kg/s
$Gcentr^{t2,s1}$	Mass flow rate flowing from centralized chiller in time period $t2$ if scenario $s1$ occurred	kg/s
$Size_{centr}^{t1}$	Capacity of centralized chiller installed in the first time period	kW
$Size_{centr}^{t2,s1}$	Capacity of centralized chiller installed in the second stage if scenario s1 occurred	kW
y_u^{t1}	Binary variable that indicates weather the user u is connected to the network in the first time period	/
$y_u^{t2,s1}$	Binary variable that indicates weather the user u is connected to the network in the second stage if scenario $s1$ occurred	/
p_i^{t1}	Relative pressure at node i in the first time period	Pa
$p_i^{t2,s1}$	Relative pressure at node i in the second time period, if scenario $s1$ occurred	Pa
up_{centr}^{t1}	Product between the variables p_{centr}^{t1} and y_u^{t1}	Pa
$up_{centr}^{t2,s1}$	Product between the variables $p_{centr}^{t2,s1}$ and $y_u^{t2,s1}$	Pa
Δp_j^{t1}	Pressure drop in branch j in the first time period	Pa
$\Delta p_j^{t2,s1}$	Pressure drop in branch j in the second time period if scenario $s1$ occurred	Pa
$GpNh^{t1}$	Product between $Gcentr^{t1}$ p_{centr}^{t1} and the initial number of full load operating hours	kg/s*Pa*h
$GpNh^{t2,s1}$	Product between $Gcentr^{t2,s1}$ $p_{centr}^{t2,s1}$ and the number of full load operating hours at the end of first time period if scenario s1 occurred	kg/s*Pa*h
$Size_{ind,u}^{t1}$	Installed capacity of individual chiller for building u in the first decision stage	kW
$Size_{ind,u}^{t2,s1}$	Installed capacity of individual chiller for building u in the second decision stage if scenario s1 occurred	kW
$z_j^{t2,s1}$	Binary variables that indicate weather a new pipe is installed in branch j in the second stage, if scenario s1 occurred	/
xz_j^{s1}	Auxiliary variable used to linearize the product between x_j^{t1} and z_j^{s1}	/

Table 4.2 Model variables

Parameter	Description	Unit
Q_u^0	Yearly cooling demand of building u at year 0	kWh
Nh_u^{t1}	Number of full load hours for building u at year 0	h
$Gext_u$	Mass flow rate requested by building u	kg/s
ρ	Water density	kg/m^3
c_p	Water specific heat	kJ/(kg*K)
L_j	Length of branch j	m
r	Discount rate	%
c_{pipe}^m	Cost per unit of pipe length, for pipes with diameter m	€/m
R_j^m	Fluid dynamic resistance per unit of mass flow rate	Pa*s^2/kg^2
π^{s1}	Probability of scenario $s1$	(%)
$incr^{s1}$	Cooling increase rate in scenario $s1$	%
c_{el}^{s1}	Electricity cost in scenario $s1$	€/kWh
$c_{chill,DC}^{s1}$	Capital cost of centralized chillers per unit of cooling power in scenario $s1$	€/kW
$c_{chill,ind}^{s1}$	Capital cost of individual chillers per unit of cooling power in scenario $s1$	€/kW
EER_{DC}	Energy efficiency ratio of centralized chillers	/
EER_{ind}	Energy efficiency ratio individual chillers	/
$c_{ETS,u}$	Capital cost of the energy transfer station in building u	€
η_{pump}	Pump efficiency	%
ΔT	Temperature difference between supply and return lines	K
p_{min}	Minimum pressure in the network	Pa

Table 4.3 Model parameters

Sets/indices	Definition
u	Generic building node
$centr$	Node of the centralized chiller
v	Generic Steiner node
j	Generic branch of the graph
m	Generic commercial pipe diameter
$s1$	Generic first period scenario
$s2$	Generic second period scenario
$t1$	First time period
$t2$	Second time period
t	Used to generalize $t1$ and $t2$
Ut	Set of building nodes
S	Set of Steiner nodes in the graph
E	Set of branches of the graph
I	Set of all nodes in the graph
M	Set of pipe diameters
Ξ_1	Set of first period scenarios
Ξ_2	Set of second period scenarios
Θ	Union of first and second time periods

Table 4.4 Definition of set and indices

Parameter	Value
EER_{DC}	6.5
EER_{ind}	2.5
η_{pump}	0.8
ΔT	7 K
p_{min}	2 bar
r	5%

Table 4.5 Values of main parameters

where Inv^{t1} refers to the investments to be taken immediately, $Inv^{t2,s1}$ refers to the cost of investments made in the second decision stage if scenario $s1$ occurred, while π^{s1} and π^{s2} are the probabilities relative to scenarios $s1$ and $s2$. The term Op^{s1} refers to the actualized operation costs relative to the first period, if scenario $s1$ appears, while $Op^{s1,s2}$ refers to the operation costs in the second period, if scenario $s2$ occurs, after the occurrence of scenario $s1$ in the first period. The term $Assets_{value}$ refers to the market value of the assets at the end of the time range. Some of the assets, indeed, are installed in a second moment, hence these will have a residual life-time at the end of the time horizon.

Investment costs

The investment costs are defined as the sum of the costs for piping, energy transfer stations and chillers.

Piping cost

Piping cost is characterised by the cost for the pipes installed in the first stage and the cost for the pipes installed in the second stage. The cost for the pipes installed from the first stage is computed as:

$$Piping^{t1} = \sum_{j}^{E} x_j^{m,t1} * c_{pipe}^{m} * L_j \tag{4.2}$$

where $x_{ij}^{t1,m}$ is a binary variable equal to 1, if the diameter m is selected for the pipe j. New pipes can be installed also at second stage, depending on the scenario. The investment cost for second stage is defined as:

$$Piping^{t2,s1} = \sum_{j}^{E} x_j^{m,t2,s1} * c_{pipe}^{m} * L_j * \frac{1}{(1+r)^{n_y/2}} \tag{4.3}$$

where r is the weighted average cost of capital, while $n_y/2$ represents the time difference in years between the first and second decision stage. These parameters are used to actualize the expenditures occurring in the second decision stage.

Energy transfer stations

The cost for energy transfer stations depends on the peak cooling demand requested

by the different buildings. This is known, as the demand peak is considered as an input of the problem. It is however unknown if a building is connected to the network or not. This cost therefore depends on the variables y_u^{t1} and $y_u^{t2,s1}$. The cost of energy transfer stations installed in the first decision stage is calculated as:

$$cost_{ETS}^{t1} = \sum_{u}^{Ut} c_{ETS,u} * y_u^{t1} \tag{4.4}$$

where $c_{ETS,u}$ is the cost to install an energy transfer station in building u. Similarly, the cost for energy transfer stations installed in the second stage is defined as:

$$cost_{ETS}^{t2,s1} = \sum_{u}^{Ut} c_{ETS,u} * y_u^{t2,s1} \frac{1}{(1+r)^{n_y/2}} \tag{4.5}$$

Chiller investment cost

The cost for a centralized chiller installed in the first stage $t1$ is calculated as:

$$Chill_{DC}^{t1} = Size_{centr}^{t1} * \sum_{s1}^{S} c_{chill,DC}^{s1} * \pi^{s1} \tag{4.6}$$

where $Size_{centr}^{t1}$ defines the capacity of the installed chiller. The terms in the sum represent the average cost per unit of installed capacity, which itself depends on the scenario. Similarly, the capital cost for chillers installed in the second stage, if the generic scenario $s1$ occurs is defined as:

$$Chill_{DC}^{t2,s1} = Size_{centr}^{t2,s1} * c_{chill,DC}^{s1} * \frac{1}{(1+r)^{n_y/2}} \tag{4.7}$$

The cost for individual chillers installed in the first and second stage is defined as:

$$Chill_{ind}^{t1} = \sum_{u}^{Ut} Size_{ind,u}^{t1} * \sum_{s1}^{S} c_{chill,ind}^{s1} * \pi^{s1} \tag{4.8}$$

$$Chill_{ind}^{t2,s1} = \sum_{u}^{Ut} Size_{ind,u}^{t2,s1} * c_{chill,ind}^{s1} \tag{4.9}$$

Operation costs

The operation costs consist in the sum of electricity expenditures to power the chillers and the pumps. They are defined as:

$$Op^{s1} = Chill^{s1}_{op,DC} + Chill^{s1}_{op,ind} + C^{s1}_{Pumping} \tag{4.10}$$

$$Op^{s1,s2} = Chill^{s1,s2}_{op,DC} + Chill^{s1,s2}_{op,ind} + C^{s1,s2}_{Pumping} \tag{4.11}$$

where:

- $Chill^{s1}_{op,DC}$ and $Chill^{s1,s2}_{op,DC}$ refer to the operating costs of the centralized chillers in the first and second time period according to scenarios $s1$ and $s2$;
- $Chill^{s1}_{op,ind}$ and $Chill^{s1,s2}_{op,ind}$ refer to the operating costs of individual chillers according to scenarios $s1$ and $s2$;
- $C^{s1}_{Pumping}$ and $C^{s1,s2}_{Pumping}$ refer to the pumping cost in the first and second time period according to scenarios $s1$ and $s2$.

Centralized chiller operation

The operating costs of the centralized chiller in the first time period depend on the connected buildings and on the yearly demand increase rate, which itself is different among the scenarios. They are therefore defined as:

$$Chill^{s1}_{op,DC} = \sum_{i=1}^{n_y/2} \sum_{u}^{Ut} y^{t1}_u * Q^0_u * (1+incr^{s1})^i * \frac{c^{s1}_{el}}{EER_{DC}} * \frac{1}{(1+r)^i} \tag{4.12}$$

where Q^0_u is the initial yearly cooling demand, while $incr^{s1}$ and c^{s1}_{el} represents the increase rate and electricity cost in scenario $s1$. Similarly, the operation costs during the second period depend on the cooling demand at the end of the first period and on the increase rate in the new time period. They are defined as:

$$\begin{aligned} Chill^{s1,s2}_{op,DC} = & \sum_{i=n_y/2+1}^{n_y} \sum_{u}^{Ut} y^{t2,s1}_u * Q^0_u * (1+incr^{s1})^{n_y/2} * (1+incr^{s2})^{i-n_y 2} \\ & * \frac{c^{s1}_{el}}{EER_{DC}} * \frac{1}{(1+r)^i} \end{aligned} \tag{4.13}$$

where the product $Q_u^0 * (1+incr^{s1})^{n_y/2}$ is the yearly cooling demand of the generic user u at the end of the first time period in scenario $s1$, while $incr^{s2}$ is the demand increase rate in the second period according to scenario $s2$.

Individual chiller operation costs

Similarly, the operation costs for individual chillers in the first and second period are evaluated as:

$$Chill_{op,ind}^{s1} = \sum_{i=1}^{n_y/2} \sum_{u}^{Ut} (1-y_u^{t1}) * Q_u^0 * (1+incr^{s1})^i * \frac{c_{el}^{s1}}{EER_{ind}} * \frac{1}{(1+r)^i} \tag{4.14}$$

$$\begin{aligned} Chill_{op,ind}^{s1,s2} = & \sum_{i=n_y/2+1}^{n_y} \sum_{u}^{Ut} (1-y_u^{t2,s1}) * Q_u^0 * (1+incr^{s1})^{n_y/2} * (1+incr^{s2})^{i-n_y/2} \\ & * \frac{c_{el}^{s1}}{EER_{ind}} * \frac{1}{(1+r)^i} \end{aligned} \tag{4.15}$$

Pumping costs

The pumping energy required to run the pumps is computed as the product between the peak pumping power and the equivalent number of full load hours. The pumping power is proportional to the product between mass flow rate and the pressure drop on the plant node. Consequently, the pumping cost of the network, which is for the first time period according to scenario $s1$ is defined as:

$$C_{pumping}^{s1} = \sum_{i=1}^{n_y/2} \frac{GpNh^{t1} * (1+incr^{s1})^i * c_{el}^{s1}}{\rho * \eta_{pump}} \tag{4.16}$$

where $GpNh^{t1}$ is the variable that defines the product between the mass flow rate at peak load, the pressure on the central node and the initial number of full load hours, while ρ and η_{pump} refer to the water density, assumed constant, and the efficiency of the pump. Similarly the pumping cost for the second time period, if scenario $s1$ occurred during the first time period and scenario $s2$ for the second one, is defined as:

$$C_{Pumping}^{s1,s2} = \sum_{i=n_y/2+1}^{n_y} \frac{GpNh^{t2,s1} * (1+incr^{s2})^{i-n_y/2} * c_{el}^{s1}}{\rho * \eta_{pump}} \tag{4.17}$$

where $GpNh^{t2,s1}$ is the variable that indicates the product between the mass flow rates at peak load and the number of full load hours at the end of the first time period according to scenario $s1$.

Residual value of the assets

The assets with a residual life-time at the end of the second time period are the pipes, the energy transfer stations and the centralized chillers installed in the second decision stage. The market value is therefore evaluated as the half of these investment cost, corrected by the actualization coefficient, as expressed in Eq. (4.18).

$$Assets_{value} = \frac{Piping^{t2,s1} + cost_{ETS}^{t2,s1} + Chill_{DC}^{t2,s1}}{2} * \frac{1}{(1+r)^{n_y/2}} \tag{4.18}$$

4.2.5 Constraints

Also this model is characterised by capacity, mass balance and pressure balance constraints. In addition, the constraints must be respected for all the possible scenarios.

Mass balance constraints

Constraints (4.19)-(4.21) ensure that mass balance is respected for chiller, user and Steiner nodes respectively.

$$\sum_{j}^{E} a_{centr,j} * G_j^{t(,s1)} + Gcentr^{t(,s1)} = 0 \qquad \forall t \in \Theta, s1 \in \Xi_1 \tag{4.19}$$

$$\sum_{j}^{E} a_{u,j} * G_j^{t1} + G_{ext,u} * y_u^{t(,s1)} = 0 \qquad \forall t \in \Theta, s1 \in \Xi_1, u \in U \tag{4.20}$$

$$\sum_{j}^{E} a_{v,j} * G_j^{t(,s1)} = 0 \qquad \forall v \in S, t \in \Theta, s1 \in \Xi_1 \tag{4.21}$$

where the apex $t(,s1)$ is used to generalize the apices $t1$ and $t2,s1$ relative to first and second stage variables. The generic term a_{ij}, present in the three equations, refers to the element of the incidence matrix that tells if the node i is an inlet or an outlet for

branch j. The subscripts $centr$, u and v refer to the index relative to the chiller node, the generic user node and the generic Steiner node.

Capacity constraints

Constraint (4.22) ensures that no more than a pipe diameter is selected for each pipe.

$$\sum_{m}^{M} x_j^{m,t(,s1)} \leq 1 \qquad \forall j \in E, t \in \Theta, s1 \in \Xi_1 \tag{4.22}$$

Constraint (4.23) defines the variable $z_j^{t2,s1}$. It is equal to one if a pipe is installed in the second stage. Otherwise, it is forced to be null.

$$\sum_{m}^{M} x_j^{m,t2,s1} = z_j^{t2,s1} \qquad \forall j \in E, t \in \Theta, s1 \in \Xi_1 \tag{4.23}$$

Constraint (4.24) indicates that in the first time period the mass flow rate in every pipe must not be larger than the maximum allowed by the selected diameter. The maximum mass flow rate indeed depends on the diameter and on the velocity limit, which is assumed equal to 1.5 m/s, coherently with ASHRAE standards [44].

$$\sum_{m}^{M} Gmax^m * x_j^{m,t1} \geq G_j^{t1} \qquad \forall j \in E \tag{4.24}$$

The capacity constraint must be respected also for the second time period variables, but two different situations may arise:

- the pipe installed in the first stage has sufficient capacity also for the additional mass flow rate that will flow in the second time period
- capacity of the pipe installed in the first stage is not sufficient

In the second situation, the capacity deficit is solved by adding a parallel pipe on the same branch. The mass flow rate is therefore divided in two pipes. It is assumed that the pipe installed in the first stage is exploited to the maximum capacity. This means that the mass flow rate that flows in there is the maximum admissible, while the remaining stream flows in the new installed pipe. This hypothesis is not optimal, but it allows to minimize the size of the new pipes to be installed. Constraint (4.25)

ensures that the mass flow rate in every branch in the second time period must respect the total capacity of the pipes installed.

$$\sum_{m}^{M} Gmax^{m} * x_{j}^{m,t1} + \sum_{m}^{M} Gmax^{m} * x_{j}^{m,t2,s1} \geq G_{j}^{t2,s1} \qquad \forall j \in E, s1 \in \Xi_1 \tag{4.25}$$

Constraint (4.26) ensures that the mass flow rate flowing in the new pipe does not exceed its maximum capacity.

$$Gdiff_{j}^{s1} - \sum_{m}^{M} Gmax^{m} * x_{j}^{m,t2,s1} \leq 0 \qquad \forall j \in E, s1 \in \Xi_1 \tag{4.26}$$

where $Gdiff^{s1}$ is the mass flow rate that flows in the new pipe. Constraint (4.27) is a big-M constraint. This is an inequality constraint used to link a continuous (or the sum of different continuous variables) and a binary variable, forcing the first to be null, if the second is equal to zero. In this case, the constraint forces $Gdiff^{s1}$ to be equal to the difference between $G_{j}^{t2,s1}$ and the maximum mass flow rate that can flow in the pre-existing pipe if a new pipe is installed in the second stage.

$$-Gdiff_{j}^{s1} + G_{j}^{t2,s1} - \sum_{m}^{M} x_{j}^{m,t1} * Gmax^{m} \leq (1 - z_{j}^{t2,s1}) * H \quad \forall j \in E, s1 \in \Xi_1 \tag{4.27}$$

where H is a sufficiently large number. Constraints (4.28) and (4.29) fix a lower bound on the size of the chiller to install in the first and second stage. It is specified that it should be at least equal to 80% of the sum of demand peaks. This is reasonable since it is unlikely that all users have a demand peak in the same instant. It is therefore assumed that there is a diversity factor of 80%.

$$Size_{centr}^{t1} \geq 0.8 * Gcentr^{t1} * c_p * \Delta T \tag{4.28}$$

$$Size_{centr}^{t1} + Size_{centr}^{t2,s1} \geq 0.8 * Gcentr^{t2,s1} * c_p * \Delta T \qquad \forall s1 \in \Xi_1 \tag{4.29}$$

Individual chillers have a smaller life-cycle equal to 15 years, hence in the second stage new chillers must be installed for buildings not connected to the network. The size of individual chillers is instead defined by constraint (4.30).

$$Size_{ind,u}^{t(,s1)} = Gext_u * (1 - y_u^{t(,s1)}) * c_p * \Delta T \qquad \forall u \in Ut, t \in \Theta, s1 \in \Xi_1 \tag{4.30}$$

Pressure drop constraints

Constraint (4.31) defines the variable $Y_j^{t(,s1)}$ as the inverse of fluid dynamic resistance per unit of mass flow rate. In order to avoid values equal to zero, the variable is forced to be equal to 1, if no pipe is installed on the branch j.

$$Y_j^{t(,s1)} = 1 + \sum_m^M x_j^{m,t(,s1)} * (\frac{1}{R_j^m} - 1) \qquad \forall j \in E, t \in \Theta, s1 \in \Xi_1 \tag{4.31}$$

Constraint (4.32) links the pressure drop variables with the relative pressures at inlet and outlet nodes of every branch.

$$\Delta p_j^{t(,s1)} = \sum_i^I a_{ij} * p_i^{t(,s1)} \qquad \forall j \in E, t \in \Theta, s1 \in \Xi_1 \tag{4.32}$$

The pressure drops in the first time period are defined with the following non-linear equation:

$$\Delta p_j^{t1} = {G_j^{t1}}^2 / Y_j^{t1} \qquad \forall j \in E \tag{4.33}$$

For the second time period, due to the possible presence of multiple pipes in parallel on the same branch, only the highest pressure drop is considered. This is guaranteed by constraints (4.34)-(4.36).

$$\Delta p_j^{t2,s1} \geq {Gdiff_j^{s1}}^2 / Y_j^{t2,s1} \qquad \forall j \in E, s1 \in \Xi_1 \tag{4.34}$$

$$\Delta p_j^{t2,s1} \geq \sum_m^M (Gmax^{m2} * R_j^m * x_j^{m,t1}) * z_j^{t2,s1} \qquad \forall j \in E, s1 \in \Xi_1 \tag{4.35}$$

$$\Delta p_j^{t2,s1} \geq {G_j^{t2,s1}}^2 / Y_j^{t1} * (1 - z_j^{t2,s1}) \qquad \forall j \in E, s1 \in \Xi_1 \tag{4.36}$$

If no pipe is installed in the second decision stage, constraints (4.34) and (4.35) just indicate that $\Delta p_j^{t2,s1}$ is greater than zero. The pressure drop is therefore computed considering that the whole mass flow rate flows in the pipe previously installed in the first stage. On the other hand, if an additional pipe is installed in the second decision stage, the right hand side of constraint (4.36) is forced to be equal to zero. The non-linearities in constraints (4.33) and (4.34) are handled by means of the cutting plane method [67], previously described in chapter 3. Hence, the problem is solved

iteratively as a MILP and at each iteration, the following constraints are introduced:

$$\Delta p_j^{t1} \geq 2 * \frac{G_j^{t1\prime}}{Y_j^{t1\prime}} * G_j^{t1} - \frac{G_j^{t1\prime 2}}{Y_j^{t1\prime 2}} * Y_j^{t1} \qquad \forall j \in E \tag{4.37}$$

$$\Delta p_j^{t2,s1} \geq 2 * \frac{Gdiff_j^{s1\prime}}{Y_j^{t2,s1\prime}} * Gdiff_j^{t1} - \frac{Gdiff_j^{s1\prime 2}}{Y_j^{t1\prime 2}} * Y_j^{t1} \qquad \forall j \in E, s1 \in \Xi_1 \tag{4.38}$$

where the apex $\prime$ refers to the solution of the previous iteration.

Constraint (4.35) can be easily linearised, since it includes products between continuous and binary variables. Auxiliary variables $xz_j^{m,s1}$ are therefore introduced to substitute the product between $x_j^{m,t1}$ and $z_j^{t2,s1}$. In addition the following McCormick constraints are introduced to guarantee that this equality is respected.

$$xz_j^{m,s1} \geq x_j^{m,t1} + z_j^{t2,s1} - 1 \qquad \forall j \in E, m \in M, s1 \in \Xi_1 \tag{4.39}$$

$$xz_j^{m,s1} \leq x_j^{m,t1} \qquad \forall j \in E, m \in M, s1 \in \Xi_1 \tag{4.40}$$

$$xz_j^{m,s1} \leq z_j^{t2,s1} \qquad \forall j \in E, m \in M, s1 \in \Xi_1 \tag{4.41}$$

Constraint (4.36) is linearized in two steps. The expression, is indeed similar to that of constraints (4.33) and (4.34), which are linearized with the cutting plane method. However, the expression includes also the product with a binary variable. An auxiliary variable $Gz_j^{t2,s1}$ is therefore introduced to substitute the product between $G_j^{t2,s1}$ and $z_j^{t2,s1}$. Moreover the following constraints are added in order to guarantee that this equality is satisfied.

$$Gz_j^{t2,s1} \geq G_j^{t2,s1} + Gmax * z_j^{t2,s1} - Gmax \qquad \forall j \in E, s1 \in \Xi_1 \tag{4.42}$$

$$Gz_j^{t2,s1} \leq G_j^{t2,s1} \qquad \forall j \in E, s1 \in \Xi_1 \tag{4.43}$$

$$Gz_j^{t2,s1} \leq Gmax * z_j^{t2,s1} \qquad \forall j \in E, s1 \in \Xi_1 \tag{4.44}$$

Finally, constraint (4.36) is linearized with the cutting plane method, already defined in Chapter 3. It consists in solving the problem iteratively and after each iteration

introducing the constraints of eq. (4.45):

$$\Delta p_j^{t2,s1} \geq 2 * \frac{Gz_j^{t2,s1\prime}}{Y_j^{t1\prime}} * Gz_j^{t2,s1} - \frac{Gz_j^{t1\prime 2}}{Y_j^{t1\prime 2}} * Y_j^{t1} \qquad \forall j \in E, s1 \in \Xi_1 \tag{4.45}$$

where the $\prime$ refers to the solution of the previous iteration. The stopping criteria used to terminate the iterations is the error in the evaluation of relative pressure on the central node, with a tolerance of 100 Pa. On the other hand the stopping criteria to terminate a single iteration is the MILP-Gap, which was set to 1.2%.

Pumping energy

The cost function includes also pumping costs, defined in equations (4.16) and (4.17). These depend on the variables $GpNh^{t1}$ and $GpNh^{t2,s1}$, which represent the product between the mass flow rate flowing in the network, the pressure at central node and the number of full load hours. They are therefore defined through non-linear relations and need to be linearized.

$$GpNh^{t1} = p_{centr}^{t1} * \sum_{u}^{U} Gext_u * Nh_u^{t1} * y_u^{t1} \tag{4.46}$$

$$GpNh^{t2,s1} = p_{centr}^{t2,s1} * \sum_{u}^{U} Gext_u * Nh_u^{t1} * (1 + incr^{s1})^{n_y/2} * y_u^{t2,s1} \tag{4.47}$$

where Nh_u^{t1} is the initial number of full load hours for building u in year 0. These variables depend on the product between continuous and binary variables, hence they can be linearized by introducing additional variables up_{centr}^{t1} and $up_{centr}^{t2,s1}$ that substitute these products. Moreover the following additional constraints must be added as well to ensure that $up_{centr}^{t(,s1)}$ is equal to the product $y_u^{t(,s1)} * p_{centr}^{t(,s1)}$.

$$up_{centr}^{t(,s1)} \geq y_u^{t,(s1)} * p_{min} \qquad \forall u \in Ut, t \in \Theta, s1 \in S1 \tag{4.48}$$

$$up_{centr}^{t(,s1)} \geq p_{centr}^{t(,s1)} + y_u^{t(,s1)} * p_{max} - p_{max} \qquad \forall u \in Ut, t \in \Theta, s1 \in S1 \tag{4.49}$$

$$up_{centr}^{t,(s1)} \leq y_u^{t,(s1)} * p_{min} + p_{centr}^{t,(s1)} - p_{min} \qquad \forall u \in Ut, t \in \Theta, s1 \in S1 \tag{4.50}$$

4.2.6 Rigid model formulation

In the model described in the previous section, it is assumed that in the second stage new pipes can be installed in the same branches where there already pipes installed in the first stage. The model therefore allows to have multiple pipes in parallel in the same branch. This assumption may not be applicable in reality, since there may not be enough space in the ground to install additional pipes close to the existing ones. Hence, a variant formulation has been implemented as well, in which it is avoided the installation of more than one pipe in the same branch of the network. This variant of the original model will be defined from now on as *rigid model*, since compared to the previous one, it guarantees less flexibility. Indeed, due to the different constraints, the network can be enlarged installing new pipes, but the flow capacity of existing branches can not be increased in the second decision stage. This model formulation therefore includes additional constraints (4.51) to ensure that in the second stage new pipes can not be installed in the branches where there are already pipes installed in the first stage.

$$\sum_{m}^{M} x_j^{m,t1} + \sum_{s1}^{\Xi_1} \sum_{m}^{M} x_j^{m,t2,s1} \leq 1 \qquad \forall j \in E \qquad (4.51)$$

4.3 Case study

Both versions of the model have been tested on a case study representing the topology of an existing district heating network connecting 107 buildings in an Italian residential neighbourhood, whose peak cooling loads are reported in Figure 4.5.

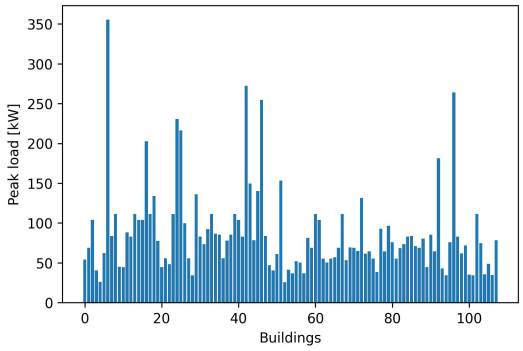

Fig. 4.5 Buildings peak loads

Figure 4.6 shows the topology and the position of buildings and the centralized chiller. The network is characterised by 304 nodes and 303 branches.

The cooling demand of these buildings has been computed by means of a model for transient simulations and the resulting total cooling power required by all buildings is 9.4 MW. In the model it is assumed that the peak power does not increase, hence the yearly demand increases only because of a rise in the number of operational hours.

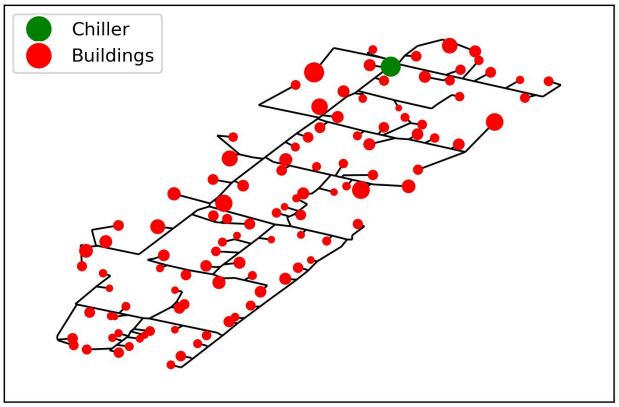

Fig. 4.6 Topology of case study

4.4 Results

In this section the main results obtained by applying the two model formulations to the case study are presented. The flexible model, characterised by 1.210.482 binary and 162.231 continuous variables converged after 22 h using a 2.10 GHz Intel(R) Xeon(R) Gold 6230R CPU.

Figure 4.7 shows the network that should be installed immediately, result of the decisions to be taken at 1^{st} stage. It should be connected to 40 buildings, with a total capacity of 4.77 MW.

Depending on the scenario, in the second decision stage the network can remain unchanged or be expanded in 23 different ways. Figure 4.8 shows few of the possible network expansions in the second stage with piping details. It should be noted that since in the second stage in some branches an additional pipe has been installed, the

ones reported in the figure refer to equivalent pipe sizes. These correspond to the size of pipes that have a section equal to the total one.

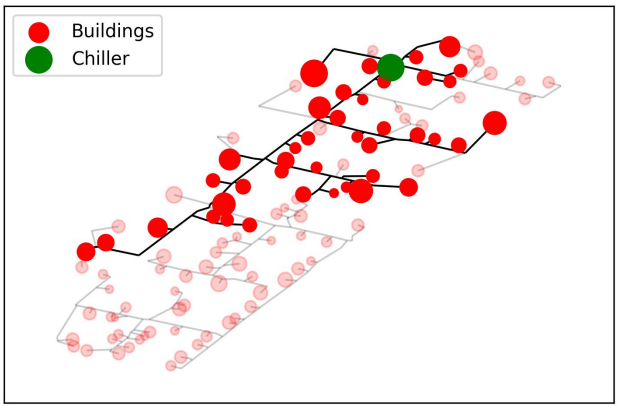

Fig. 4.7 Optimal first stage network design

These results evidence that it is more convenient to install a smaller network at the initial stage and to enlarge it in the future, if conditions are good enough (e.g. higher cost of electricity and larger increase rate of cooling demand). This allows to reduce the risks related to the uncertainties. Indeed it is avoided the realization of a larger investment from the beginning, that could result non convenient, if cooling demand or energy prices do not increase in the future. In fact, if a larger network is built already from the first stage and the cooling demand does not increase or the electricity cost is lower than expected, the higher initial investment costs would not be compensated by sufficient operation savings. As a consequence, the total costs would be larger than the ones obtained by realizing a smaller network and installing individual cooling systems in the remaining buildings.

Figure 4.9 compares the solution obtained with the stochastic approach and two obtained deterministically considering a single scenario with the lowest (lowest cost of electricity, lowest increase rate of cooling demand, lowest capital cost of individual chillers, highest capital cost of centralized chillers) and highest potential (highest cost of electricity, highest increase rate, highest capital cost of individual chillers, lowest capital cost of centralized chillers) of district cooling, respectively. The graph shows how these solutions behave in the different scenarios. The three curves do not have the same profile, since moving from a scenario to another one may have a positive impact on a solution, while a negative or negligible one on the others. Moreover, in order to make the graph more readable, the scenarios are sorted

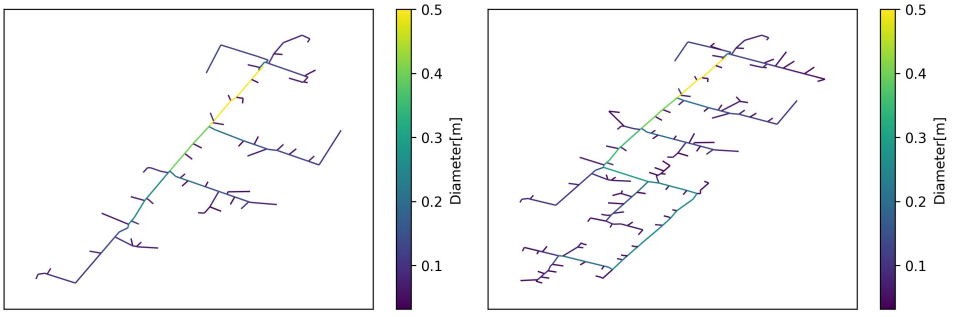

(a) c_{el}=0.10 €/kWh, *incr*=0%, $c_{chilll,DC}$=250 €/kW, $c_{chill,ind}$=600 €/kW

(b) c_{el}=0.50 €/kWh, *incr*=0%, $c_{chilll,DC}$=250 €/kW, $c_{chill,ind}$=600 €/kW

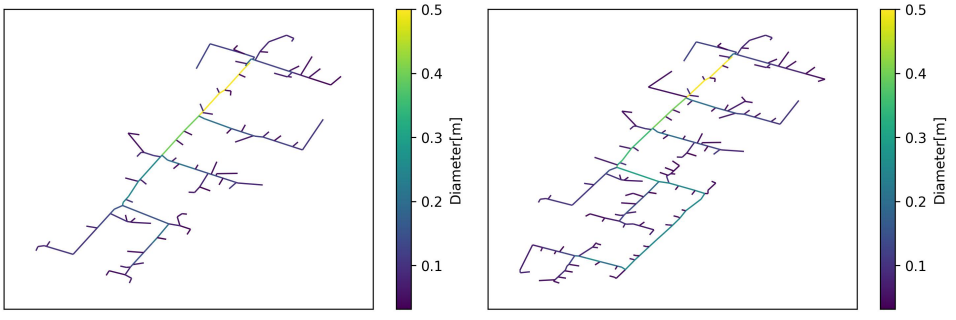

(c) c_{el}=0.50 €/kWh, *incr*=3%, $c_{chilll,DC}$=416 €/kW, $c_{chill,ind}$=400 €/kW

(d) c_{el}=0.50 €/kWh, *incr*=4%, $c_{chilll,DC}$=600 €/kW, $c_{chill,ind}$=600 €/kW

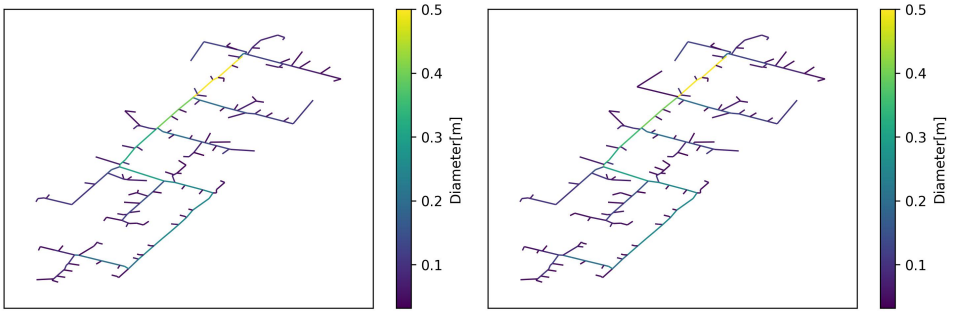

(e) c_{el}=0.30€/kWh, *incr*=3%, $c_{chilll,DC}$=250 €/kW, $c_{chill,ind}$=400 €/kW

(f) c_{el}=0.30 €/kWh, *incr*=4%, $c_{chilll,DC}$=600 €/kW, $c_{chill,ind}$=600 €/kW

Fig. 4.8 Subset of possible second stage network designs in different scenarios

to give a monotonic stochastic curve. It can be observed that the stochastic solution is the most robust, as it tends to work well for all possible scenarios, while the other two tend to be optimal only in few cases. In particular, in the solution *Deterministic 1*, which was obtained considering the scenario with the lowest potential for district cooling, the total cost is lower compared to the stochastic solution, only in scenarios characterised by a lower cost of electricity and cooling demand. In particular, in the scenario characterised by minimum cost of electricity, cooling demand, cost of individual chillers and maximum cost of centralized chillers, this solution is 24% less expensive than the stochastic one. On the other hand, in scenarios with larger values of electricity cost and cooling demand, the total cost can be up to 29% larger than the one obtained with the stochastic solution.

On the other hand, the solution *Deterministic 2* tends to work slightly better than the stochastic one in scenarios characterised by higher district cooling potential. In the best case, this solution is 10% less expensive than the stochastic one. However, in scenarios where district cooling is less convenient, the cost can be up to 33% larger compared to the stochastic solution. Indeed, due to the higher number of buildings connected to the network, capital costs are larger, but the savings achievable by district cooling are lower and not sufficient, when electricity cost and cooling demand are lower.

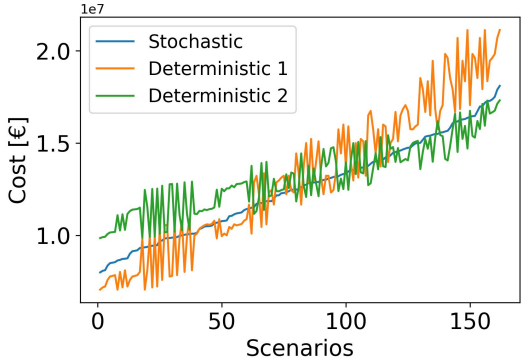

Fig. 4.9 Comparison between stochastic and deterministic solutions

The expected value of the cost function, evaluated for the three different solutions in all possible scenarios is reported in Table 4.6. The stochastic solution is, on average, up to 5% less expensive than a deterministic one. Figure 4.10 shows the expected net present value and payback time for the stochastic and *Deterministic 2* solutions. Solution *Deterministic 1* was not included in the analysis since it corresponds to the

Solution	Expected value of cost fun. [M€]
Stochastic(flexible)	12.63
Deterministic 1	13.28
Deterministic 2	13.19
Stochastic (rigid)	12.68

Table 4.6 Expected value of cost function evaluated with the different solutions

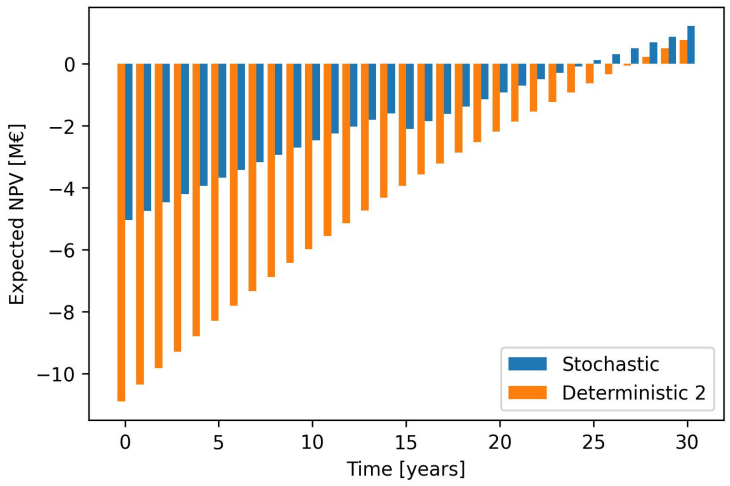

Fig. 4.10 Net Present Value and payback time analysis

case where all the buildings are cooled individually and no district cooling network is installed. The analysis has been carried out considering that the district cooling utility sells chilled water at a price that is dependent on the scenario and corresponds to the cost the users would pay if they installed individual cooling systems. It can be observed that the expected payback time of the stochastic solution is 25 years, while for the solution *Deterministic 2* is 28 years. In addition, the final expected value of net present value of the stochastic solution is 58% larger, with an initial capital investment 54% lower.

4.4.1 Impact of parameters uncertainty

In this subsection it is analysed how the uncertainty of the different parameters influences the optimal solution. Figure 4.11 shows the number of buildings connected in the second stage (including the ones already connected in the first stage), as a function of the uncertain parameters that are revealed after the first time period.

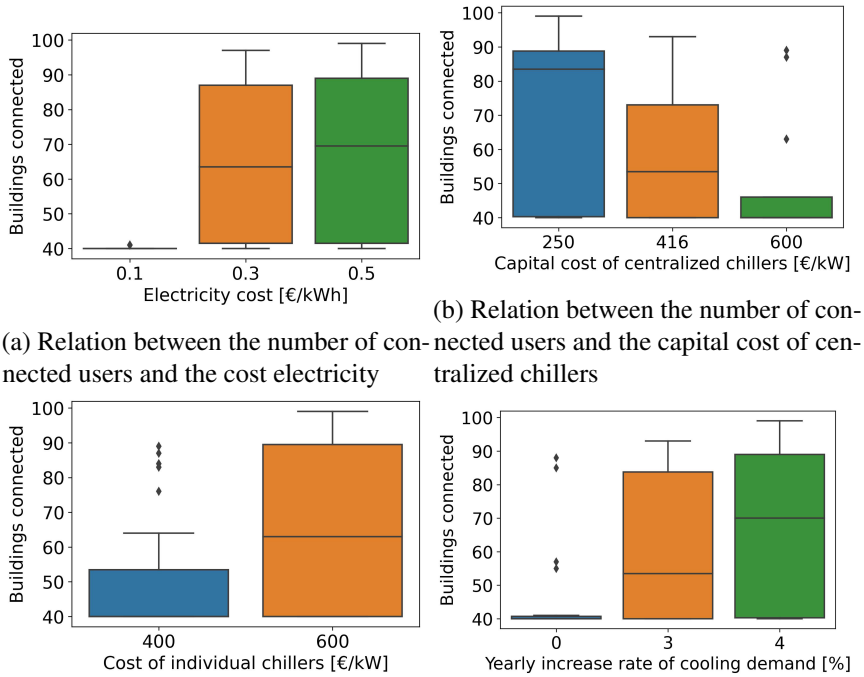

(a) Relation between the number of connected users and the cost electricity

(b) Relation between the number of connected users and the capital cost of centralized chillers

(c) Relation between the number of connected users and the capital cost of individual chillers

(d) Relation between the number of connected users and the demand increase rate

Fig. 4.11 Influence of the different parameters on the results

Electricity cost

The electricity cost has a strong impact on the results. Among the eighteen scenarios with an electricity cost of 0.10 €/kWh, in fifteen of these, no further buildings shall be connected in the second stage. Moreover, in the other three scenarios, only one new building is connected in the second stage. On the other hand, if the electricity cost is equal to 0.3 €/kWh, in 50% of the cases more than twenty-three buildings should be connected in the second stage. Lastly, with an electricity cost of 0.5 €/kWh, in half of the scenarios more than 30 new connections should be added in the second decision stage.

Capital cost of centralized chillers

Among the eighteen scenarios with a capital cost of centralized chillers equal to 250 €/kW, in ten of these more than 43 additional buildings shall be connected in the second stage. On the other hand, with a cost of 416 €/kW this happens only

in four scenarios. With a capital cost of 600 €/kW, in 50% of the cases, one new building would be connected at most. Hence, also the uncertainty related to the cost of centralized chillers has an impact on the results.

Capital cost of individual chillers

Among the twenty-seven scenarios with a capital cost of individual chillers equal to 400 €/kW, in seventeen of these, no additional buildings shall be connected to the network in the second stage. On the other hand, in twelve cases, more than ten buildings shall be connected. If this cost is equal to 600 €/kW, in twelve cases, more than 43 buildings shall be connected in the second stage. As a consequence, the impact of the uncertainty of the cost individual chillers is limited with respect to the other parameters.

Yearly demand increase

The increase rate of cooling demand is one of the parameters with the highest impact on the results, as one could expect. In thirteen of the eighteen scenarios in which cooling demand does not increase during the first time period, no new buildings shall be connected in the future. In 56% of the scenarios in which the yearly demand increase rate is equal to 3% in the first time period, at least ten new buildings must be connected to the network in the second stage. Lastly, in nine out of the eighteen scenarios characterised by an increase rate of 4% during the first period, more than 30 new buildings shall be connected in the second stage.

Combined impact of electricity cost and cooling demand increase rate

The results show that the uncertain parameters with the highest impact are the electricity cost and the yearly demand increase. In Figure 4.12 a heat map that presents the combined impact these two parameters is shown. The values reported in the heat map table, represent the median number of total buildings connected in the second stage (including the ones already connected in the first stage), in all scenarios characterised by those values of electricity cost and cooling demand increase rate. Both parameters have a large impact. In particular, highest differences are observed when varying the increase rate of cooling demand. However, if electricity cost

is minimum, the network would remain as it is regardless of the cooling demand increase. The same applies, if cooling demand does not increase during the first time period, regardless of the electricity cost.

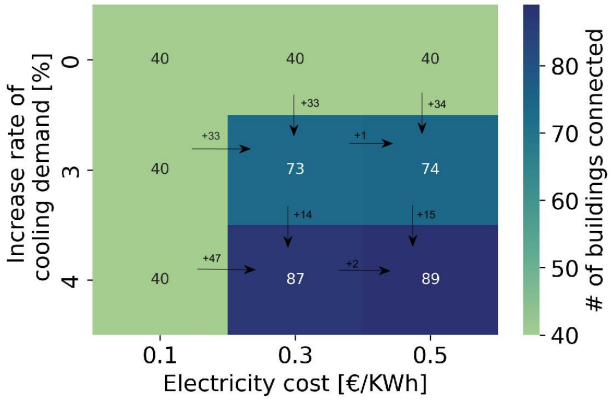

Fig. 4.12 Combined impact of electricity cost and cooling demand

4.4.2 Rigid model

In this part the results obtained with the rigid version of the model are presented (i.e. it is avoided the installation of new pipes in the second stage in the same branches where there are already pipes previously installed in the first stage).

Figure 4.13 shows the network that should be installed from the beginning according to this model. The topology is similar to the one of the previous model, but 50 buildings would be connected from the beginning, hence ten more with respect to the flexible formulation. The reason is due to the fact that the network pipes can not be expanded in the future, so larger diameters are installed from the beginning, leading also to the connection of additional buildings.

However, in this case, the number of possible enhancements in the second stage is equal to seventeen, six less with respect to the flexible model formulation. Six of these are shown in Figure 4.14.

Compared to the *flexible model*, in this case the number of users connected in the second stage is sensibly lower. Indeed the maximum amount of connected buildings

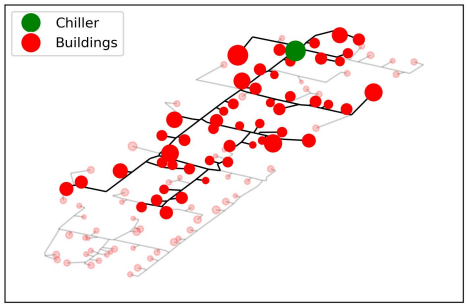

Fig. 4.13 Network that should be installed from the beginning according to rigid model version

is 64, while in the flexible version it is 99. This result was expected, since the pipe capacities can not be modified as in the *flexible model*.

Figure 4.15 shows the topology of a network that represents the intersection of the networks obtained by the two models. This network therefore connects only the buildings that are present in both solutions. In figures 4.15a and 4.15b the branches are coloured on the base of the diameter selected in the first stage by each model. It can be observed that for most of the edges, the diameter is the same in the two solutions. However, in some branches, the rigid model selected a larger diameter. This is also shown more clearly in figure 4.15c, where the branches in which the rigid model selects a larger diameter are highlighted. Indeed, the rigid model selects larger pipes, since no future pipe modifications are allowed. In the subnetwork common to both solutions, the average pipe diameter selected by the rigid model is 158 mm, while the average one selected by the flexible model is 150 mm. The expected value of the cost obtained by the rigid model formulation is shown in Table 4.6 and is 0.4% higher than the one found previously. Hence, a greater flexibility would guarantee slightly larger savings.

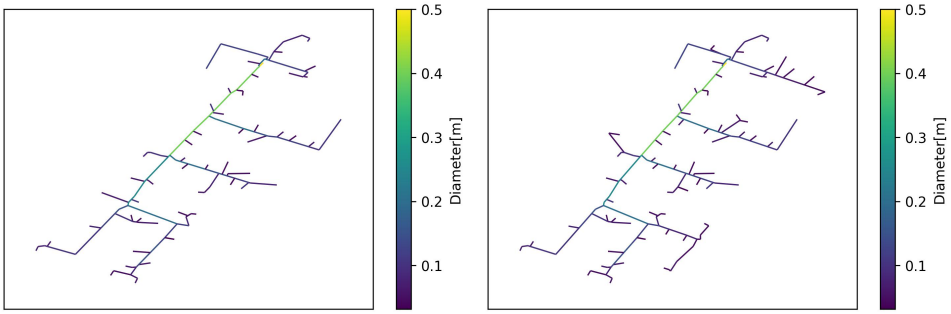

(a) c_{el}=0.10 €/kWh, *incr*=0%, $c_{chillIDC}$=250 €/kW, $c_{chill,ind}$=600 €/kW

(b) c_{el}=0.30 €/kWh, *incr*=0%, $c_{chillIDC}$=250 €/kW, $c_{chill,ind}$=600 €/kW

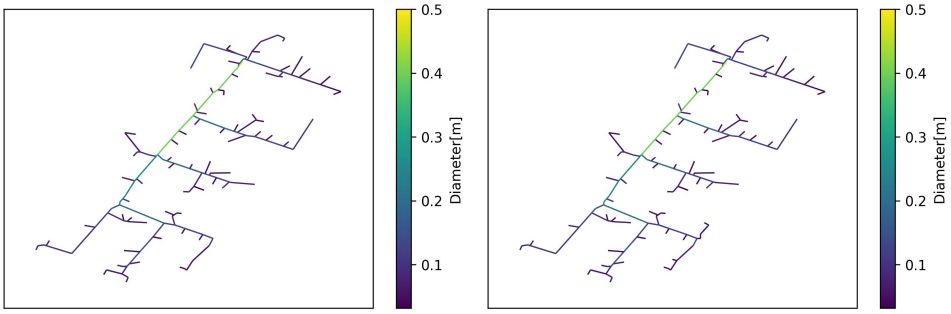

(c) c_{el}=0.30 €/kWh, *incr*=0%, $c_{chillIDC}$=416 €/kW, $c_{chill,ind}$=600 €/kW

(d) c_{el}=0.40 €/kWh, *incr*=3%, $c_{chillIDC}$=250 €/kW, $c_{chill,ind}$=400 €/kW

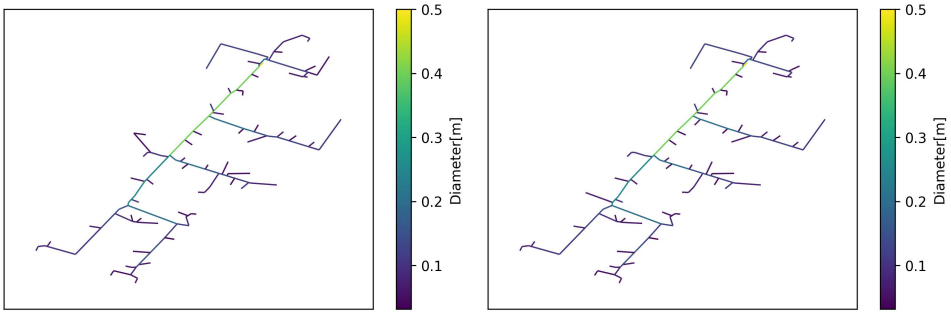

(e) c_{el}=0.30 €/kWh, *incr*=3%, $c_{chillIDC}$=416 €/kW, $c_{chill,ind}$=400 €/kW

(f) c_{el}=0.30 €/kWh, *incr*=3%, $c_{chillIDC}$=600 €/kW, $c_{chill,ind}$=400 €/kW

Fig. 4.14 Second stage network designs for different scenarios according to rigid model

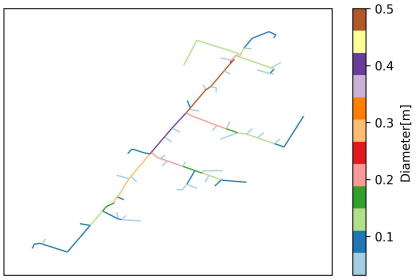

(a) Diameter selection at 1st stage in rigid model formulation

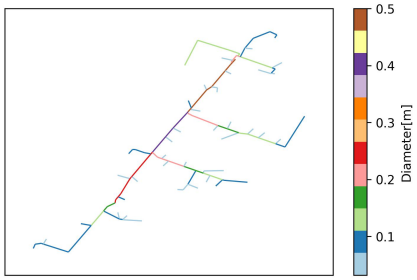

(b) Diameter selection at 1st stage in flexible model formulation

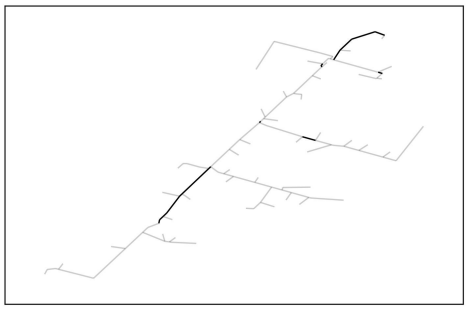

(c) Branches where rigid model selects larger diameters

Fig. 4.15 Comparison of diameter selection between rigid and flexible model solutions

4.4.3 Impact of residual value of equipment

All previous results have been obtained by considering a positive cash flow in the last year, due to the residual value of assets. Indeed, theoretically equipment that did not complete its life-time, can be used for new projects, such as a renovation of the district cooling system. However, it is also difficult to estimate the real residual value of partially worn-out parts. In this paragraph the results obtained by considering a null residual value of the equipment at the end of project life are presented.

Figure 4.16 shows the optimal first stage network obtained by the flexible model formulation. The initial number of connected users would be 44, hence about 10% more than when considering residual value in the cost function. Depending on the scenario, the network can remain as is or be enhanced in three different ways at the second decision stage, as shown in Figure 4.17.

Figure 4.18 shows the distribution of the number of new connections added in the second stage according to the scenarios. It can be observed that if no residual value of equipment is taken into account, the maximum number of new buildings connected in the second stage would be 13, while it would be 59 if residual value is considered in the cost function. Moreover, only in 6 cases out of 54, the network would be enhanced in the second stage, if residual value is not included in the cost function. If this is taken into account, the network would be expanded in the second stage, in 29 scenarios out of 54.

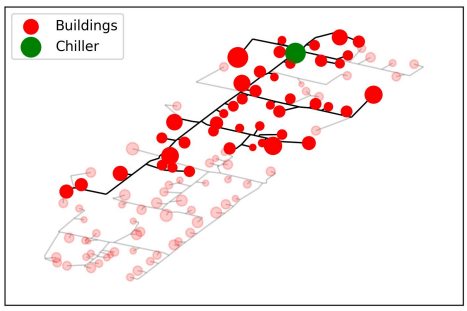

Fig. 4.16 Initial network layout if residual value is not taken into account

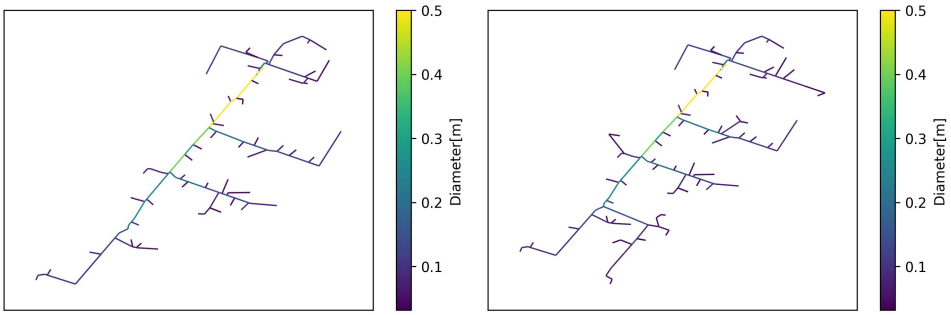

(a) c_{el}=0.30 €/kWh, *incr*=3%, $c_{chillIDC}$=250 €/kW, $c_{chill,ind}$=600 €/kW

(b) c_{el}=0.30 €/kWh, *incr*=4%, $c_{chillIDC}$=250 €/kW, $c_{chill,ind}$=600 €/kW

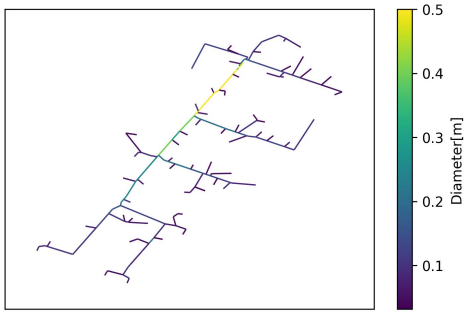

(c) c_{el}=0.50€/kWh, *incr*=4%, $c_{chillIDC}$=250 €/kW, $c_{chill,ind}$=600 €/kW

Fig. 4.17 Possible network enhancement in the second stage if no residual value of equipment is considered

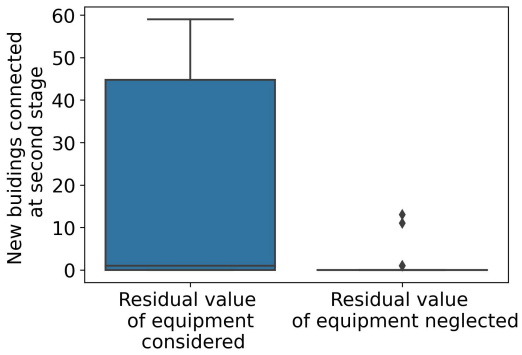

Fig. 4.18 Impact of residual value of equipment on second stage decisions

4.5 Discussion and concluding remarks

The results showed that it is more convenient to start with a smaller district cooling network and to eventually enhance it in the future. In this way, the district cooling network can be enlarged if the demand or the electricity cost increases. At the same

time, this solution limits the risks related to the possible future decrease of district cooling potential, by lowering the initial investment costs with the installation of a smaller network.

From the analysis of the impact of the uncertainty on the optimal solution, it can be deduced that all the parameters affect the results. However, the electricity cost and the evolution of cooling demand are the ones with the highest impact.

The comparison of the stochastic model with other deterministic approaches proved that the latter on average tend to provide 5% more expensive solution and three years larger payback time.

Concerning the rigid model formulation, it tends to install larger pipes from the beginning in order to be able to connect additional buildings in the second stage. On the other hand, the impact of the rigid formulation in terms of expected value of the cost function is limited to 0.4%.

Regarding the residual value of asset at the end of project life, if this is not taken into account in the cost function, the model tends to select a slightly wider network from the beginning. However, in 89% of the scenarios the network is not expanded in the second stage. Indeed, installing new pipes, substations or chillers in the second stage would imply, following the assumptions of the model, using them for only half of their life if the residual value is not taken into account. Hence, the achievable operation savings would not be large enough to compensate the additional capital investment. The only scenarios in which the investment of new district cooling equipment is compensated by operation savings in the second time period, are the ones characterised by the highest potential of district cooling. This result attests that the value and the use of assets at the end of project life has a strong impact on the solution, influencing both first and second stage decisions.

The developed models can be suitable to support decision makers in the different design phases of district cooling systems. Indeed, these systems should operate for a large time-horizon, where most of parameters are uncertain and could sensibly change in the long period. By taking into account the uncertainty of different parameters, these models select a robust network design that can eventually be modified in the future, if conditions become more convenient for district cooling technology. At the same time, the robust network design allows to mitigate the risks related to a possible decrease of district cooling potential in the future.

Chapter 5

Genetic algorithm for the optimization of the location of chillers and storages in a district cooling network

The content of this chapter has been previously presented at 35th International conference on Energy Efficiency, Cost, Optimization and Environmental Impact of Energy Systems (ECOS) in Copenhagen in July 2022 and has been published in the following paper [103]:

Manfredi Neri, Elisa Guelpa and Vittorio Verda. "Trade-off between optimal design and operation in district cooling networks" Smart Energy 13(2024): 100127

5.1 Introduction

In this chapter a further improvement to the heuristic algorithm previously implemented in chapter 3 is presented. This new model is able, not only to optimize the optimal set of buildings to be connected and the network layout, but also the position of chillers and storages, while fixing the storage strategy a priori. Indeed, the previously implemented heuristic algorithm proved to effectively optimize the layout and the set of buildings to be connected to a district cooling network, but has some

limitations, since it is applicable only to one-plant networks without cold storage. In addition, optimizing simultaneously the buildings to be connected and the position of the chillers would help to fully exploit the potential of district cooling, as the buildings to be connected and the plant position depend on each other. This chapter therefore proposes a further improvement to the previously implemented model and the application to two different case studies, where the optimization impact has been assessed.

5.2 Model description

5.2.1 Assumptions

The model is based on the following assumptions:

- The network is tree-shaped.
- Thermal losses are neglected, hence the temperature is homogenous on both supply and return lines.
- The cooling power production of every chiller is constant and storages are used for peak shaving and valley filling.
- The demand of each building is always satisfied by the same chiller. This assumption is based on the fact that, in order to minimize pumping costs, the cooling demand of buildings should be satisfied by chiller plants close to them.
- Every chiller relies on a specific storage, hence the extra/deficit production is absorbed/released always by the same storage).

District cooling operation is therefore not optimized, since it is assumed that the chillers operate at constant load and that the storages are sized accordingly.

5.2.2 Model variables and parameters

The model is characterized by two types of integer decision variables: x_u and x_j. The variable x_u indicates whether the generic user u is connected or not to the network

Variable value	Meaning
$x_u = 0$	Building u not connected
$x_u = j$	Demand of building u satisfied by chiller j
$x_j = k$	Chiller j is connected to storage k

Table 5.1 Encoding of model variables

Set/Index	Description
Ut	Set of users
Ch	Set of chillers
St	Set of Storages
S	Set of Steiner nodes
M	Set of pipe diameters
E	Set of network branches
Θ	Set of time steps
u	Index referring to the generic user
j	Index referring to the generic chiller
k	Index referring to the generic storage
l	Index referring to the generic branch
v	Index referring to the generic Steiner node
t	Index referring to the generic time step

Table 5.2 Sets and indices defined in both models

and by which chiller is fed. It can range between zero and the number of possible chiller locations. If it is equal to zero, the user u is not connected to the network, while if it is equal to j, it is connected and fed by the chiller indexed with j. Similarly, the variable x_j indicates on which storage the generic chiller j relies on. Table 5.1 summarizes how these variables are encoded. The other variables, such as the size of chillers and storages, the mass flow rate flowing in every branch of the network, the cooling power production and the cooling energy absorbed or released by the storage, are all dependent on x_u and x_j and are evaluated simultaneously with the cost function. The nomenclature for the indices, sets and parameters is defined in Table 5.2 and 5.3, while in Table 5.4 are shown the values of the main parameters used for the optimizations.

Parameter	Description
EER_{DC}	EER of large-scale chiller in district cooling networks
EER_{ind}	EER for small scale chillers in individual cooling systems
$G^t_{ext,u}$	Mass flow rate requested by generic user u at time t [kg/s]
L_l	Length of branch l [m]
c^t_{el}	Cost of electricity at time t [€/kWh]
$c_{chill,DC}$	Cost of centralized chiller per unit of size [€/kW]
$c_{chill,ind}$	Cost of individual chiller per unit of size [€/kW]
$c_{storage}$	Cost of storage per unit of size [€/kWh]
$c_{ETS,u}$	Cost of energy transfer station installed at user u [€]
c^m_{pipe}	Cost of pipe with diameter m per unit of length [€/m]
ΔT	Temperature difference between supply and return [K]
c_p	Specific heat [kJ/(kJ*K)]
n_d	Duration of cooling season [days]
n_y	Life cycle of the system [years]
r	Discount rate [%]
Δt	Time interval between two steps [s]
N	Number of time steps in Θ
$maxG^h$	Maximum mass flow rate admissible for a pipe with diameter m [kg/s]
$minG^h$	Lower bound of the maximum mass flow rate for a pipe with diameter m [kg/s]
η_{charge}	Charge efficiency of thermal energy storage [%]
$\eta_{discharge}$	Discharge efficiency of thermal energy storage [%]

Table 5.3 Parameters

Parameter	Value
EER_{DC}	6.5 [101]
EER_{ind}	2.7 [101]
$c_{storage}$	20 €/kWh [104]
$c_{chill,DC}$	400 €/kW [101]
$c_{chill,ind}$	600 €/kW [101]
n_y	30 y
n_d	60 d
r	5%
ΔT	7°C
η_{pump}	80% [105]
η_{charge}	95%
$\eta_{discharge}$	95%
N	24
Δt	1 h

Table 5.4 Values of the parameters

5.2.3 Cost function

The cost function is the sum of capital and operation expenditures, as shown in eq. (5.1).

$$cost_{tot} = cost_{chillers} + cost_{op,chillers} + cost_{piping} + cost_{pumping} + cost_{ETS} + cost_{storage} \tag{5.1}$$

Cost of energy transfer stations

The size and the cost of energy transfer stations depend on the demand peak of the single buildings, whose demand profiles are inputs of the model, hence they are known a priori. The only unknown is whether a building is connected to the network or not. Hence, the capital cost of energy transfer stations is defined as:

$$cost_{ETS} = \sum_{u|x_u>0}^{Ut} c_{ETS,u} \tag{5.2}$$

where $c_{ETS,u}$ is the cost of the energy transfer station of building u. The condition $u|x_u > 0$ indicates that only buildings connected to the district cooling network are taken into account.

Capital cost of chillers and storages

The capital cost of chillers and storages is proportional to their installed capacity. Concerning the chillers, as in the previous models, there are two possible options: individual chillers characterized by larger cost per unit of size and centralized chillers characterized by lower cost per unit of size. The total capital expenditure for chillers is therefore defined as:

$$cost_{chillers} = \sum_{j}^{Ch} c_{chill,DC} * S_j + \sum_{u|x_u=0}^{Ut} c_{chill,ind} * S_u \tag{5.3}$$

where the first term refers to the cost of centralized chillers and the second term refers to the cost of individual chillers. The condition $u|x_u = 0$ indicates that only buildings not connected to the network, hence with an individual cooling system, are taken into account. S_j is the size of the generic centralized chiller indexed with

j, while S_u refers to the size of the independent chiller of the generic user indexed with u. The size of individual chillers is known a priori, since it depends only on the demand peak, which is an input of the model. On the other hand, the size of centralized chillers depends on the variables x_u and x_j, since it is assumed that every user is fed by only one chiller and that every chiller operates at constant power. The mass flow rate inserted from a generic chiller into the network is evaluated as:

$$G^t_{ext,j} = -\frac{1}{N}\sum_{t}^{\Theta}\sum_{i|x_i=j}^{Ut} G^t_{ext,u} + Losses \qquad \forall j \in Ch \tag{5.4}$$

where N is the number of time steps and $G^t_{ext,u}$ is the mass flow rate of chilled water requested by the generic user u at time t. The condition $u|x_u = j$ indicates that only the users fed by chiller j are considered. The Losses term refers to the additional mass flow rate that the chillers should introduce in order to compensate the heat losses of thermal energy storages. This term is calculated by computing the theoretical mass flow rate inserted from the chillers and that would be absorbed by the thermal energy storages in the ideal case of unitary efficiency and multiplying it by a loss factor, which itself is evaluated as:

$$L_f = 1 - \eta_{charge} * \eta_{discharge} \tag{5.5}$$

where η_{charge} and $\eta_{discharge}$ are the thermal energy storage efficiencies during charge and discharge. The mass flow rates absorbed or released by the thermal energy storages are evaluated as stated in eq. (5.6):

$$G^t_{ext,k} = -\sum_{j|x_j=k}^{Ch}(G^t_{ext,j} + \sum_{u|x_u=j}^{Ut} G^t_{ext,u}) \qquad \forall k \in St \tag{5.6}$$

where $G^t_{ext,k}$ is the generic mass flow rate absorbed/released by the generic storage indexed with k at time t. The terms between parentheses represent the difference between the flow rate demanded by the users and the one inserted into the network by the chillers. If this quantity is negative, it means that the chillers are producing more cooling power than the requested one, so the rest is stored. If it is positive, the chillers alone can not satisfy the users demand, so the the rest is provided by the storages. The condition $j|x_j = k$ indicates that only the chillers connected to the k storage are taken into account, as for hypothesis it is assumed that the extra/deficit

mass flow rate of every chiller is always absorbed/released by the same storage. Once the mass flow rates are evaluated, the sizes and costs of chillers and storages can be easily determined. The size of the generic chiller is therefore given by the cooling power that it has to produce, which is equal for all time steps, as hypothesized.

$$S_j = G^t_{ext,j} * c_p * \Delta T \qquad \forall j \in Ch \tag{5.7}$$

where c_p is the specific heat and ΔT is the temperature difference between supply and return pipes. The sizes of the storages depend on the cumulate function of the cooling energy absorbed/released. In particular, they are equal to the difference between the maximum and the minimum of this function. In fact, this value indicates the minimum size that a storage must have to be able to satisfy the demand.

$$S_k = \max \sum_{t=0}^{t} G^t_{ext,k} * c_p * \Delta T * \Delta t - \min \sum_{t=0}^{t} G^t_{ext,k} * c_p * \Delta T * \Delta t \qquad \forall k \in St \tag{5.8}$$

The capital cost of storages is successively computed as defined in eq. (5.9):

$$cost_{storage} = \sum_{k}^{St} S_k * c_{storage} \tag{5.9}$$

Chillers operation costs

The operation cost of centralized and individual chillers is evaluated similarly to the models described in the previous chapters. The main difference is that, in this case, there are more chiller plants, so the costs are evaluated for all plants and then summed. Also in this case, the operation costs are evaluated for a reference day and multiplied by the number of utilization days of the system within a year. This assumption is justified by the fact that the daily demand profile tends to be cyclic, as it depends especially on the use of the cooling systems, which itself depends on other factors like working hours and daily routines. On the other hand, the daily peaks vary and depend on the climate conditions. The shape of the demand curve has a certain pattern that depends on the type of building and on the users' routines, while the amplitude of the curve depends mostly on the climate conditions. Eq. 5.10 and

5.11 define the operation costs of centralized and invidudal chillers, respectively:

$$cost_{op,chillers-DC} = \sum_{t}^{\Theta} \sum_{j}^{Ch} \left(\frac{G^t_{ext,j} * c_p * \Delta T * \Delta t}{EER_{DC}} * c^t_{el} \right) * n_d * \sum_{n=1}^{n_y} \frac{1}{(1+r)^n} \tag{5.10}$$

$$cost_{op,chillers-ind} = \sum_{t}^{\Theta} \sum_{u|x_u=0}^{Ut} \left(\frac{G^t_{ext,u} * c_p * \Delta T * \Delta t}{EER_{ind}} * c^t_{el} \right) * n_d * \sum_{n=1}^{n_y} \frac{1}{(1+r)^n} \tag{5.11}$$

where $G^t_{ext,u}$ is the mass flow rate requested by user u at time t. The total chillers operation cost is defined as:

$$cost_{op,chillers} = cost_{op,chillers-DC} + cost_{op,chillers-ind} \tag{5.12}$$

Piping cost

In order to evaluate the piping cost, it is necessary to compute first the mass flow rates in every branch of the network. Once the mass flow rates entering or exiting from each node are evaluated, the mass flow rate in every branch can be computed by solving the continuity equation in every node, which in matrix form is written as:

$$A * G + G_{ext} = 0 \tag{5.13}$$

The diameters are chosen so that the maximum velocity does not exceed 1.5 m/s. For each pipe it is therefore selected the smallest diameter that can satisfy this constraint. The piping cost is then be evaluated as:

$$cost_{piping} = \sum_{l}^{E} \sum_{m}^{M} L_l * x^m_l * c^m_{pipe} \tag{5.14}$$

where L_l is the length of the branch l, x^m_l is an auxiliary binary variable that indicates whether the diameter m is selected for the branch l and c^m_{pipe} is the cost per unit of length for a pipe with diameter m.

Pumping cost

After the mass flow rates and the pipe diameters have been evaluated, the pressure drops and pumping costs can be computed. The pressure drop at the generic time

instant along the generic pipe is calculated with the Darcy-Weisbach equation (5.15):

$$\Delta p_l^t = 8 * \frac{(f * L_l / D_l + \beta_l) * {G_l^t}^2}{(\rho * D_l^4 * \pi^2)} + \rho * g * \Delta z_l \tag{5.15}$$

Where:

- ρ is the density;
- f is the friction coefficient;
- D_l is the diameter of the pipe l;
- β_l is the sum of the coefficients of localized pressure drops;
- $G_l(t)$ is the mass flow rate flowing in pipe l at time t;
- g is the gravitational acceleration;
- Δz_l is the height difference between the exit and entry node of the pipe l;
- $\Delta p_l(t)$ is the pressure drop on the pipe l at time t.

It is hypothesized that the pumping stations are located in the same positions of the chillers and storages, hence in all the nodes in which mass flow rate enters into the network. The mechanical power provided by the pumps is therefore calculated as defined in Eq. (5.16):

$$P_{pump,mech}^t = \sum_{in}^{Ch \cup St} \frac{G_{ext,in}^t \Delta p_{in}^t}{\rho} \tag{5.16}$$

Where the index *in* refers to the generic chiller or storage node from which a mass flow rate is inserted into the network, Δp_{in}^t is the pressure increase due to the presence of a pump and η_{pump} is the efficiency of the pump. The electric power required by the pumps is computed by dividing the mechanical power with the efficiency of the pumps.

$$P_{pump,el}^t = \frac{P_{pump,mech}^t}{\eta_{pump}} \tag{5.17}$$

The pumping cost is then evaluated multiplying the energy consumed by the pumps in each time interval by the cost of electricity, as defined in eq. (5.18):

$$cost_{pumping} = \sum_t^{\Theta} P_{pump,el}^t * \Delta t * c_{el}^t * n_d * \sum_{n=1}^{n_y} \frac{1}{(1+r)^n} \tag{5.18}$$

5.2.4 Clustering approach and iterative procedure

Also this model is coupled with the clustering approach to ease the convergence of the algorithm. However, in this case, a further iterative procedure has been implemented, which consists in solving the problem with an increasing number of clusters. At each iteration a genetic algorithm is used to solve the problem, using the previous known solution as a member of the initial population.

This method, hence, exploits the knowledge of a coarser optimal solution, obtained with a lower number of variables and searches a more accurate one in its neighbourhood, introducing additional variables. The procedure starts with a sufficiently low number of clusters and at each step, a cluster is divided in two new clusters. The iterations are stopped when the prefixed number of clusters is reached.

5.3 Case studies

The model has been applied to two different case studies in order to demonstrate how it can unleash the full potential of district cooling in different urban contexts. These case studies consider the topology of two existing distribution networks, which are part of the Turin district heating system. They were chosen, since the information about the buildings is known and they have realistic layouts, which can be found also in district cooling networks. A second reason for this choice, is that the two topologies are very different from each other, and the aim of the study is also to show how the optimal layout may change with different shapes of urban districts.

The cooling demand of the buildings has been calculated for a typical summer day using a dynamic model, described in the norm UNI EN ISO 52016-1 [106], whose inputs are only the building volumes and the weather data. The model handles the uncertainty of the thermophysical properties through stochastic distributions.

Figure 5.1 shows the electricity cost curve that was considered for this study. It was extracted from the historical archive of the Italian electricity market. In particular, it was considered the monthly average of the day-ahead market for January 2022 [100].

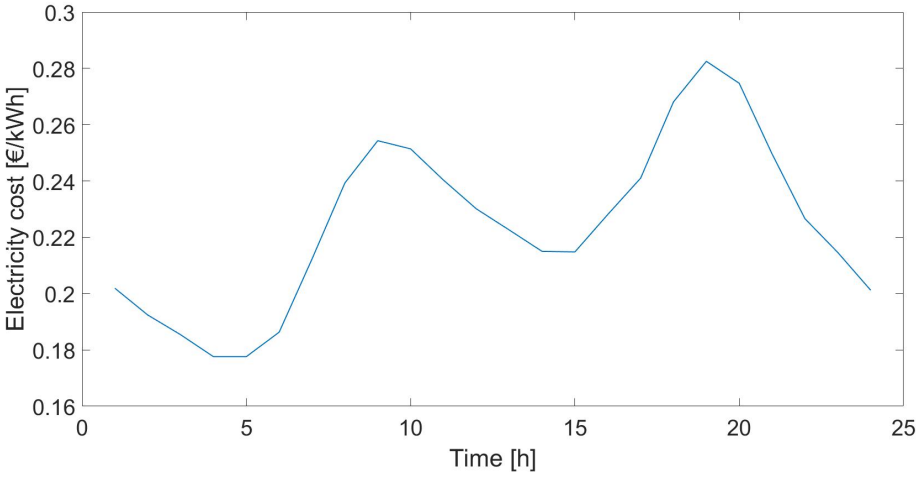

Fig. 5.1 Electricity cost daily variation

Case study 1

The topology of the first case study is the same of the case study B presented in chapter 3. In this case, however, the cooling demand of every building has been calculated using a dynamic model, whose input data are only the volumes of the buildings and the meteorological data. The cooling demand resulting from the simulation model has been then used as an input for the optimization model.

Firstly, it was considered a district cooling network that feeds all the buildings and that has a chiller located in a central position (Figure 5.2). However, this design does not provide any economic advantages if compared to individual cooling. As a consequence, the optimization tool was applied to the case study to find a better configuration that is economically convenient. Three possible positions for chillers and eight possible positions for storages have been considered as shown in Figure 5.3.

Case study 2

The second case study is obtained considering the topology of another Italian residential district heating system. The network is 5.3 km long and feeds 107 users. As for the previous case study, it was first considered a unique network that satisfies all the users in the area and that is fed by a centralized chiller, as shown in Figure 5.4.

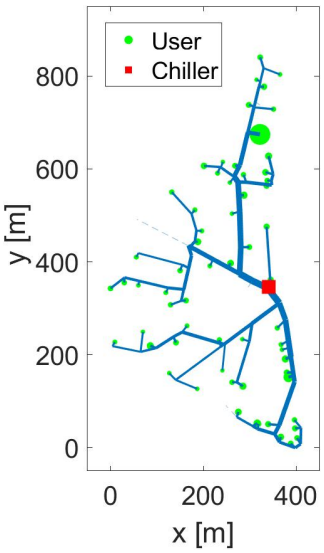

Fig. 5.2 Case study 1: non-optimal network

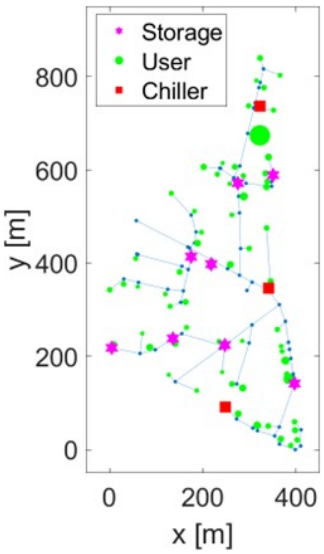

Fig. 5.3 Case study 1: set of possible locations for chillers and storages

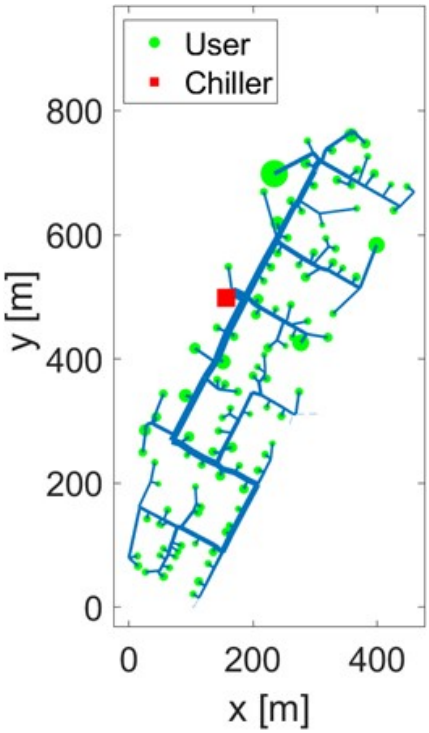

Fig. 5.4 Case study 2: non-optimal network

This network configuration is not optimal and not economically competitive with conventional individual cooling systems, as will be seen in the results reported in the next section. Consequently, the optimization model has been applied also to this case study to find a more feasible solution. Three possible chiller locations and six possible storage locations have been considered, as shown in Figure 5.5

5.4 Results

In this section the main results obtained for both case studies with and without the optimization model are presented. Moreover, the results have been compared with the case in which all users are cooled individually, in order to determine the savings achievable with district cooling.

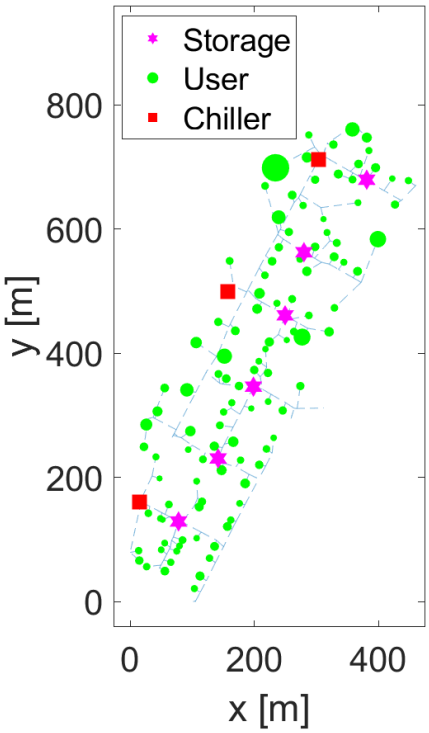

Fig. 5.5 Case study 2: set of possible locations for chillers and storages

5.4.1 Case study 1

In Figure 5.6 the costs relative to the *Case study 1* are shown for three different solutions: the non-optimized single plant district cooling network, the optimal solution, and the case where all the buildings are cooled individually without any district cooling system. It can be observed that the most expensive solution is the non-optimized district cooling network, where the total costs amount to 7.54 M€. This solution is 17.6% more expensive than the conventional one of individual cooling, due to extremely large capital expenditures, which amount to 5.9 M€. The largest costs are represented by piping and the installation of energy transfer stations. Moreover, pumping cost constitutes the 10.7% of operation expenditures, hence it shall not be neglected. These results show that without a smart design, the advantages of a district cooling system are limited or even null, as in this case. However, thanks to the optimization tool, it is possible to reduce the total expenditures and unleash the full potential of district cooling. The total costs amount to 6.1 M€, therefore the optimal solution is 20% cheaper than the non-optimal one, while if compared with individual cooling the costs are 4.8% lower.

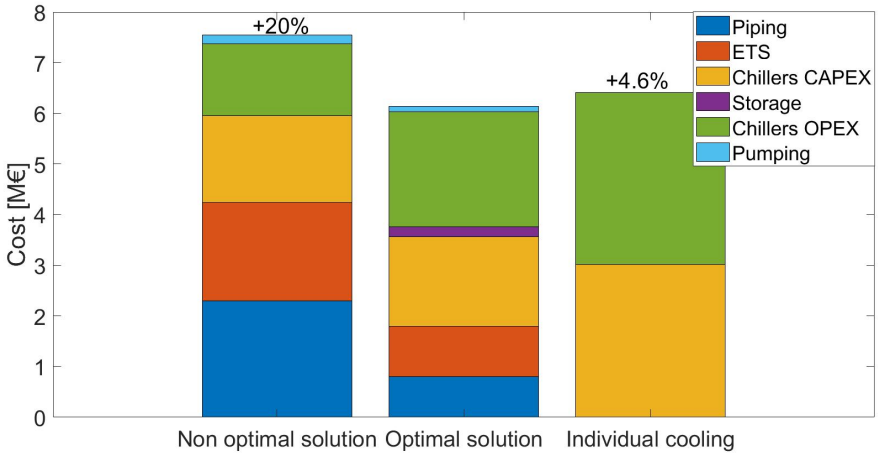

Fig. 5.6 Case study 1: economic results

Figure 5.7 shows the optimal solution layout. It consists of two independent networks that feed two limited portions of the reference area, each fed by a chiller and a storage. This outcome is not surprising, since the solver suggests realizing two networks in the areas with the largest cooling energy demand. Therefore, the solver avoids connecting the other areas, since the capital costs would increase, while the additional savings in terms of operational expenditures would not be significant, due to the lower cooling demand of the other buildings. For the same reason, it is more convenient to install two independent networks, since if they were unified, the total length and therefore the piping and pumping costs would be larger, while only few additional buildings would be connected. Consequently, the larger capital costs would not be compensated by sufficient additional savings in terms of operation costs.

Network energy density

The two district cooling networks have a total length of 1.57 km and satisfy the demand of 30 buildings for a total of 1.4 GWh per year. The average linear energy density is therefore equal to 890 kWh/m. In order to evaluate the threshold of linear energy density for this case study a sensitivity analysis has been carried out varying the pipe lengths. It resulted that the network length could be increased by up to 33% and it would still be more convenient than individual cooling. This means that the threshold linear energy density for this case study is 670 kWh/m. Any value of

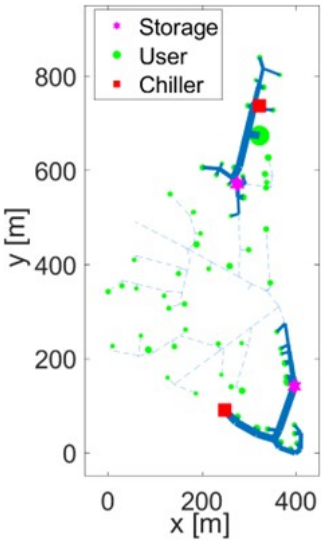

Fig. 5.7 Case study 1: optimal solution

energy density below this threshold would provide a non-convenient district cooling network compared to individual cooling systems.

5.4.2 Case study 2

In Figure 5.8 the economic results for the second case study are shown. Also in this case, without an appropriate network design, district cooling is not convenient. In fact, the non-optimal solution is the most expensive one, with total expenditures that amount to 11.85 M€. Compared to individual cooling, this solution is 6.8% more expensive. Thanks to the optimization tool, these costs can be reduced to 10.58 M€. Hence trough the optimization tool it is possible to save 4.8% of the costs, if compared with individual cooling and 12% if compared with the non-optimized solution. Piping and energy transfer stations costs are reduced by 7%, while the chillers capital expenditures are 52% lower with respect to the non-optimal solution, thanks to the installation of the storages, that allow to dimension the chillers according to average daily demand, rather than on the peaks. The cost of storage installation amounts to 0.57 M€ and represents the 5.4% of total costs. Pumping cost is equal to 0.29 M€ and represents 10.4% of operation costs.

In Figure 5.9 the optimal network configuration is shown. The district cooling system, in this case, is characterised by a unique large network fed by three chillers and three storages. Moreover, most of the buildings are connected to the network,

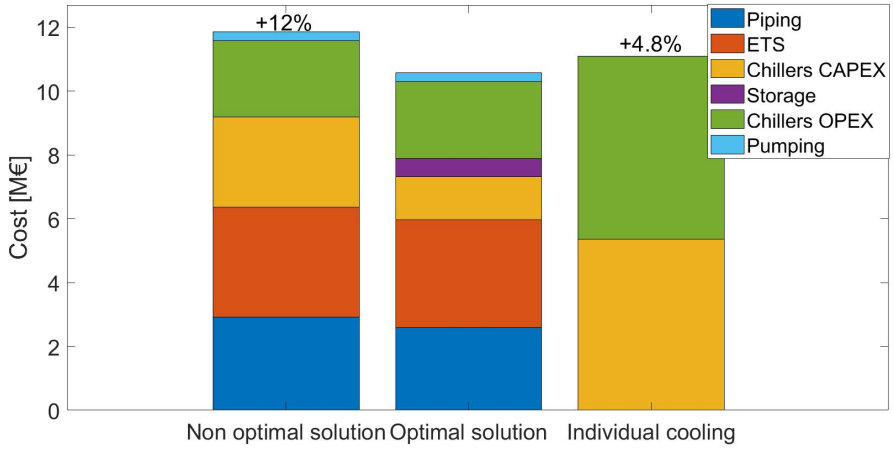

Fig. 5.8 Case study 2: economic results

while only few are cooled with individual systems. In fact, the buildings are more concentrated in this case study, with respect to the previous one, where they are more dispersed. Therefore, this area has a higher potential for district cooling, since the solution suggests that almost all the users should be connected.

Network energy density

The network is connected to 103 buildings, with a total yearly demand of 4.1 GWh and has an extension of 4.9 km. As a consequence the average linear energy density of the district cooling system is 839 kWh/m. The network would be convenient also with branches up to 18% longer. The threshold value for the economic feasibility of district cooling in this case is therefore equal to 711 kWh/m.

5.5 Discussion and concluding remarks

The results of the case studies proved that the optimization tool can be effective in the design phase of a district cooling network. In both case studies the optimization model allowed to find a network configuration economically feasible. Without this tool, it would have been impossible to fully unleash the district cooling potential of these areas.

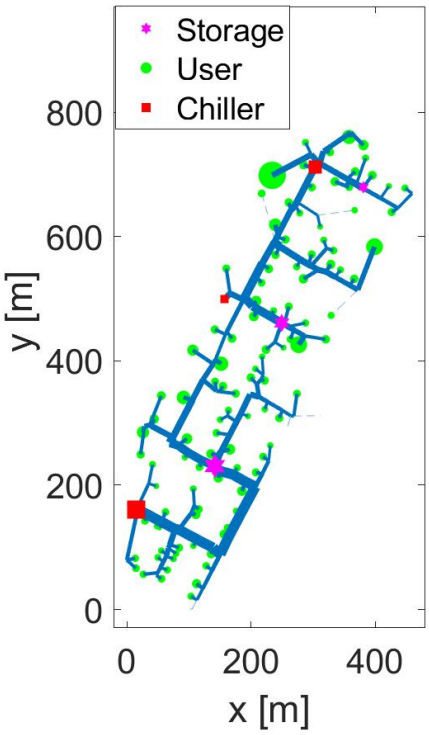

Fig. 5.9 Case study 2: optimal solution

Moreover, the model in the first case study suggested that it would be more convenient to install multiple smaller networks localised in the areas with largest cooling demand, rather than a unique larger network that feeds more buildings. In fact, piping and pumping costs increase with the network width, while the savings in terms of operation costs only depend on the annual cooling demand. As a consequence, it is more convenient to feed smaller areas with larger cooling demand.

The results also showed that the demand density strongly affects the potential of district cooling. In the second case study, indeed, the buildings are more concentrated, and it resulted that a district cooling network is highly convenient and that almost all users should be connected. Moreover, the optimal solution consists in a unique wider network, but fed by three chillers and three different thermal energy storages. It is, in fact, preferable having multiple chillers and storages in different locations in order to minimize the piping and pumping costs. The tool highlighted also the importance of thermal energy storages, that can be used for peak shaving and valley filling, allowing to install smaller chillers, reducing investment costs.

Lastly, it was computed the linear energy density for two optimal solutions and the relative threshold for the economic feasibility of district cooling. The values that were obtained for the two case studies differ by only 5.6%. Consequently, they could be used for a preliminary estimate of the potential of district cooling in an urban context.

Chapter 6

Trade-off between optimal design and operation in district cooling networks

The content of this chapter has been previously published in the following paper [103]:

Manfredi Neri, Elisa Guelpa and Vittorio Verda. "Trade-off between optimal design and operation in district cooling networks" Smart Energy 13(2024): 100127

6.1 Introduction

The previous model implemented in Chapter 5 is able to unleash the potential of district cooling networks, but does not optimize the storage strategy. Indeed, the model is based on the assumption that chillers operate with constant load and that cold storages are only used for peak shaving and valley filling. This allows to minimize the capacity of chillers, but major savings could be obtained by optimizing simultaneously the design and the operation. Indeed, by installing larger chillers and storages, power-to-cool strategies may be adopted and the chillers could be operated more during off-peak hours, in order to exploit the lower electricity prices.

As a consequence, in this chapter, a novel model for the combined design and operation optimization of district cooling networks is presented. The model is defined as a mixed integer quadratic constrained programming and optimizes the position of chillers and storages, their capacities and their daily operation. Contrarily

to the previous implemented models, this one does not optimize the set of buildings to be connected, but uses it as an input parameter, together with the network layout and cooling demand.

The model has been applied to one of the previous case studies and the results have been compared with the ones obtained by the heuristic model presented in Chapter 5 to assess the impact of optimizing simultaneously design and operation. In addition, a sensitivity analysis has also been performed to observe how the results may differ by varying the equipment costs, the electricity prices and the cooling demand. The main goal of this study is therefore to identify in which cases optimizing only the design is sufficient and in which ones a combined optimization of design and operation provides significant benefits.

6.2 Design and operation optimization model

This model has the objective of minimizing the sum of operation and capital expenditures of a district cooling network. The model is non-linear and non-convex and is formulated as Mixed Integer Quadratic Constrained Programming (MIQCP) and solved using Gurobi [107]. The reason for which it is chosen a non-linear non-convex model is linked to the presence of bi-linear constraints, whose linearization is complex to handle. Indeed, it is not possible to linearize all the non-linearities, as it was done with the MILP model in chapter 3, since in this case, multiple chiller plants and storages are considered. Table 6.1 defines the variables of the model, while the sets, indices and the parameters are the same already defined for the heuristic model in Table 5.2 and 5.3.

6.2.1 Cost function

The cost function is the same defined in chapter 5 and is equal to the sum of operation and capital expenditures. There are however two slight differences, due to the fact that the set of buildings to be connected is known a priori. The first is that capital and operation costs of individual chillers are not considered. The second is that the cost of energy transfer stations is a fixed cost, since it does not depend on the decision variables.

Variable	Description
S_j	Size of generic chiller j
S_k	Size of generic storage k
x_l^h	Binary variable equal to 1 if the diameter h is selected for pipe l
G_l^t	Mass flow rate flowing in pipe l at time t
$G_{ext,j}^t$	Mass flow rate entering from chiller j at time t into the network
$G_{ext,k}^{t+}$	Mass flow rate absorbed from storage k at time t
$G_{ext,k}^{t-}$	Mass flow rate released from storage k at time t
C_k^t	Capacity of the storage k at time t
R_l	Fluid dynamic resistance of pipe l per unit of mass flow rate
p_s^t	Pressure on generic node s at time t
Δp_l^t	Pressure drop on pipe l at time t
$Gabs_l^t$	Absolute value of G_l^t
P_j^t	Pumping power required by pump at chiller node j and time t
P_k^t	Pumping power required by pump at storage node k and time t
$G2_l^t$	Product between G_l^t and its absolute value
$Gmax_l$	Maximum mass flow rate flowing in pipe l
yG_l^t	Binary variable that is equal to 1 if the maximum mass flow rate in pipe l occurs at time t

Table 6.1 List of model variables

6.2.2 Constraints

The model is characterized by linear and non-linear constraints, which are defined as follows.

Mass balance constraints

The following constraints ensure that mass balance is respected for every type of node. Eq (6.1) is the mass balance applied to the chiller nodes for all time steps.

$$\sum_{l}^{E} a_{j,l} * G_l^t + G_{ext,j}^t = 0 \qquad \forall j \in Ch, t \in \Theta \tag{6.1}$$

Eq.(6.2) reports the mass balance applied to the storage nodes for all time steps. The variable $G_{ext,k}^{t+}$ represents the mass flow rate absorbed by a storage at the genetic time steps t, while $G_{ext,k}^{t-}$ is the mass flow rate released at time t. The first variable is positive, while the second is negative, as the convention is that the mass flow rate exiting from the network has positive sign, while negative if it is entering in the network.

$$\sum_{l}^{E} a_{k,l} * G_l^t + G_{ext,k}^{t+} + G_{ext,k}^{t-} = 0 \qquad \forall k \in St, t \in \Theta \tag{6.2}$$

Eq. (6.3) represents the mass balance applied to the user nodes for all time steps. In this case, the mass flow rate exiting from the network is known, since it depends on the demand of the users.

$$\sum_{l}^{E} a_{i,l} * G_l^t = - G_{ext,u}^t \qquad \forall u \in Ut, t \in \Theta \tag{6.3}$$

Eq. (6.4) is the mass balance applied to a generic intermediate node v at all time instances. These nodes are characterised by null external mass flow rates.

$$\sum_{l}^{E} a_{v,l} * G_l^t = 0 \qquad \forall v \in S, t \in \Theta \tag{6.4}$$

Constraint in Eq. (6.5) is a balance on the thermal energy storage, linking its variation of residual capacity with the mass flow rates entering or exiting from it, taking into

account the thermal storage efficiency for charge and discharge.

$$C_k^t - C_k^{t-1} - G_{ext,k}^{t+} * c_p * \Delta T * \Delta t * \eta_{charge} - \frac{G_{ext,k}^{t-} * c_p * \Delta T * \Delta t}{\eta_{discharge}} = 0 \quad \forall k \in St, t \in \Theta \tag{6.5}$$

Moreover, the additional constraint in Eq. (6.6) is added in order to impose a daily cycle of charge/discharge.

$$C_k^0 - C_k^N - G_{ext,k}^{0+} * cp * \Delta T * \Delta t * \eta_{charge} - \frac{G_{ext,k}^{0-} * c_p * \Delta T * \Delta t}{\eta_{discharge}} = 0 \quad \forall k \in St \tag{6.6}$$

where the superscripts 0 and N refer to the first and last time steps.

Capacity constraints

The constraint in Eq. (6.7) ensures that the cooling power produced by a chiller is not larger than its capacity.

$$G_{ext,j}^t * c_p * \Delta T \leq S_j \qquad \forall t \in \Theta, j \in Ch \tag{6.7}$$

Constraint in Eq. (6.8) instead guarantees that the maximum storage capacity is not exceeded.

$$C_k^t \leq S_k \qquad \forall k \in St, t \in \Theta \tag{6.8}$$

Pressure constraints

Constraint in Eq. (6.9) defines the pressure drop in a generic pipe. Since the pressure drop depends on the square of mass flow rate, a new variable called $G2_l^t$ is introduced to represent the product between mass flow rate and its absolute value. This is different than the square of mass flow rate, which is always positive, since in this case the pressure drop and the mass flow rate must have the same sign.

$$\Delta p_l^t - G2_l^t * \sum_m^M x_l^m * R_l^m = 0 \qquad \forall t \in \Theta, l \in E \tag{6.9}$$

Constraint in Eq. (6.10) links the pressure at the inlet and outlet of each pipe with its pressure drop. The indices l_{in} and l_{out} indicate the input and outlet nodes of the generic pipe indexed by l.

$$p^t_{l_{in}} - p^t_{l_{out}} - \Delta p^t_l = 0 \qquad \forall t \in \Theta, l \in E \tag{6.10}$$

Constraint in Eq. (6.11) guarantees that the pressure at user nodes is larger than a minimum value.

$$p^t_u \geq p_{min} \qquad \forall u \in Ut, t \in \Theta \tag{6.11}$$

The bilinear constraints in Eq. (6.12) and (6.13) define the variables P^t_j and P^t_k, which represent the electrical power required by the pumps located in chillers and storage nodes.

$$P^t_j + G^t_{ext,j} * \frac{p^t_j}{\rho * \eta_{pump}} = 0 \qquad \forall j \in Ch, t \in \Theta \tag{6.12}$$

$$P^t_k + G^{t-}_{ext,k} * \frac{p^t_k}{\rho * \eta_{pump}} = 0 \qquad \forall k \in St, t \in \Theta \tag{6.13}$$

Constraint in Eq. (6.14) defines the variable $G2^t_l$ as the product between the mass flow rate flowing in branch l at time t and its absolute value.

$$G2^t_l - Gabs^t_l * G^t_l = 0 \qquad \forall l \in E, t \in \Theta \tag{6.14}$$

Absolute value is not a linear function; therefore it is linearized by introducing the constraints in Eq. (6.15) and (6.16), which ensure that the variable $Gabs^t_l$ is equal to the absolute value of G^t_l.

$$-Gabs^t_l + G^t_l \leq 0 \qquad \forall l \in E, t \in \Theta \tag{6.15}$$

$$Gabs^t_l + G^t_l \geq 0 \qquad \forall l \in E, t \in \Theta \tag{6.16}$$

Topology constraints

Constraint (6.17) guarantees that only one diameter is selected for each pipe.

$$\sum_{m}^{M} x_l^m = 1 \qquad \forall l \in E \tag{6.17}$$

Constraints (6.18) and (6.19) restrict the maximum mass flow rate in each pipe to a defined range.

$$Gmax_l - \sum_{m}^{M} x_l^m * maxG^m \leq 0 \qquad \forall l \in E \tag{6.18}$$

$$Gmax_l - \sum_{m}^{M} x_l^m * minG^m \geq 0 \qquad \forall l \in E \tag{6.19}$$

Constraints (6.20) and (6.21) ensure that the variable $Gmax_l$ is equal to the maximum mass flow rate in branch l. These auxiliary constraints therefore linearize the max function, introducing additional binary variables. The first is a *big-M constraint*, where H is a constant whose value is larger than the upper bound of $Gmax_l$. Consequently, if the maximum occurs at t, yG_l^t is equal to zero and in order to satisfy both constraints, $Gmax_l$ must be equal to $Gabs_l^t$. If the maximum occurs at another instant different than t, the first constraint is satisfied only if yG_l^t is equal to one.

$$Gmax_l - yG_l^t * H - Gabs_l^t \leq 0 \qquad \forall l \in E, t \in \Theta \tag{6.20}$$

$$Gabs_l^t - Gmax_l \leq 0 \qquad \forall l \in E, t \in \Theta \tag{6.21}$$

6.3 Case study

The model has been applied to the *case study 2* of chapter 5. Both cooling demand and the electricity cost profile are shown in Figure 6.1. It can be observed that the demand is larger in the time interval between 10 AM and 8 PM, reaching a peak demand of about 7 MW. The electricity cost presents two peaks at 8 AM and 7 PM. During the night, the cooling demand is null since HVAC systems are mainly operated during the day in the warmest hours. However, also electricity cost is low, reaching a minimum at 5 AM, due to the lower electricity demand during the night. These profiles suggest the possibility to implement power-to-cool strategies.

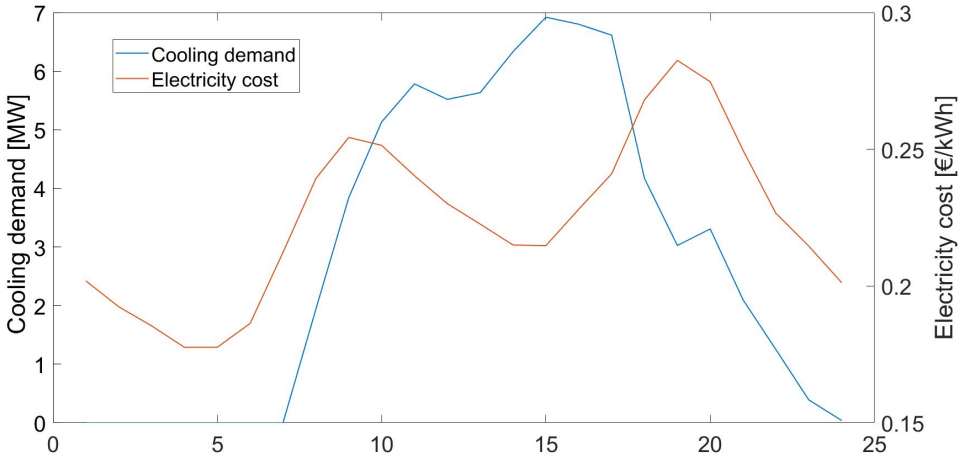

Fig. 6.1 Daily profiles of cooling demand and electricity cost

In particular, chillers could operate at higher load during the night, when electricity is cheaper and the demand is low. The cooling energy could be therefore stored and released when the electricity is expensive and demand is larger. This strategy has a limit, which depends on the size of chillers and pipes. In fact, if only operation costs are considered, the optimal solution would be to produce the whole daily cooling demand when the electricity cost is minimum. However, this solution would require extremely large components and the capital costs would be too large. Conversely, if only capital costs are minimized, the solution would consist in a constant cooling production, since in this way the size of chillers and pipes would be minimum. On the other hand, the operation schedule in this solution would not be optimal. As a consequence, one of the goals of this analysis is to determine if there is a trade-off between the two solutions. The objective is therefore to verify if it is beneficial installing larger chillers and pipes in order to be able to have a better operation schedule and to obtain major savings.

6.4 Results

In this section are presented the results obtained by the heuristic and the Mixed Integer Quadratic Programming Models. The simulations have been carried out on a laptop with the CPU Intel Core i7-510 1.8 GHz.

Chiller/storage coord. (x,y)	Size (Operation and design opt)	Size (Design opt.)
(380.8374,679.2562)	4.9 MWh	5.1 MWh
(141.6696,230.7191)	14.5 MWh	13.9 MWh
(249.4144, 461.0040)	9.3 MWh	9.0 MWh
(303.7968, 712.3305)	1.0 MW	0.7 MW
(157.0443, 499.1148)	0.5 MW	1.0 MW
(15.3938, 160.3585)	1.6 MW	1.4 MW

Table 6.2 Sizes of chillers and storages

6.4.1 Design optimization (heuristic)

The maximum number of clusters was fixed to 20 and the model took 25 minutes to find the optimal solution, which is shown in Figure 6.2a. According to the solution, 103 out of 107 users should be connected to the district cooling network and three chillers should be installed, each connected to a different storage.

6.4.2 Design and operation optimization (MIQCP)

The optimal set of users and the network layout found with the heuristic algorithm has been considered as an input for the MIQCP model. The demand profile is therefore known, while the sizes of chillers and storages is optimized, as well as their scheduling. The optimization did not converge to the global optimum in three days. However, it was found a solution with an optimality gap of 2%, which means that the local optimum found is, to the utmost, 2% more expensive than the global one. The large computational cost and the difficulty to converge are due to the large number of variables and the bilinear constraints, which not only are non-linear, but also they cause the non-convexity of the problem.

In Figure 6.2b the resulting optimal network layout is shown. The sizes of chillers and storages are slightly different from the ones obtained with the design optimization model. In fact, the total storage and chiller capacity is almost the same, but it is distributed differently in the two solutions. This is also summarized in Table 6.2.

In Figure 6.3 the optimal hourly scheduling for chillers and storages is shown. It can be observed that the cooling power produced by the chillers is almost constant during the day, since the ratio between the average and the peak load is 98%. The

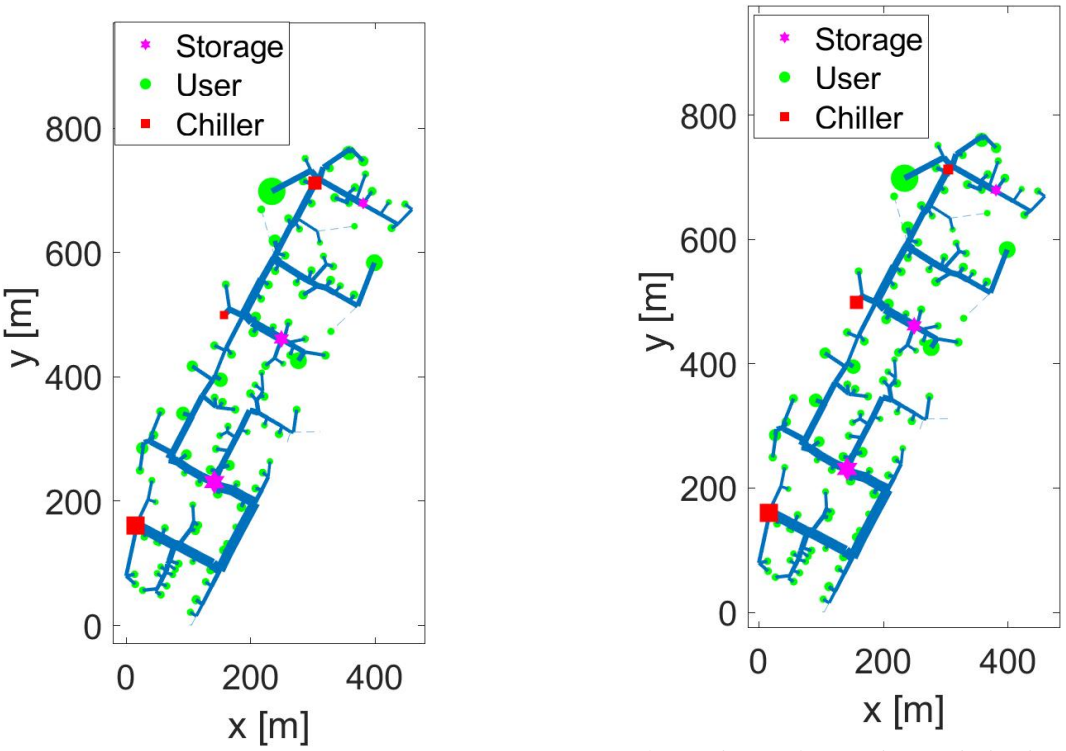

(a) Design optimization model

(b) Design and operation optimization model

Fig. 6.2 Optimal network design according to the two models

storages are therefore used mainly for peak shaving and valley filling. They, in fact, store the extra cooling energy produced during the night and release it when the production of chillers alone can not satisfy the demand.

Figure 6.4 shows the cost details of this solution and the comparison with the design optimization solution. With respect to the solely design optimization, the costs are 0.5% lower. The results therefore are similar to the solution obtained with the design only optimization model.

6.5 Sensitivity analysis

The previous results show that for this case study it is possible to design and size a district cooling network considering a constant cooling power production by the chillers with negligible cost increase. Indeed, the results obtained with the model for both design and optimization are very similar to the ones obtained with the model for

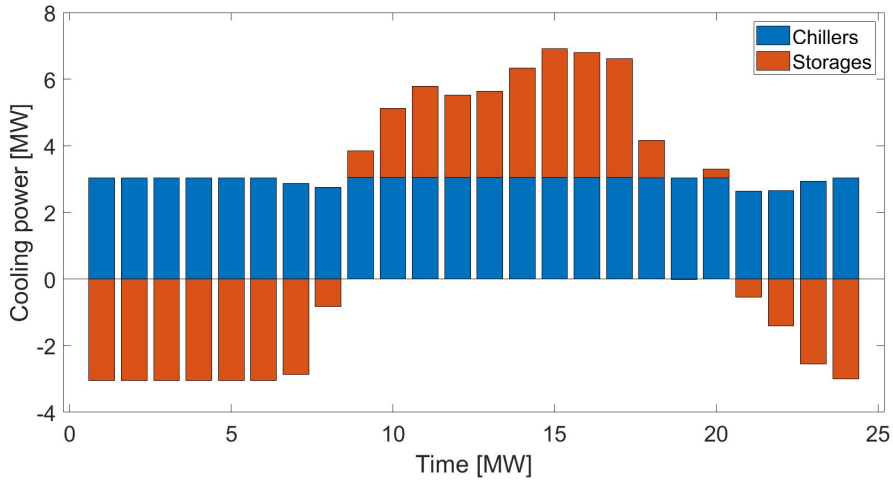

Fig. 6.3 Optimal chillers and storages hourly scheduling

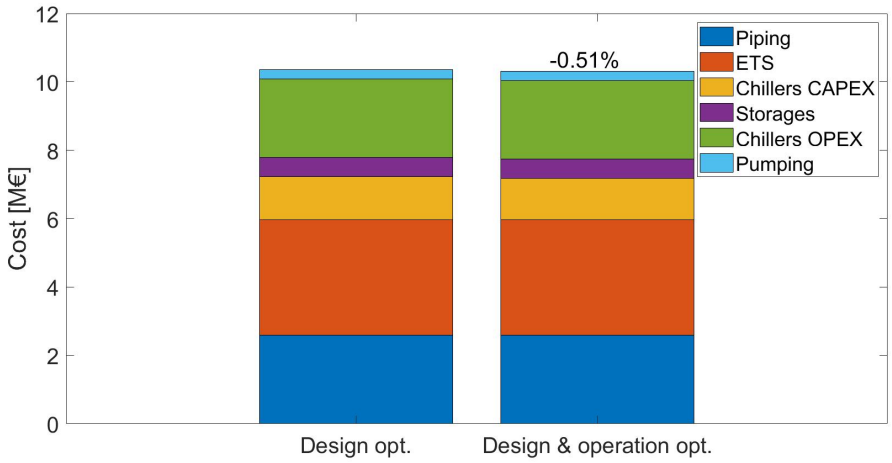

Fig. 6.4 Cost comparison between the optimal solutions obtained by the different models

design optimization. However, the savings obtained by optimal operation depend on the electricity cost, cost of equipment and number of cooling days. Electricity cost is highly uncertain as it can vary significantly, as a response to market trends and geopolitical crisis. Equipment cost is also uncertain, as in literature it is common to find price ranges, but not the exact values, which depend on many factors, such as the labour cost for installation, which varies from country to country. Lastly, the number of cooling days depends mainly on the climate zone.

In this section the results of a sensitivity analysis are presented. This is done to determine how these parameters influence the optimization results and how the

Scenario	Electricity cost profile	Capital cost of centralized chillers	Number of cooling days
0	Standard (January 2022)	400 €/kW	60
1	Middle (January 2022+50%)	400 €/KW	60
2	High (May 2022)	400 €/kW	60
3	Standard (January 2022)	320 €/kW	60
4	Standard (January 2022)	480 €/kW	60
5	Standard (January 2022)	400 €/kW	300
6	High (May 2022)	400 €/kW	300

Table 6.3 Summary of scenarios

operation strategy of chillers and storages changes with larger electricity cost or cooling demand and with different equipment installation costs. Hence, the analysis has been carried out on seven different scenarios, differing in terms of electricity cost profile, capital cost of centralized chillers or number of cooling days.

Figure 6.5 shows the electricity cost profiles considered for this analysis. *Scenario 0* indicates the standard scenario used in the previous simulations, while in *Scenario 1* and *Scenario 2* two different cost profiles were considered. *Scenario 1* is obtained increasing by 50% the electricity cost of *Scenario 0*. *Scenario 2* was instead obtained by selecting a day of May 2022, in which it was observed a large peak of electricity cost and a wide difference between minimum and maximum electricity cost. This therefore does not represent a typical profile, observable every day, but it is rather an exception and an extreme situation that occurred during a period characterized by high electricity cost, due to different external geopolitical factors. *Scenario 2* therefore offers more opportunities for scheduling optimization. The two scenarios, named *Scenario 3* and *Scenario 4*, instead, are obtained by lowering or increasing the capital cost of chillers by 20% with respect to *Scenario 0*. Lastly, *Scenario 5* and *Scenario 6* are obtained considering a larger number of cooling days and the cost profiles used in *Scenario 0* and *Scenario 2*, respectively. These two scenarios were considered to determine how the results can differ if cooling demand is not seasonal. Table 6.3 summarizes the parameters used for all the seven scenarios.

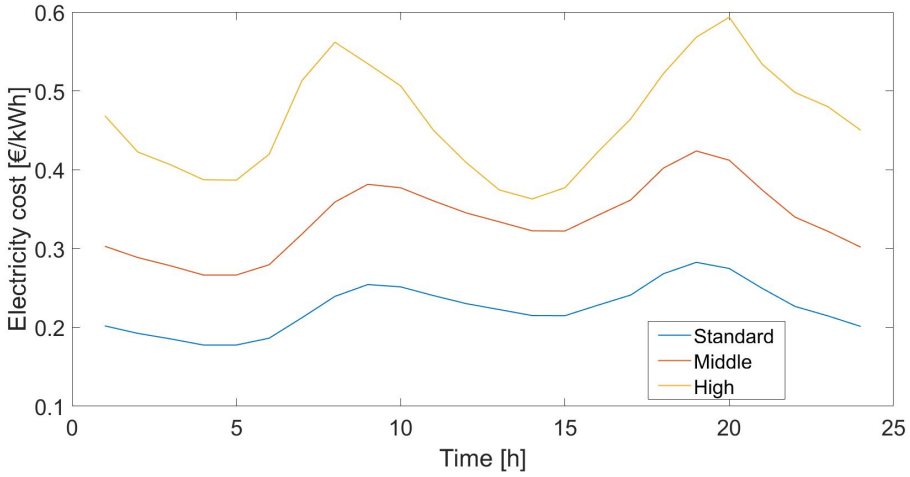

Fig. 6.5 Electricity cost profiles taken into account

6.5.1 Results

In the following subsections the optimal operation strategy is presented for each of the scenarios. In addition, Figure 6.6 shows the comparison in terms of total costs between design only and combined optimization model solutions for all the new scenarios.

Scenario 1

Figure 6.7 reports the hourly chiller and storage operation for scenario 1, obtained through the model for optimal design and operation. In this case, the chillers tend to operate almost constantly during the whole day, apart from 8 AM and in the evening, when the production is sensibly lower. In particular, at 9 PM the cooling power produced by the chiller is minimum and equal to 2.15 MW, while the maximum is 3.14 MW. The ratio between average and peak cooling production is equal to 95%, since the load is sensibly lower only in few hours, while in the rest of the day is almost constant.

As shown in Figure 6.6, for Scenario 1 the design and operation optimization (MIQCP) model allows to save 0.34% more in terms of total life cycle costs with respect to the solution obtained the design optimization (heuristic).

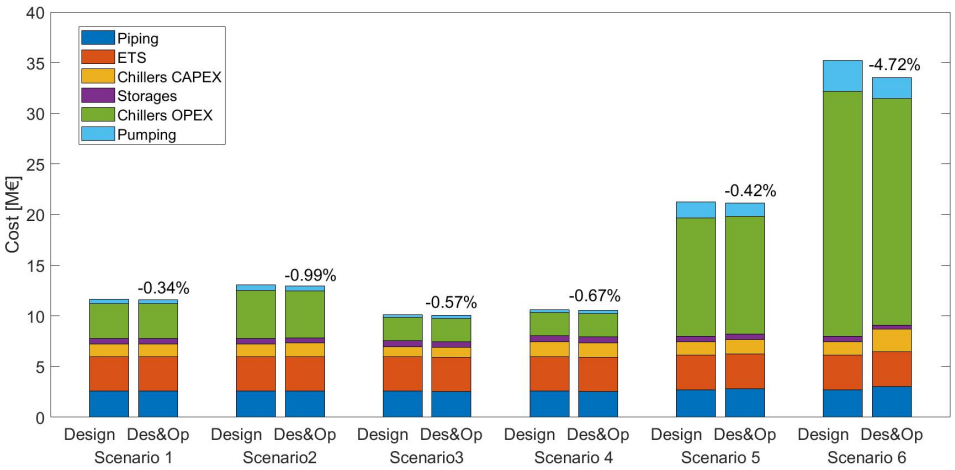

Fig. 6.6 Cost comparison between model solutions in different scenarios

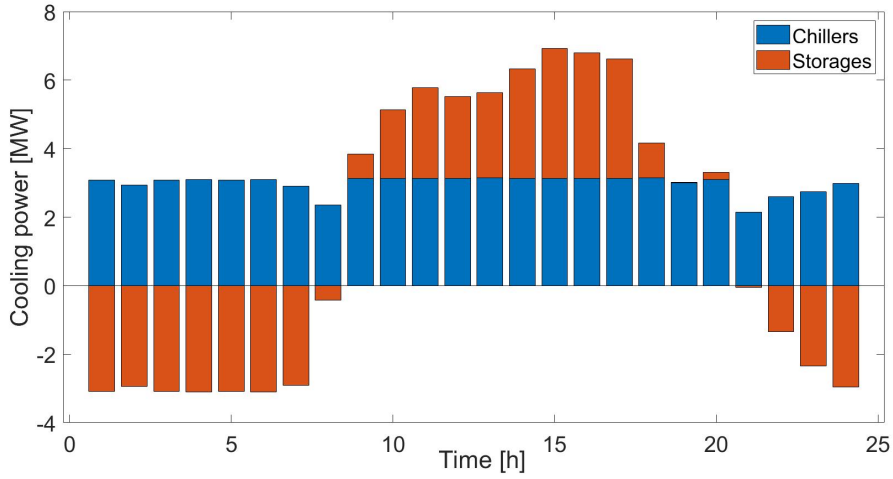

Fig. 6.7 Optimal operation in scenario 1

Scenario 2

Figure 6.8 shows the optimal hourly operation according to the design and operation optimization model for *Scenario 2*. In this case, the chillers operation tends to exploit more the variations of the electricity cost. The cooling power, indeed, ranges between 0.95 MW and 3.46 MW. Hence, compared to the Scenario 0, the installed chiller capacity is 11.6% larger. On the other hand, the ratio between the average and peak cooling production (capacity factor) is 86%.

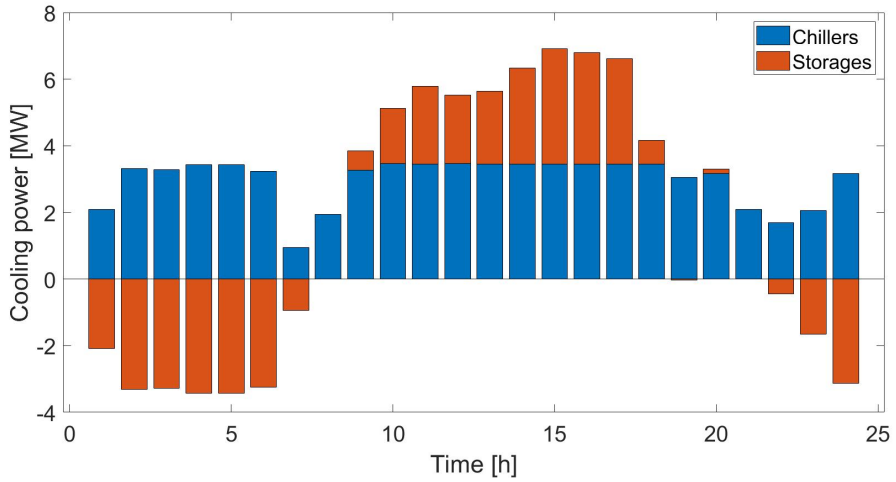

Fig. 6.8 Optimal operation in scenario 2

Figure 6.6 shows that in *Scenario 2* the additional savings that the design and operation optimization model allow to achieve amount to 1% with respect to design only optimization.

Scenario 3

Figure 6.9 shows the optimal daily operation according to the design and operation optimization model for *Scenario 3*. Also in this case, the cooling production is almost constant during the day. In particular, only in the two hours with highest cost of electricity, the production is lower than 2.1 MW, while for the remaining 22 hours, the chillers operate constantly with a total load of 3.05 MW. The ratio between average and maximum load is 97%.

Figure 6.6 shows that in this scenario, optimizing simultaneously operation and design would allow to save 0.57% more with respect to optimizing only the design.

Scenario 4

Figure 6.10 shows the optimal schedule of chillers and storages according to the design and operation optimization model for *Scenario 4*. In this case, the chillers operate constantly, with a load of 2.99 MW, hence the ratio between average and maximum load is 100%.

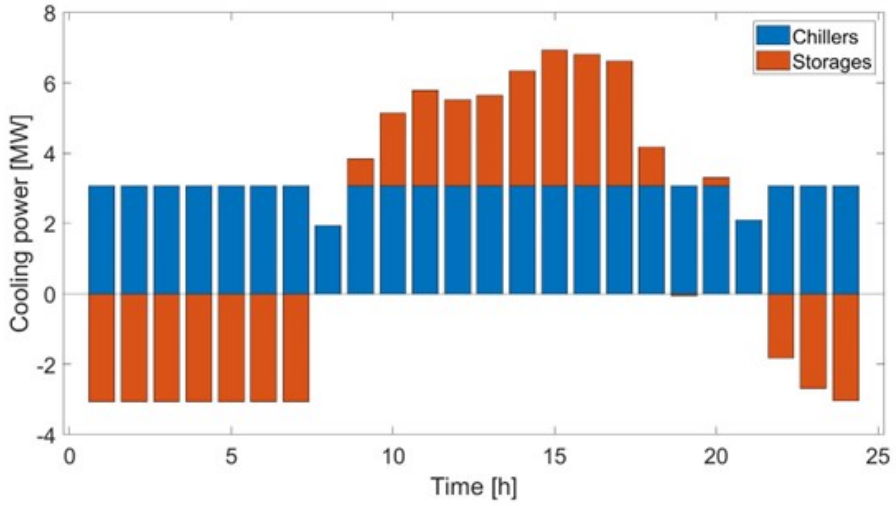

Fig. 6.9 Optimal operation in scenario 3

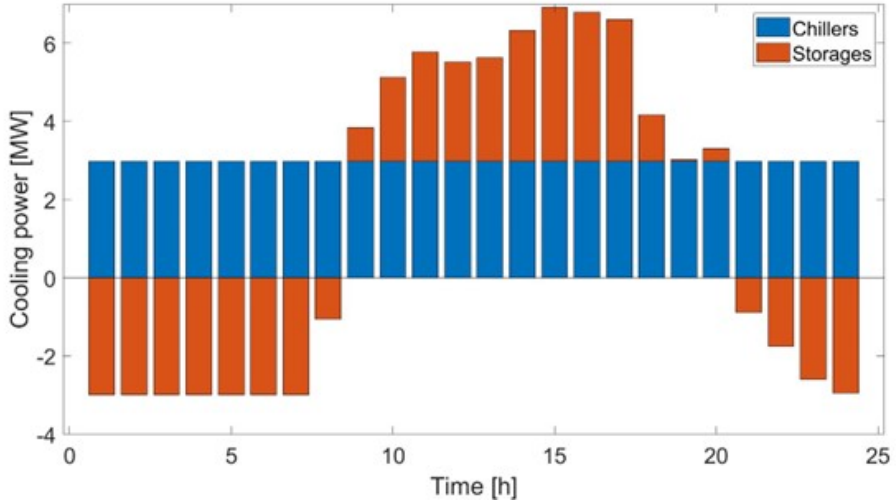

Fig. 6.10 Optimal operation in scenario 4

Figure 6.6 shows that for *Scenario 4*, the design and operation optimization solution is 0.7% less expensive, with respect to the one obtained by the design only optimization model. The reason for the difference, in this case is related to the assumption made in the design optimization model, for which the cooling production of chillers is discrete, rather than continuous, as it depends on the buildings that should be fed. On the other hand, the design and optimization model is more flexible, since the chillers can operate freely as long as the network energy and mass balances are respected. As a consequence the search space is wider and a better solution can be found.

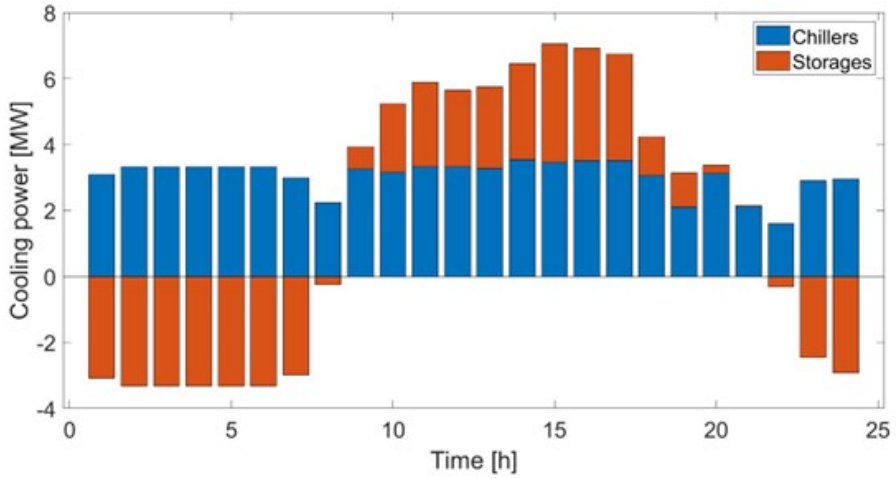

Fig. 6.11 Optimal operation in *Scenario 5*

Scenario 5

Figure 6.11 shows the optimal dispatch of cooling power from chillers and storages for *Scenario 5*. The maximum, minimum and average cooling power produced by the chillers are 3.54 MW, 1.61 MW and 3.04 MW, respectively. The chiller capacity factor is therefore 86%, which is sensibly lower compared to scenario 0.

Figure 6.6 shows that in this case, optimizing simultaneously operation and design allows to save 0.4% more in terms of total life cycle costs.

Scenario 6

Figure 6.12 shows the optimal daily operation for *Scenario 6*. It can be observed that the chiller production is very discontinuous and not constant. The maximum cooling power produced by the chillers is 5.4 MW, with a capacity factor of 56%.

From Figure 6.6 it can be observed that in *Scenario 6*, characterised by the maximum fluctuation of electricity cost and days of use of the district cooling system, optimizing simultaneously design and operation allows to save 4.7% more with respect to optimizing only the design. It can also be observed that in the design and operation optimization solution the cost for chillers installation is higher, but this is compensated by lower cost of chillers operation and pumping.

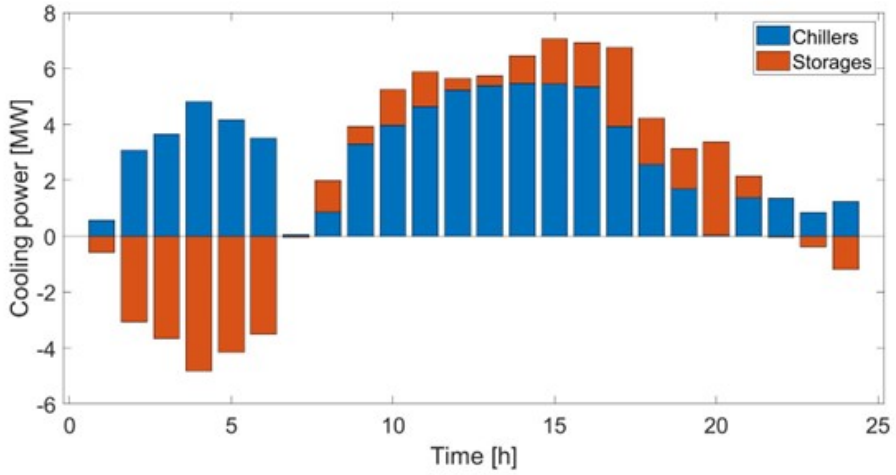

Fig. 6.12 Optimal operation in scenario 6

6.6 Discussion and concluding remarks

The design optimization model manages to optimize simultaneously the position of chillers and storages and the set of buildings to be connected, while keeping the computational time low, thanks to the combination of the iterative algorithm and the clustering approach. In case of larger electricity costs, with daily fluctuations, the model may provide non-optimal results, as it optimizes only the design. On the other hand, the sensitivity analysis showed that if cooling demand is seasonal, even with larger volatility in the electricity prices, the relative difference in terms of objective function from the optimum found with a design and operation optimization model is around 1%.

The design and operation optimization model manages to optimize both the size of the equipment and the operating schedule. If on one hand the model is more accurate than the first one, on the other hand it is highly computationally expensive, due to the complexity and the presence of non-linearities.

The results obtained for scenarios from 0 to 4, show that the scheduling optimization of the district cooling network does not influence the design, hence operation and design optimization problems can be separated. The priority is to minimize the capital expenditures, which represent most of life cycle costs. The optimal solution suggests, indeed, to operate the chillers at constant load, minimizing in this way the capital costs, since pipes and chillers would need smaller sizes due to the absence

of peak load. Hence, the impact of operation optimization is negligible and optimizing simultaneously the operation and the design of a district cooling network is not necessary. Similar results are achieved with different electricity tariffs. The sensitivity analysis also showed that by lowering the chiller costs, the results do not change sensibly. The analysis hence confirmed that within the ranges of chiller and electricity costs considered in the sensitivity analysis, the size of chillers in district cooling systems can be chosen so that they can operate at constant load. The installation of larger chillers would be justified only for larger differences between peak and off-peak electricity prices. In that case, the operation savings would be larger and could compensate the larger initial investment.

The sensitivity analysis also showed that if cooling demand is not seasonal, but is present throughout the entire year (scenarios 5 and 6), the impact of optimizing simultaneously design and operation is higher. Indeed, in these cases the relative difference in terms of total costs between the two models can be as high as 4.7% if there is sufficient difference between off-peak and peak tariffs. Hence, if cooling demand is not seasonal, the model that optimizes both design and operation would be more appropriate, especially if there is large volatility of electricity price.

Chapter 7

Design and operation optimization of a district cooling network in Singapore

7.1 Introduction

In this chapter, the heuristic design optimization model is further improved and integrated with MILP models, forming a hierarchical structure to solve a more complex optimization problem, compared to the ones presented in the previous chapters. The objective of this model is to optimize not only the topology, the set of buildings to connect and the position of chillers, but also the operation, the network supply temperature and the storage technology to be installed. Indeed, the new model takes into account the space occupancy costs and the effects of supply temperature on the chillers EER and on pumping costs.

Moreover, the previous models are based on the assumption that centralized chillers are more efficient than individual ones. While this is true for buildings with small cooling demand, where chillers with smaller capacities are installed, it may not be the case for buildings with larger cooling demand, such as malls or offices. Indeed, in these buildings it is possible to just install large efficient chillers, without the need to connect them to a district cooling network. In these cases the economic advantages of district cooling systems compared to individual cooling solutions are less evident. However, district cooling can be still economically feasible for

different reasons. The first is that the operation of chillers in district cooling systems is closer to design conditions, thanks to the installation of multiple capacities that reduce chiller operation in partial load conditions. The second main reason is that district cooling networks can rely also on free sources (i.e. waste heat from industrial plants or free cooling from large water basins) which help to obtain further energy and cost savings, compared to individual cooling systems. Thirdly, few centralized chillers tend to occupy overall less space than the multiple residential ones. As a consequence, district cooling can help reducing space occupancy, which in the major cities can represent a non-negligible cost. Lastly, integrating district cooling networks with thermal storage allows to reduce the capacity of installed chillers and their operation costs.

These gaps have been addressed by optimizing the design and operation of a district cooling network in a neighbourhood of Singapore, characterised by commercial and office buildings with large cooling demand. Different scenarios have been considered to study the impact of increasing the indoor set point temperature and how the presence of waste heat can enhance district cooling potential, reducing the total costs and the payback time. In addition, the influence of electricity tariff structure and space occupancy cost on the optimal network topology and on the design and operation of chillers and storages has also been analysed.

7.2 Hierarchical model

The objective of the model is to optimize the design and operation of district cooling systems, minimizing the total overall costs, characterised by the sum of capital and operation expenditures. In particular, the model optimizes the following aspects:

- the set of buildings to be connected;
- the pipe diameters and network topology;
- the position of production plants;
- the capacity and hourly operation of chillers and storages;
- the type of storage technology;
- the network supply temperature.

The model represents a further improvement to the previous implemented heuristic approach. It is based on a hierarchical structure, characterised by a master problem at superior level and two groups of subproblems at inner level. The master problem is solved by a genetic algorithm that finds iteratively the optimal values of its variables, and at each iteration the subproblems are solved by means of Mixed Integer Linear Programming models.

The objective of the genetic algorithm is to find the optimal set of buildings to be connected to the district cooling network, the position of the plants, the supply temperature and the maximum velocity admissible in each commercial diameter. The goal of the first class of subproblems is to optimize the capacity and operation of chillers and storages in each plant. As a consequence, for each plant a MILP problem is solved to find the optimal capacity of chillers and storages and the daily operation. The objective of the second subproblem is instead to optimize the network topology, providing as output the tree-network with the shortest total length.

The subproblems are solved, fixing the master problem variables. The latter are varied iteratively through the genetic algorithm and at each iteration the values of the variables are used as input parameters to solve the two classes of subproblems, whose outputs are needed to compute the master problem cost function. The model has therefore a nested structure, where the outer part is characterised by the master problem. The flowchart of the hierarchical model is shown in Figure 7.1.

7.2.1 General assumptions

The hierarchical model is based on the following assumptions.

- Different plant positions can be selected and each of them includes chillers and thermal storages.
- Heat gains in pipes are neglected due to the low temperature difference between the network and the ground.
- The demand of each building is always satisfied by a specific plant.
- When varying the network supply temperature, the heat transfer areas of heat exchangers are assumed to be constant. It is assumed that the logarithmic average temperature difference between the secondary and primary loops

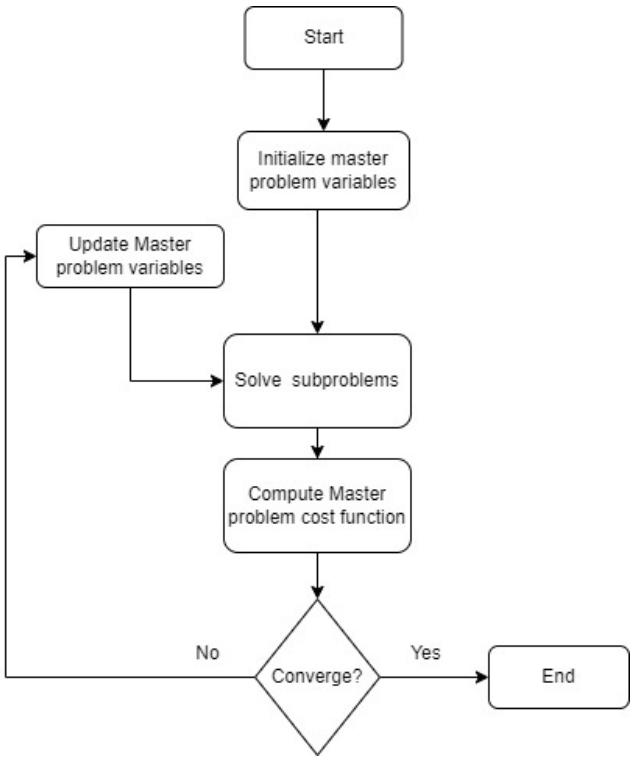

Fig. 7.1 Hierarchical model flowchart

can be considered constant. Consequently, if network supply temperature increases, the return temperature decreases to maintain the same logarithmic temperature difference.

- The impact of partial load on the EER of chillers is taken into account in the case of individual chillers, but it is neglected in the case of centralized chillers. This assumption enables a simplification of the model without affecting the results. Indeed, according to the results, the centralized chillers tend to work almost always at full load, thanks to the peak shaving enabled by thermal storages (Figure 7.10). Moreover, since multiple chillers are installed in each plant, when demand is lower, it could be possible to turn on just few of the installed chillers, maximising their efficiencies.

- Only a storage technology can be installed in each plant.

- Sensible thermal energy storage is charged using chilled water at the network supply temperature, while ice and PCM storages require cooling power at -5°C and 3°C, respectively.

7.2.2 Master Problem

Variables

The master problem is characterised by three different types of decision variables. As in the heuristic model of chapter 5, the first group of variables is formed by the integer variables x_u, which indicate by which plant the demand of the building u is satisfied. These can range from zero to the number of possible plant positions. The values assumed by these variables are therefore indices pointing to specific plant sites. The difference with the heuristic model of Chapter 5 is that in this case, it is assumed that the storages are installed in the same locations of the chiller plants.

The second group includes continuous variables named $vmax_m$, which indicate the velocity limit for every commercial diameter. These are used therefore to select the pipe diameters, after the evaluation of the mass flow rates.

Finally, the last group is characterised by only one continuous variable, $T_{ch,s}$, which indicates the supply temperature of the network. Its upper bound depends on the supply temperature of the secondary loop, as it is assumed that the temperature difference at the pinch-point must be greater than 2°C for technical reasons.

Cost function

The objective is to minimize the sum of capital and operation expenditures. In this case, however, also occupancy costs are taken into account. The investment and operation costs of individual chillers can be directly computed, once the master problem variables are set. The capital and space occupancy costs of individual chillers installed in the buildings not connected to the district cooling network are computed as defined in equations (7.1) and (7.2):

$$cost^{cap}_{ch,ind} = \sum_{u|x_u=0}^{Ut} c^{i}_{chill,ind} \tag{7.1}$$

$$cost^{occ}_{ch,ind} = \sum_{u|x_u=0}^{Ut} s^{u}_{ch,ind} * c_{occ} * \sum_{n=1}^{N_y} \frac{1}{(1+r)^n} \tag{7.2}$$

where $c^{u}_{chill,ind}$ is the capital cost of the chillers to be installed in building u, $s^{u}_{ch,ind}$ is the space occupied by the chiller and c_{occ} is the yearly cost of space occupancy per

unit of surface, while the terms needed to compute the actualization factor, r and N_y, are the interest rate and the lifetime of the investment, respectively.

The operating costs of individual chillers are evaluated as:

$$cost^{op}_{ch,ind} = \sum_{u|x_u=0}^{Ut} \sum_{t}^{\Theta} Q^t_u / EER^t_u * c^t_{el} * \Delta t * \sum_{n=1}^{N_y} \frac{1}{(1+r)^n} \tag{7.3}$$

where Q^t_u is the cooling demand of building u at time t, while EER^t_u and c^t_{el} are the energy efficiency ratio of the chiller and the cost of electricity at time t, respectively. The EER indeed depends on the chiller load and on the outdoor temperature, which differs between day and night. The cost of electricity is also function of time, since the tariff is different during peak and off-peak hours.

The other cost terms can be evaluated only after solving the inner subproblems. The solutions of the capacity and operation optimization subproblems provide the operating and the investment costs of centralized chillers and thermal storages installed in each plant site. Piping and pumping costs are instead computed once the topology is optimized. Indeed, the optimization of the topology allows to evaluate the mass flow rates by solving the system of mass balance equations. This allows also to choose the pipe diameter for each pipe. In particular, it is selected the smallest feasible commercial diameter for which the flow velocity is lower than the specified limit $vmax_m$, which is defined when setting the master problem variables.

7.2.3 Capacity and operation optimization of chillers and storages

One of the subproblems to be solved is the optimization of the capacity and operation of chillers and storages. The chiller positions and the cooling demand they supply are determined through the master problem variables, while the optimal size and operation of chillers and storages in each plant are found by means of a Mixed Integer Linear Programming(MILP) model.

This model selects the quantity of chillers to install choosing from different types that have different capacities. In addition, absorption chillers may be installed, if waste heat is available in the plant site. The storage size and the technology type are also selected by the model, which can choose between ice, a commercial PCM,

Type	Cost	Latent heat [kJ/kg]	Density [kg/m^3]	Charging temperature [° C]	Life cycle [y]
Ice	50 €/m^3	350	917	-5	30
Commercial PCM	10 €/kWh	180	800	3	10
STES	50 €/m^3	0	1000	4-9	30

Table 7.1 Thermal storage properties

and sensible thermal storage. Ice and PCM are characterised by higher volumetric capacity, thanks to the latent heat, but they require lower supply temperatures during the charging phase. The main properties of the three technologies are all reported in table 7.1.

Variables

The variables and the parameters of the model are described in Table 7.2 and 7.3. The hourly cooling demand and the network supply temperature instead are input parameters, as they are set when assigning the values of the master problem variables.

Variable	Description	Unit
$Q^t_{ch,w}$	Coling power produced by compression chillers of plant w at time t	kW
$Q^t_{abs,w}$	Cooling power prdocued by absorption chillers of plant w at time t	kW
$Q^t_{PCM,w}$	Cooling power stored/released by PCM storage of plant w at time t	kW
$Q^t_{STES,w}$	Cooling power stored/released by sensible thermal storage of plant w at time t	kW
$Q^t_{Ice,w}$	Cooling power stored/released by ice thermal storage of plant w at time t	kW
$x^t_{PCM,w}$	Binary variable that indicates if PCM of plant w is charged at time t	/

$x^t_{Ice,w}$	Binary variable that indicates if Ice thermal storage of plant w is charged at time t	/
$C^t_{STES,w}$	Residual capacity of sensible thermal energy storage of plant w at time t	kWh
$C^t_{PCM,w}$	Residual capacity of PCM storage of plant w at time t	kWh
$C^t_{Ice,w}$	Residual capacity of Ice storage of plant w at time t	kWh
$S_{STES,w}$	Sensible thermal storage maximum capacity in plant w	kWh
$S_{PCM,w}$	PCM storage maximum capacity in plant w	kWh
$S_{Ice,w}$	Ice storage maximum capacity in plant w	kWh
$N_{abs.w}$	Number of installed absorption chillers in plant w	/
$N^k_{ch,w}$	Number of installed chillers of size k in plant w	/
$N^k_{ch,st,w}$	Number of chillers of size k usable to produce chilled water at lower temperatures in plant w	
$Q^t_{ch,0,w}$	Cooling power produced by chillers in the form chilled water at $\theta_{ch,s}$ in plant w	kW
$Q^t_{ch,PCM,w}$	Cooling power produced by chillers of plant w at time t at the temperature level required to charge PCM storage	kW
$Q^t_{ch,Ice,w}$	Cooling power produced by chillers of plant w at time t at the temperature level required to charge Ice storage	kW
$MaxQ_{ch,st,w}$	Maximum chiller power producible at lower temperature levels in plant w	kW
$y_{PCM,w}$	Binary variable that indicates if PCM storage is installed in plant w	/
$y_{STES,w}$	Binary variable that indicates if sensible storage is installed in plant w	/

$y_{Ice,w}$	Binary variable that indicates if Ice storage is installed in plant w	/

Table 7.2 Variables of design and operation of plant sites optimization subproblem

Cost function

The objective of this optimization subproblem is to minimize the sum of capital and operation expenditures of chillers and storages in each plant site. These are characterised by the following costs:

- chillers capital cost
- chillers space occupancy cost
- storage capital cost
- storage space occupancy cost
- chillers operation cost

The capital cost of the centralized chillers installed in the generic plant w is defined as:

$$cost^{cap}_{ch,w} = \sum_{k}^{K} N^{k}_{ch,w} * c_k + N_{abs,w} * c^{cap}_{abs} \tag{7.4}$$

where c_k is the capital cost to install a compression chiller of type k, $N^k_{ch,w}$ is the integer variable referring to the number of chillers of type k to be installed, while c^{cap}_{abs} is the capital cost to install an absorption chiller and $N_{abs,w}$ is the number of absorption chillers to be installed.

The cost of space occupancy of these chillers is defined as:

$$cost^{occ}_{ch,w} = (\sum_{k}^{K} N^{k}_{chmw} * s_k * + N_{abs,w} * s_{abs}) * c_{occ} \sum_{n=1}^{N_y} \frac{1}{(1+r)^n} \tag{7.5}$$

where s_k and s_{abs} refer to the space occupied by compression chillers of type k and by absorption chillers. Similarly, the capital and space occupancy cost of thermal

Parameter	Description	Unit
c_k	Cost of compression chiller k	€
c_{abs}^{cap}	Capital cost of absorption chiller	€
s_k	Space occupancy of chiller k	m^2
S_{ch}^k	Capacity of compression chiller k	kW
$Q_{waste-heat}^t$	Waste heat available at time t	kW
S_{abs}	Capacity of absorption chiller	kW
c_{occ}	Cost of occupancy	€/(m^2*year)
s_{PCM}	Space occupied by PCM storage per unit of installed capacity	m^2/kWh
s_{PCM}	Space occupied by ice storage per unit of installed capacity	m^2/kWh
s_{STES}	Space occupied by sensible storage per unit of installed capacity	m^2/kWh
EER_0^t	EER of chiller operating at nominal supply temperature at time t	/
EER_{PCM}^t	EER of chiller if charging PCM storage at time t	/
EER_{Ice}^t	EER of chiller if charging ice storage at time t	/
EER_{abs}^t	EER of absorption chiller at time t	/
$c_{abs^{OM}}$	Operation and maintenance cost of absorption chiller	€/kWh
$Q_{demand,w}^t$	Cooling demand provided by plant w at time t	kW
H	large number used in big-M constraints	

Table 7.3 Parameters of design and operation of plant sites optimization subproblem

storages are evaluated as defined in eq. (7.6) and (7.7):

$$cost^{cap}_{st,w} = S_{PCM,w} * c_{PCM} + S_{Ice,w} * c_{Ice} + S_{STES,w} * c_{STES} \tag{7.6}$$

$$cost^{occ}_{st,w} = (S_{PCM,w} * s_{PCM} + S_{Ice} * s_{Ice} * + S_{STES,w} * s_{STES}) * c_{occ} * \sum_{n=1}^{N_y} 1/(1+r)^n \tag{7.7}$$

where $S_{PCM,w}$, $S_{ICE,w}$ and $S_{STES,w}$ refer to the installed capacity of PCM, ice and sensible thermal storage in plant w, while c_{PCM}, c_{ICE} and c_{STES} refer to the capital cost of these storages per unit of installed capacity. The terms s_{PCM}, s_{STES} and s_{Ice} refer to the specific space occupancy of thermal energy storages per unit of capacity, expressed as m^2/kWh. The operation cost of the chillers depends on the amount of cooling energy produced at the different temperature levels and is defined as:

$$\begin{aligned} cost^{op}_{ch,w} = & (\sum_{t}^{\Theta} (\frac{Q^t_{ch,0,w}}{EER^t_0} + \frac{Q^t_{ch,PCM,w}}{EER^t_{PCM}} + \frac{Q^t_{ch,Ice,w}}{EER^t_{Ice}} * \Delta t * c^t_{el} + Q^t_{abs,w} * \Delta t * c^{OM}_{abs}) \\ & * \sum_{n=1}^{N_y} \frac{1}{(1+r)^n} \end{aligned} \tag{7.8}$$

where EER^t_0, EER^t_{PCM}, EER^t_{Ice} refer to the EER of the chillers when producing chilled water at supply temperatures of network, PCM and ice storage, respectively. The EER is also dependant on the time step, since during the night, the cooling water temperature in the condenser can decrease thanks to lower outdoor temperatures. The terms $Q^t_{ch,0,w}$, $Q^t_{ch,PCM,w}$, $Q^t_{ch,Ice,w}$ refer to the cooling power produced by the chillers when they supply water at nominal temperature and when charging PCM or ice storage. The cost of electricity is defined by c^t_{el} and varies with time, since there are different tariffs for off-peak and peak hours. $Q^t_{abs,w}$ refers to the cooling power produced by absorption chillers, while c^{OM}_{abs} is the cost for operation and maintenance of absorption chillers per unit of cooling energy produced.

Constraints

The model constraints are mainly energy balance equations or capacity constraints. Eq. (7.9) is an energy balance constraint of the cooling power produced by the

chillers, absorbed/released by the storages and requested by the buildings.

$$Q^t_{ch,w} + Q^t_{abs,w} + Q^t_{PCM,w} + Q^t_{Ice,w} + Q^t_{STES,w} = Q^t_{demand,w} \qquad \forall t \in \Theta \qquad (7.9)$$

where $Q^t_{ch,w}$, $Q^t_{PCM,w}$, $Q^t_{Ice,w}$, $Q^t_{STES,w}$ refer to the cooling power produced by the chillers, absorbed or released by PCM, ice or sensible thermal storages, respectively. $Q^t_{demand,w}$ is the cooling demand that at time t must be satisfied and is given by the sum of the cooling demand of all the buildings that are fed by the plant w,which depends on the variables x_u, as defined in equation (7.10)

$$Q^t_{demand,w} = \sum_{u|x_u=w} Q^t_u \qquad \forall t \in \Theta \qquad (7.10)$$

Constraints (7.11)-(7.13) are energy conservation equations, indicating that the residual storage capacity at time t depends on the storage capacity at the previous time-step and on the cooling energy absorbed or released by storages in the time interval between the two time-steps.

$$C^t_{PCM,w} = C^{t-1}_{PCM,w} - Q^t_{PCM,w} * \Delta t \qquad \forall t \in \Theta \qquad (7.11)$$

$$C^t_{Ice,w} = C^{t-1}_{Ice,w} - Q^t_{Ice,w} * \Delta t \qquad \forall t \in \Theta \qquad (7.12)$$

$$C^t_{STES,w} = C^{t-1}_{STES,w} - Q^t_{STES,w} * \Delta t \qquad \forall t \in \Theta \qquad (7.13)$$

where $C^t_{PCM,w}$,$C^t_{Ice,w}$ and $C^t_{STES,w}$ are the capacities at time t of PCM, ice or sensible thermal energy storages. Inequality constraints (7.14)-(7.16) indicate that the residual storage capacity must not exceed the installed storage capacity.

$$C^t_{PCM,w} \leq S_{PCM,w} \qquad \forall t \in \Theta \qquad (7.14)$$

$$C^t_{Ice,w} \leq S_{Ice,w} \qquad \forall t \in \Theta \qquad (7.15)$$

$$C^t_{STES,w} \leq S_{STES,w} \qquad \forall t \in \Theta \qquad (7.16)$$

Constraint (7.17) indicates that cooling power produced by compression chillers must not exceed the installed chiller capacity.

$$Q^t_{ch,w} \leq \sum_k^k N^k_{ch,w} * S^k_{ch,w} \qquad \forall t \in \Theta \qquad (7.17)$$

Constraint (7.18) is a big-M constraint that ensures that the cooling power produced at the temperature level required by PCM($3°C$) is null, if the PCM thermal energy storage is not charged at time t.

$$Q^t_{ch,PCM,w} \leq H * x^t_{PCM,w} \qquad \forall t \in \Theta \tag{7.18}$$

where H is a sufficiently large number at least equal to the upper bound of $Q^t_{ch,PCM,w}$, while $x^t_{PCM,w}$ is a binary variable that indicates if the PCM storage is charging. Similarly, constraint (7.19) ensures that the cooling power produced at -5 ° C is equal to zero if ice thermal storage is not charging.

$$Q^t_{ch,Ice,w} \leq H * x^t_{Ice,w} \qquad \forall t \in \Theta \tag{7.19}$$

where $x^t_{Ice,w}$ is a binary variable that indicates if the ice thermal energy storage is charging at time t. Constraints (7.20) and (7.21) instead indicate that the amount of cooling energy stored by PCM or ice thermal storage must not exceed the cooling power produced by the chillers at the specific temperature levels required to charge these storages.

$$Q^t_{PCM,w} \leq Q^t_{ch,PCM,w} \qquad \forall t \in \Theta \tag{7.20}$$

$$Q^t_{Ice,w} \leq Q^t_{ch,Ice,w} \qquad \forall t \in \Theta \tag{7.21}$$

Constraint (7.22) ensures that the cooling power produced by the chillers to charge either PCM or ice thermal storages does not exceed the installed chiller capacity for this scope.

$$Q^t_{ch,PCM,w} + Q^t_{ch,Ice,w} \leq \sum_{k}^{K} N^k_{ch,st,w} * S^k_{ch,w} \qquad \forall t \in \Theta \tag{7.22}$$

where $N^k_{ch,st,w}$ is the number of chillers of type k installed to charge PCM or ice thermal energy storages. Constraint (7.23) indicates that the installed chillers used to charge PCM or ice thermal energy storages are a subset of the total installed chillers.

$$N^k_{ch,st,w} \leq N^k_{ch,w} \qquad \forall k \in K \tag{7.23}$$

Constraint (7.24) indicates that cooling power produced in the form of chilled water at the network supply temperature must be lower than or equal to the available

capacity at time t. When neither PCM nor ice storage is being charged, this capacity corresponds to the total one, while if either PCM or ice storage is being charged, it corresponds to the installed chiller capacity that is not used to charge storages.

$$Q^t_{ch,0,w} \leq \sum_k^K (N^k_{ch,w} - N^k_{ch,st,w} * (x^t_{PCM,w} + x^t_{Ice,w})) * S^k_{ch,w} \qquad \forall t \in \Theta \qquad (7.24)$$

The constraint is non-linear, since it includes the products between $N^k_{ch,st,w}$ and the variables $x^t_{PCM,w}$ and $x^t_{Ice,w}$. However, these are products between integer and binary variables and can be easily linearized by including additional variables and McCormick constraints.

Constraint (7.25) ensures that the cooling power produced by absorption chillers does not exceed the amount of cooling that can be produced by absorption chillers. This depends on the available waste heat and on the EER of the absorption chillers.

$$Q^t_{abs,w} \leq Q^t_{waste-heat,w} * EER^t_{abs} \qquad \forall t \in \Theta \qquad (7.25)$$

where $Q^t_{waste-heat,w}$ is the available waste heat in plant w and EER^t_{abs} is the EER of the absorption chiller.

Constraint (7.26) ensures that the cooling power produced by absorption chillers does not exceed the installed capacity.

$$Q^t_{abs,w} \leq N_{abs,w} * S_{abs,w} \qquad \forall t \in \Theta \qquad (7.26)$$

Constraint (7.27) limits to one the number of storage technologies installed in each plant.

$$y_{PCM,w} + y_{STES,w} + y_{Ice,w} \leq 1 \qquad (7.27)$$

Constraints (7.28)- (7.30) ensure that the capacity of a storage is equal to zero, if that technology is not installed.

$$S_{PCM,w} \leq H * y_{PCM,w} \tag{7.28}$$

$$S_{Ice,w} \leq H * y_{Ice,w} \tag{7.29}$$

$$S_{STES,w} \leq H * y_{STES,w} \tag{7.30}$$

Constraint (7.31) is an energy balance indicating that the cooling power produced by chillers is equal to the sum of the cooling power produced at all temperature levels.

$$Q^t_{ch,w} = Q^t_{ch,0,w} + Q^t_{ch,PCM,w} + Q^t_{ch,Ice,w} \qquad \forall t \in \Theta \tag{7.31}$$

Lastly, constraints (7.32)-(7.34) force the energy storages to complete full charge/discharge cycles everyday.

$$\sum_{t}^{\Theta} Q^t_{PCM,w} = 0 \tag{7.32}$$

$$\sum_{t}^{\Theta} Q^t_{STES,w} = 0 \tag{7.33}$$

$$\sum_{t}^{\Theta} Q^t_{Ice,w} = 0 \tag{7.34}$$

7.2.4 Topology optimization subproblem

The second subproblem to be solved, once the master problem variables are set, is the network topology optimization. The optimization subproblem to be solved is also called Steiner tree problem and consists in finding the tree network that connects the selected chillers and buildings, minimizing the total network length. This is a generalization of the minimum spanning tree, since in this case, Steiner nodes (internal nodes) can be either included or not in the final network. On the other hand, when solving minimum spanning tree problems the Steiner nodes are always included. As a consequence, solving a Steiner tree problem allows to find a better solution, since the search space is wider.

The problem is modelled as a Mixed Integer Linear Programming, where the cost function is represented by the total length, while the constraints are mass balances that ensure flow conservation in the network.

Variables

The model is characterised by the following four types of variables.

- A group of binary variables z_{ij}^{+} that indicate if the branch that connects node i with node j is selected and if the flow is directed from node i to node j.
- A group of binary variables z_{ij}^{-} that indicate if the branch that connects node i with node j is selected and if the flow is directed from node j to node i.
- A group of continuous non-negative variables $Gmax_{ij}^{+}$ that indicate the mass flow rate flowing from node i to node j
- A group of continuous non-positive variables $Gmax_{ij}^{-}$ that indicate the mass flow rate flowing from node j to node i.

The mass flow rates are therefore split in two groups of variables based on their flow directions.

Cost function

The objective of this model is to find the set of edges that constitute the tree network with the minimum total length and which connects the selected plants and buildings. The objective function is therefore given by eq. (7.35)

$$L_{tot} = \sum_{ij}^{E} (z_{ij}^{+} + z_{ij}^{-}) * L_{ij} \tag{7.35}$$

where L_{tot} is the total length of the network, L_{ij} is the length of the generic branch that connects nodes i and j, while z_{ij}^{+} and z_{ij}^{-} are binary variables that indicate if branch (i, j) is selected and which flow direction.

Constraints

The constraints defined for this model are flow balances that guarantee the mass flow conservation in the network. Constraint (7.36) indicates that only one flow direction can be selected for each branch.

$$z_{ij}^{+} + z_{ij}^{-} \leq 1 \qquad \forall (i,j) \in E \tag{7.36}$$

If z_{ij}^{+} is equal to one, it means that the mass flows from i to j, while if z_{ij}^{-} is equal to one, it flows in the opposite direction.

Constraints (7.37)-(7.38) enforce a mass flow rate to zero, if its branch is not selected in the final layout.

$$Gmax_{ij}^{+} \leq M * z_{ij}^{+} \qquad \forall (i,j) \in E \tag{7.37}$$

$$-Gmax_{ij}^{-} \leq H * z_{ij}^{-} \qquad \forall (i,j) \in E \tag{7.38}$$

where H is a sufficiently large number.

Constraint (7.39) represent a generic mass balance applied to every node.

$$\sum_{i}^{V_j} (Gmax_{ij}^{+} + Gmax_{ij}^{-}) = Gmax_{ext}^{j} \qquad \forall j \in V \tag{7.39}$$

where $Gmax_{ext}^{j}$ is the maximum mass flow rate entering into or exiting from the network from node j. It depends on the values of the master problem variables x_u and on the peak demand of the different buildings. V^j represents the set of nodes adjacent to the generic node j.

7.3 Case study

The hierarchical framework has been applied to a Singaporean case study. The neighbourhood, object of the study, is a commercial district characterised by 18 buildings with a total cooling demand of 130 MW. Four possible plant positions have been considered, which are shown in Figure 7.2 together with the neighbourhood topology and the position of the 18 buildings. The radius of the red circles in Figure 7.2 is proportional to the cooling demand of the buildings.

The total demand curve of the neighbourhood is shown in Figure 7.3. The demand reaches 40 MW during the night, since most buildings require cooling only during peak hours.

7.3.1 Scenarios

Eight different scenarios have been considered to study the feasibility of district cooling in a densely populated tropical area under different conditions. The scenarios differ from each others in terms of i) indoor temperature set-point, ii) availability of waste heat, iii) EER of absorption chillers, iv) electricity tariffs and v) cost for space occupancy. Table 7.4 summarizes the different conditions that define the eight scenarios.

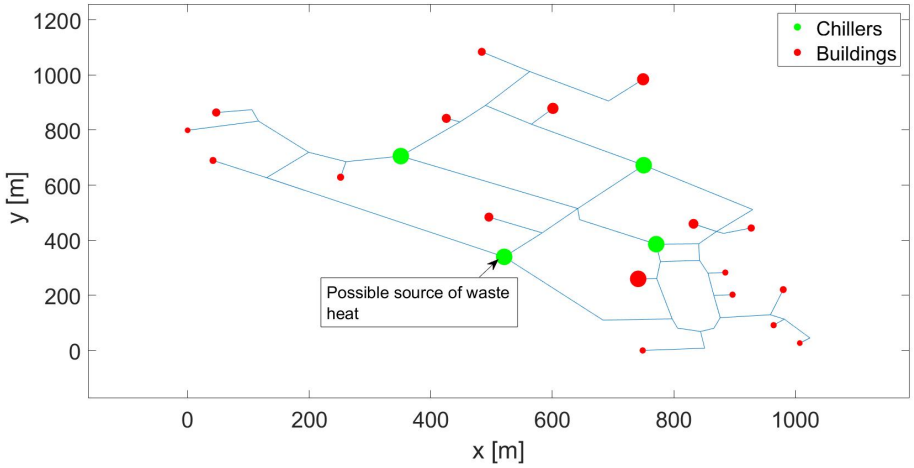

Fig. 7.2 Neighbourhood topology and possible chiller locations

Scenario 1: Baseline

In the baseline scenario the indoor set-point temperature is assumed to be equal to 22.5°C. The temperature difference between the indoor set-point and the entering airflow is assumed to be 11°C, following ASHRAE standards [108]. As a consequence the air is cooled down to 11.5°C. It is also assumed that 50% of indoor air is recirculated with outdoor air having a temperature of 33° C and relative humidity of 75%. With these informations and assuming a logarithmic mean temperature

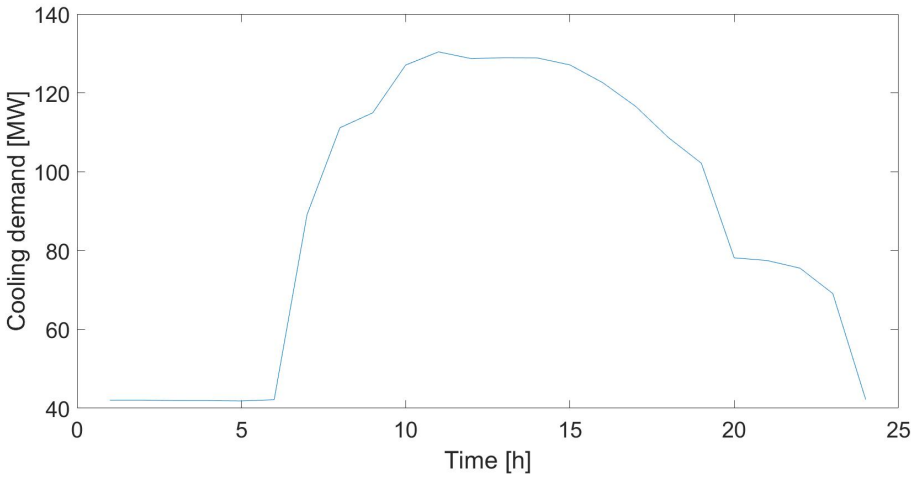

Fig. 7.3 Overall demand curve

difference of 5°C between air and water in the air handling units, it is possible to fix the supply and return temperature of the chilled water in the secondary loops of the energy transfer stations. By varying the supply temperature of the district cooling network is therefore possible to compute the return temperature, fixing a logarithmic temperature difference of 3° C between the primary and secondary loops. In this scenario no availability of waste heat is considered, while the electricity price is equal to 0.28 SGD/kWh in the peak hours and 0.17 SGD/kWh during off-peak hours [109]. Lastly, the space occupancy cost is considered equal to 70 $/(sqf*y) [110].

Scenario 2

In this scenario, it is assumed an indoor set point temperature of 25.5°C, which is the upper limit according to Singaporean thermal comfort guidelines [111]. Due to the higher set-point temperature, a lower cooling demand is considered. A previous study found that for each Celsius degree increase in set-point temperature, the cooling demand decreases by 6% [112]. As a consequence, for this scenario it was considered a 18% lower cooling demand. In addition, the logarithmic temperature differences in the air handling units and in the substation heat exchanger are lowered by 18% as well, since the heat transfer areas are assumed to be equal to the baseline scenario. This therefore leads to a higher upper bound of network supply temperature.

Scenario 3,4,5,6

These scenarios are characterised by the availability of waste heat in one of the plant sites (Figure 7.2). The scenarios differ from each other in terms of waste heat available and EER of absorption chillers, which depends on the temperature of the waste heat source. In scenario 3 and 4 a waste heat of 10 MW is considered, while in scenario 5 and 6 the waste heat available is equal to 25 MW. Concerning the waste heat temperature, in scenarios 3 and 5, it is equal to 75°C, while in scenarios 4 and 6 it is equal to 84 °C. In these scenarios, the indoor temperature set-point, the electricity tariff and the space occupancy cost are the same as in the baseline scenario.

Scenario 7

Scenario 7 differs from the baseline in terms of electricity cost. The off-peak price does not change, while the peak price is assumed to be equal to 0.4 SGD/kWh.

Scenario 8

In scenario 8 it is assumed that the cost of space occupancy increases every year by 5%, while all the other parameters are the same as in the baseline. This scenario has been considered, since most likely space occupancy cost will continue to increase in the future.

7.3.2 Chillers parameters

In the analysis four types of compression chillers and one type of absorption chiller have been considered. The main properties are reported in Table 7.5. The performance curves of the chillers were obtained from the catalogues of Trane, manufacturer of heat pumps, chillers and HVAC equipment and from the library of the software DesignBuilder. They are bicubic or quadratic functions that express the nonlinear relation between EER and the partial load or the supply chilled water and condensing water temperatures. Figure 7.4 shows the bicubic performance curve of compression chillers as a function of supply and condensing water temperatures. Figure 7.5 shows the bicubic curves of the EER as a function of the chiller load for

Scenario	Set point temperature [°C]	Cost of electricity [$/kWh]	Space occupancy cost	Waste heat
Baseline	22.5	Peaks: 0.28 SGD/kWh Off-peaks: 0.17 SGD/kWh	70 $/sqf	No
2	25.5	Peaks: 0.28 SGD/kWh Off-peaks: 0.17 SGD/kWh	70 $/sqf	No
3	22.5	Peaks: 0.28 SGD/kWh Off-peaks: 0.17 SGD/kWh	70 $/sqf	10 MW, T_{wh}=75°C
4	22.5	Peaks: 0.28 SGD/kWh Off-peaks: 0.17 SGD/kWh	70 $/sqf	10 MW, T_{wh}=84°C
5	22.5	Peaks: 0.28 SGD/kWh Off-peaks: 0.17 SGD/kWh	70 $/sqf	25 MW, T_{wh}=75°C
6	22.5	Peaks: 0.28 SGD/kWh Off-peaks: 0.17 SGD/kWh	70 $/sqf	25 MW, T_{wh}=84°C
7	22.5	Peaks: 0.4 SGD/kWh Off-peaks: 0.17 SGD/kWh	70 $/sqf	No
8	22.5	Peaks: 0.28 SGD/kWh Off-peaks: 0.17 SGD/kWh	increasing 5% every year	No

Table 7.4 Summary of scenarios conditions

Typology	Capacity [MW]	Space occupancy [m^2]	Cost[M€]
Compression	0.5	28.68	0.23 [82]
Compression	1	31.45	0.45 [82]
Compression	3	44.16	0.9 [82]
Compression	10	89.38	4.5 [82]
Absorption	5	17.2	3.3 [113]

Table 7.5 Main Chillers parameters

the different chillers, setting the supply chilled water and condensing water temperatures to the standard ones (6.7 °C and 35°C, respectively). As previously mentioned, the load curves were used only for individual chillers, since centralized ones tend to work more homogeneously, thanks to the installation of multiple chillers, which allows to minimize the effect of partial load. Figure 7.6 shows the performance curves of absorption chillers as a function of chilled water temperature.

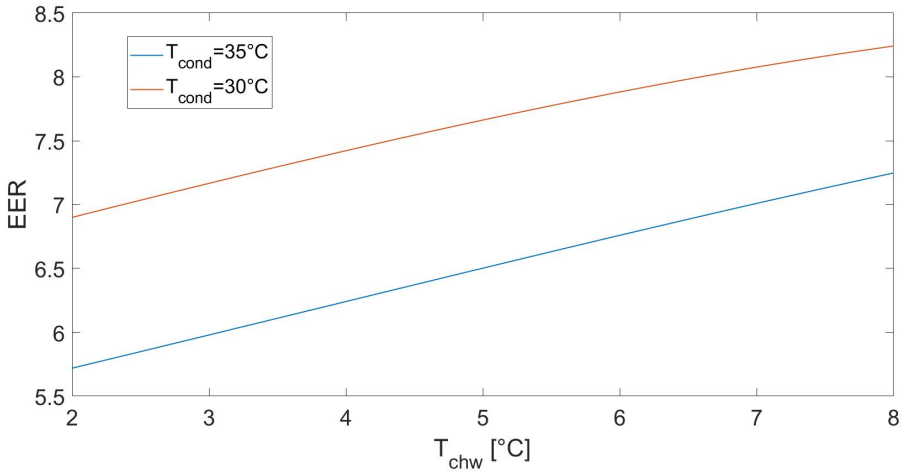

Fig. 7.4 Performance curve of compression chillers

7.4 Results

In this section the results obtained from the application of the model to the Singapore case study are reported. The section is structured in six subsections that show the results in the different scenarios in terms of optimal topology, operation, storage technology, supply temperature, district cooling potential compared to traditional cooling and net present value.

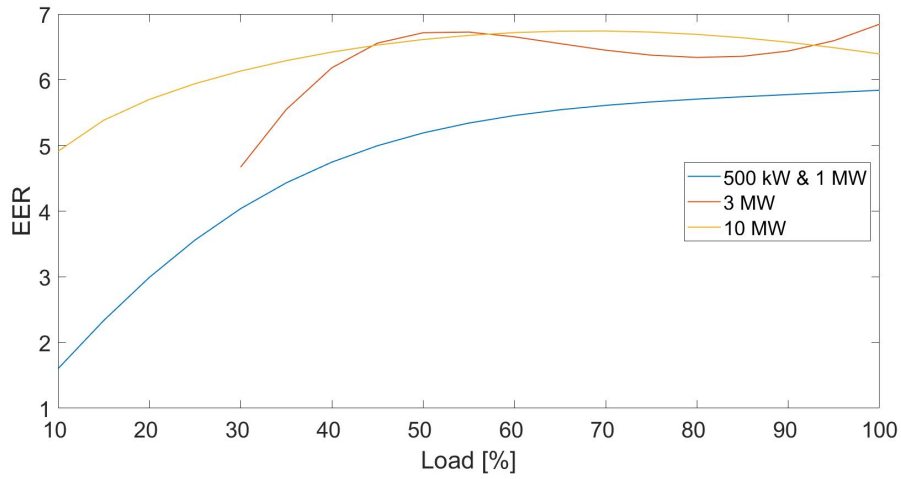

Fig. 7.5 EER in partial load conditions and T_{chw}=6.7°C and T_{cond}=35°C

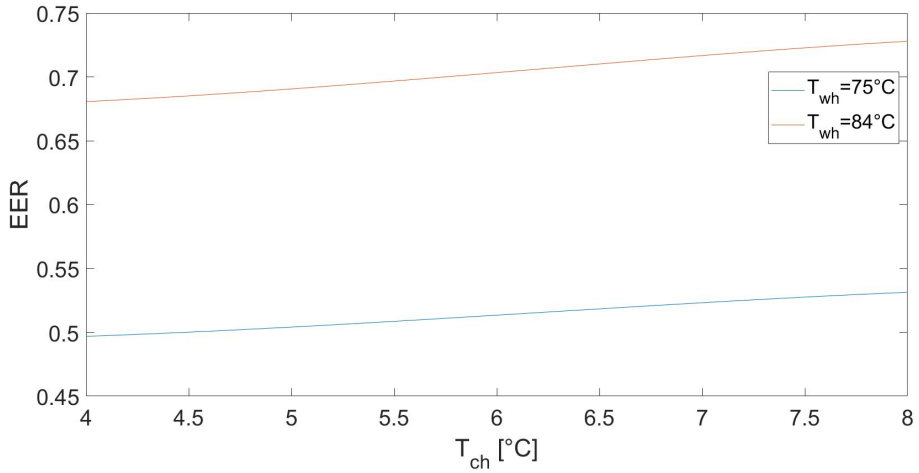

Fig. 7.6 Performance curves of absorption chillers

7.4.1 Optimal topology

Figure 7.7 shows the optimal topology in the different scenarios. It can be observed that the number of connected buildings increases if the potential of district cooling compared to individual cooling is higher. Indeed, in the baseline scenario 12 buildings out of 18 are connected, while when absorption chillers are installed the number of connected buildings rises up to 16.

In scenario 7, the solution consists in connecting 15 buildings and installing two independent networks, each fed by a chiller plant. The reason for this design is that

it allows to reduce pressure drops and pumping costs. Indeed, with higher electricity price, pumping has a major weight on the total costs.

The building in the node with coordinates (740, 260) is a data centre with a cooling demand of 30 MW and is never connected in any scenario. The reason is that district cooling would not provide any advantage, since already very efficient chillers can be installed there and they would always work at constant load, with high performances, since the data centre cooling demand is constant.

7.4.2 Comparison with individual cooling

Figure 7.8 shows the cost comparison between the optimal solutions found by the model and two suboptimal solutions: one obtained connecting all buildings to the same chiller plant and the other refers to the case in which no district cooling is installed and all the buildings are cooled individually.

In the baseline scenario, installing individual cooling systems in every building is 3.3% more expensive than the optimal solution. At the same time, connecting all the buildings to the network is 4.4% more expensive.

These differences change from one scenario to another. When waste-heat is available(scenarios 3,4,5,6), the optimal solution is up to 16.5% less expensive than the one where all buildings are cooled individually.

Moreover, the electricity cost has a large impact on the potential of district cooling, as in scenario 7 the individual cooling solution is 7.6% more expensive than the optimal one.

Levelized cost of individual cooling

The set of buildings to be connected to the district cooling network depends on the potential savings achievable compared to individual cooling. If the costs for individual cooling are already low, district cooling may not bring significant savings and may result unfeasible. This is the case of some of the buildings of the case study, including the previously mentioned data centre. These buildings could be connected to the district cooling network if the selling price of cooling energy decreases, which is possible only if the district cooling costs are lowered(i.e. installing absorption

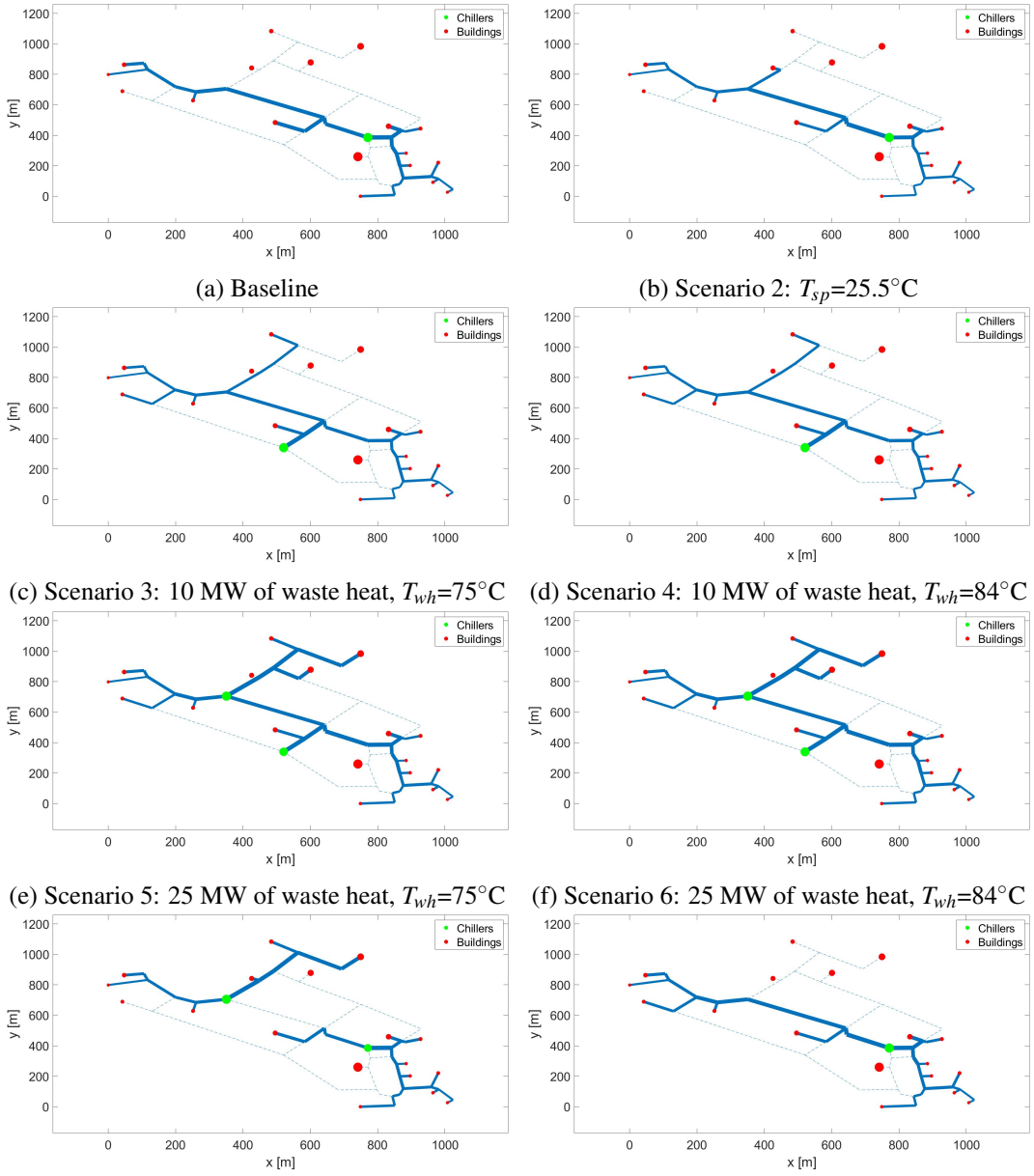

(a) Baseline

(b) Scenario 2: T_{sp}=25.5°C

(c) Scenario 3: 10 MW of waste heat, T_{wh}=75°C

(d) Scenario 4: 10 MW of waste heat, T_{wh}=84°C

(e) Scenario 5: 25 MW of waste heat, T_{wh}=75°C

(f) Scenario 6: 25 MW of waste heat, T_{wh}=84°C

(g) Scenario 7: Peak electricity price=0.4 SGD/kWh

(h) Scenario 8: Space occupancy cost increasing 5% every year

Fig. 7.7 Optimal topology in the different scenarios

chillers to exploit the available waste heat), or if individual cooling costs increase(i.e. increase of electricity cost).

Figure 7.9 shows the levelized cost of individual cooling for the 18 buildings in the baseline scenario. These are computed dividing the total individual cooling costs by the amount of cooling energy requested. The six points in red represent the

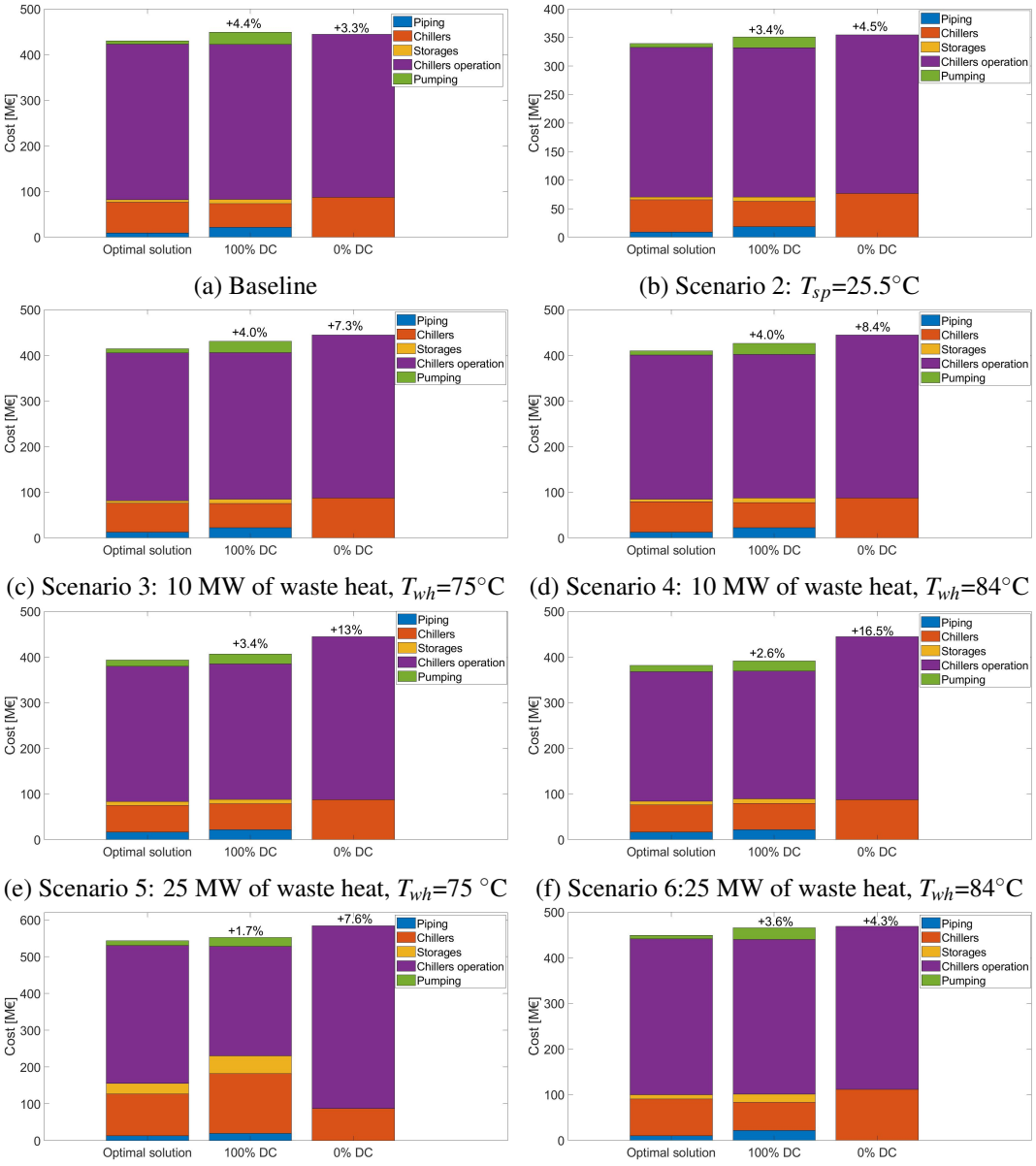

(a) Baseline

(b) Scenario 2: T_{sp}=25.5°C

(c) Scenario 3: 10 MW of waste heat, T_{wh}=75°C

(d) Scenario 4: 10 MW of waste heat, T_{wh}=84°C

(e) Scenario 5: 25 MW of waste heat, T_{wh}=75 °C

(f) Scenario 6:25 MW of waste heat, T_{wh}=84°C

(g) Scenario 7: Peak electricity price=0.4 SGD/kWh

(h) Scenario 8: Space occupancy cost increasing 5% every year

Fig. 7.8 Cost comparison with conventional cooling in the different scenarios

buildings not connected to the network, which indeed are characterised by the lowest levelized costs and distances from the installed plant. The figure also suggests that the minimum selling price per unit of cooling energy should be greater than 0.039 €/kWh to make district cooling economically feasible. Lower selling prices would

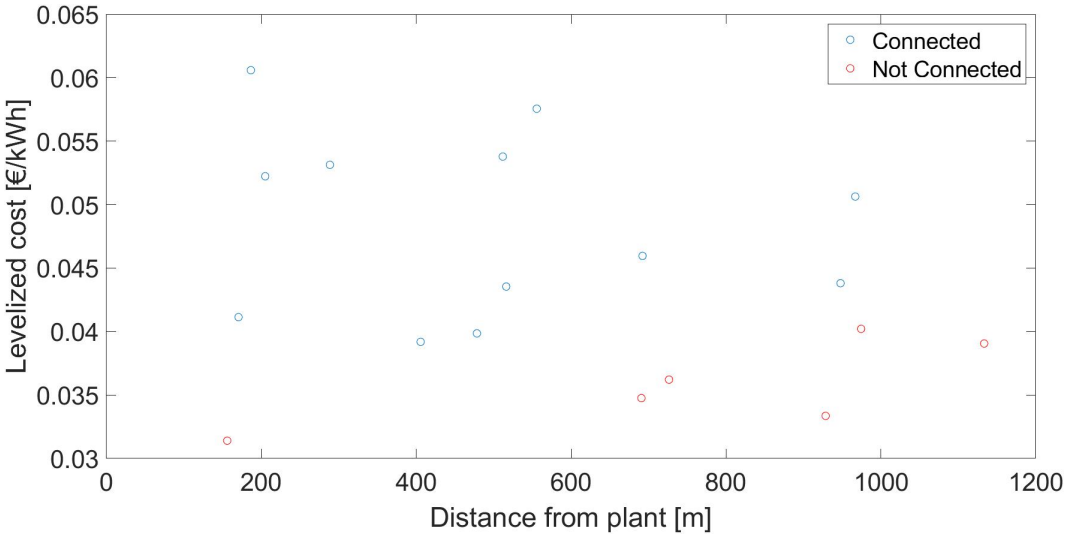

Fig. 7.9 Levelized cost of cooling for different buildings in the baseline scenario

not cover the costs of this technology. The price could be decreased, by reducing district cooling costs(i.e. exploiting the waste heat through absorption chillers).

7.4.3 Optimal operation

Figure 7.10 shows the optimal hourly operation in the different scenarios. In almost all scenarios, chillers are operated with almost constant load throughout the day, apart from the evening hours when they only produce the amount of cooling power demanded by the users. In the rest of the day, the cooling power produced is constant, while the storages are charged during the night, and discharged during the morning and afternoon hours. The reason why during the evening hours the production is lower is due to the fact that cooling demand is lower, while the electricity is more expensive in these hours, since the peak tariff is between 7 AM and 11 PM.

In scenario 7, the strategy is completely different, since the chillers are operated almost only during the night, due to the larger costs of electricity during peak hours, with respect to the baseline scenario; as a consequence, larger capacities of chillers and storages are installed.

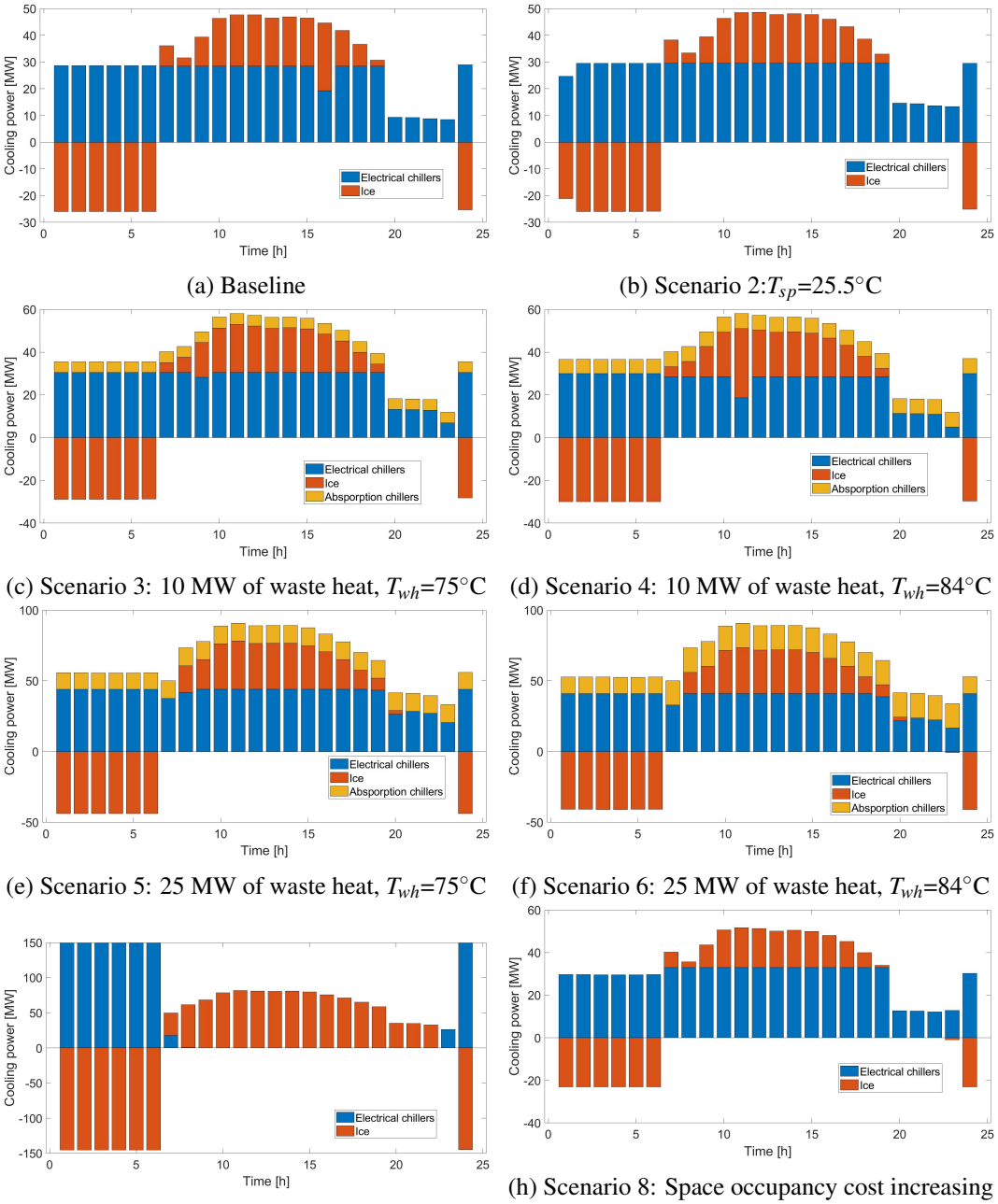

(a) Baseline

(b) Scenario 2:T_{sp}=25.5°C

(c) Scenario 3: 10 MW of waste heat, T_{wh}=75°C

(d) Scenario 4: 10 MW of waste heat, T_{wh}=84°C

(e) Scenario 5: 25 MW of waste heat, T_{wh}=75°C

(f) Scenario 6: 25 MW of waste heat, T_{wh}=84°C

(g) Scenario 7: $c_{el,peak}$=0.4 SGD/kWh

(h) Scenario 8: Space occupancy cost increasing 5% every year

Fig. 7.10 Optimal hourly operation in the different scenarios

7.4.4 Optimal storage technology

Figure 7.11 shows the comparison between different storage solutions in each of the eight scenarios. The first three solutions *STES(heur.)*, *PCM (heur.)* and *ICE (heur.)* represent heuristic solutions obtained considering the installation of sensible, PCM

or ice storage, respectively. In addition, in these solutions the chillers are always operated with constant load, so the operation strategy is not optimized. It can be observed that the sensible storage solution is the most expensive, due to the larger space occupation compared to PCM or ice storage.

The solutions *PCM(opt)* and *Ice(opt)* refer to solutions obtained considering PCM or ice storage and no fixed operation strategy, contrarily to the previous three solutions. In these cases, the operation strategy and the design are combinedly optimized. Apart from scenarios 7 and 8, the differences between these solutions are around 1%, which means that in most cases PCM storage and ice storage are almost equivalent in terms of overall costs. The reason is that the higher operation costs of chillers occurring when producing ice are balanced by lower space occupation and longer life cycle. The results of these solutions are significantly different from the ones obtained with the heuristic assumption of constant chiller operation. Optimizing the size and operation of chillers and storage without this constraint allows to save from 4.2% to 27.5% in terms of total costs, depending on the scenario. The main reason is that if it is assumed an always constant chiller operation, larger storages would be needed and they would be charged also when it is not convenient, such as during the evening hours(i.e. when the demand is lower than the average, but the electricity price is larger).

In scenario 8, the difference between ice thermal storage and PCM optimal solutions is larger since the space occupancy cost increases by 5% every year. As a consequence, ice thermal storage results 3.6% cheaper since it is characterised by higher volumetric capacity. In scenario 7, the difference between ice thermal storage and PCM optimal solutions is also larger, since greater capacities are installed, due to the major price difference between peak and off-peak electricity prices. The figure shows also the benefits of thermal storage comparing the optimal solutions with ones lacking storage. In the baseline scenario, a district cooling network without a storage would be 9.1% more expensive in terms of total costs, since the chillers would be operated with higher loads during peak hours. This difference reaches 20.8% in scenario 7, where the electricity cost in peak hours is larger.

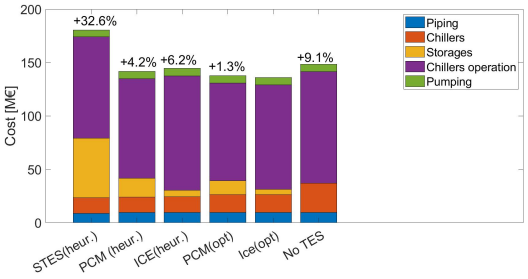

(a) Baseline

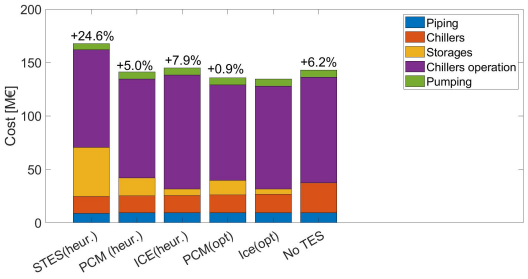

(b) Scenario 2: T_{sp}=25.5°C

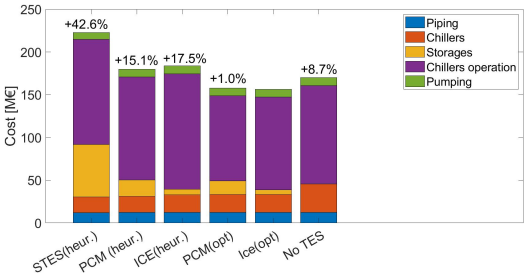

(c) Scenario 3: 10 MW of waste heat, T_{wh}=75°C

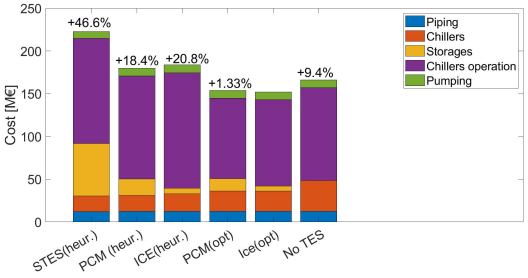

(d) Scenario 4 10 MW of waste heat, T_{wh}=84°C

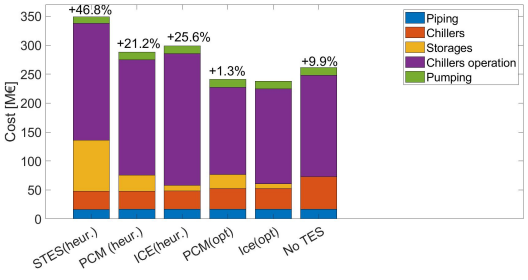

(e) Scenario 5: 25 MW of waste heat, T_{wh}=75°C

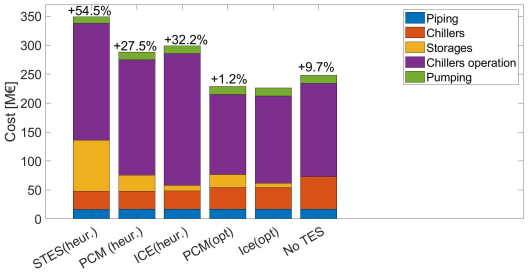

(f) Scenario 6: 25 MW of waste heat, T_{wh}=84°C

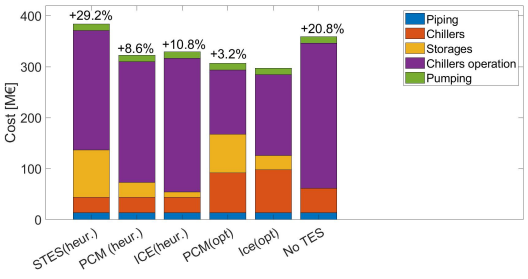

(g) Scenario 7: $c_{el,peak}$=0.4 SGD/kWh

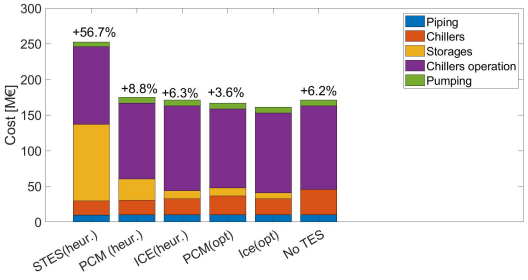

(h) Scenario 8: Space occupancy cost increasing 5% every year

Fig. 7.11 Optimal storage technology in the different scenarios

7.4.5 Optimal supply temperature

Figure 7.12 shows the optimal supply temperature in the different scenarios. Apart from scenario 2 and 7, the optimal supply temperature is always around 5°C. The optimal temperature is between the lower and upper bounds, as it corresponds to

the trade-off between pumping and chiller operation costs. Indeed, with a lower temperature, the chiller would operate at lower efficiency, but the temperature difference between supply and return would be higher, requiring lower mass flow rates and therefore lower pumping power. It can also be observed that when absorption chillers are used, the cost difference between the optimal supply temperature and the upper bound increases. The main reason is that the EER varies differently in compression and absorption chillers, due to different performance curves.

In Scenario 7 the optimal supply temperature corresponds to the lower bound of 4°C, since chillers are always operated to charge ice thermal storage at −5°C. As a consequence, the chiller efficiency is already affected by that and supplying the network at a higher temperature has a minor impact on the coefficient of performance. The network is therefore operated at a temperature of 4° C in order to minimize the pumping costs.

Lastly, in scenario 2 the optimal supply temperature is higher, thanks to the higher indoor set-point temperature that allows to increase the network supply and return temperatures.

7.4.6 Net present value analysis

Figure 7.13 shows the impact of increasing the indoor temperature set-point on the net present value and payback-time, by comparing scenario 2 with the baseline. In the analysis, the price of chilled water set by the utility represents the average levelized cost for individual cooling, since that represents the threshold for the economical feasibility of district cooling. The results of the analysis show that by increasing by 3° C the indoor temperature set-point, the payback time decreases from 14 to 11 years. In addition, with the increase of set point temperature, 43% higher NPV would be achieved at the end of lifetime.

Figure 7.14 shows the impact of waste heat utilization on the net present value and payback time of a district cooling system. It can be observed that if the waste heat available and the EER of the absorption chillers increase, the final net present value can increase by up to 3.5 times thanks to the lower costs and larger revenues. In addition, the payback time can be reduced by 5 years in scenario 6, the one characterised by the highest values of waste heat and source temperature.

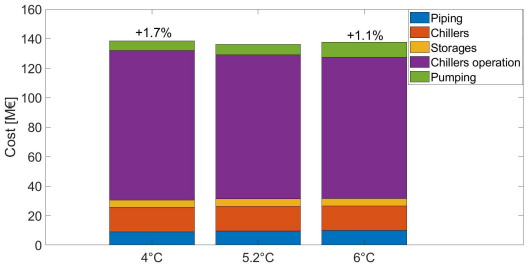

(a) Baseline

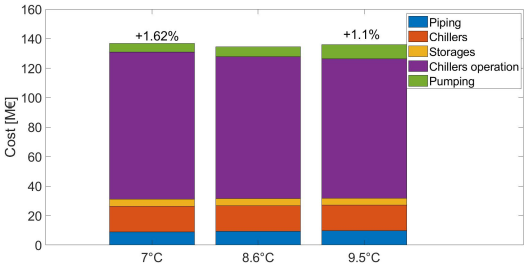

(b) Scenario 2: T_{sp}=25.5°C

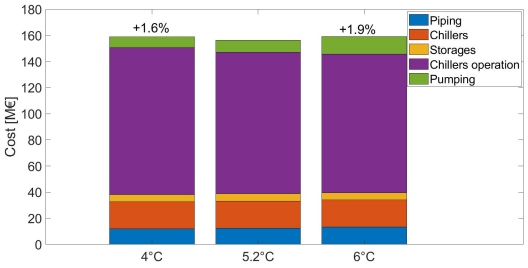

(c) Scenario 3: 10 MW of waste heat, T_{wh}=75°C

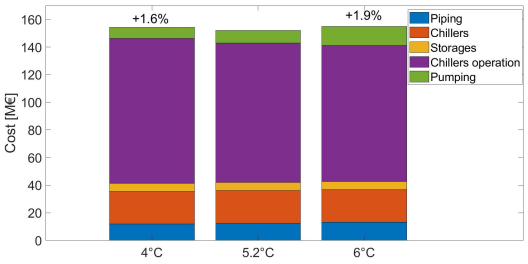

(d) Scenario 4: 10 MW of waste heat, T_{wh}=84°C

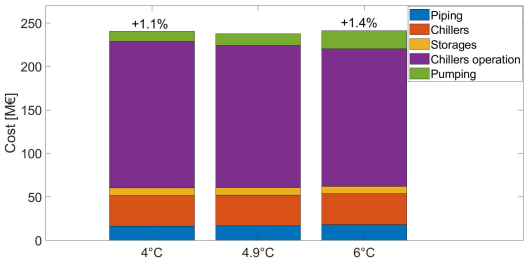

(e) Scenario 5: 25 MW of waste heat, T_{wh}=75°C

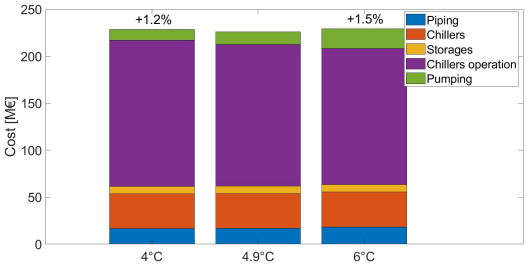

(f) Scenario 6: 25 MW of waste heat, T_{wh}=84°C

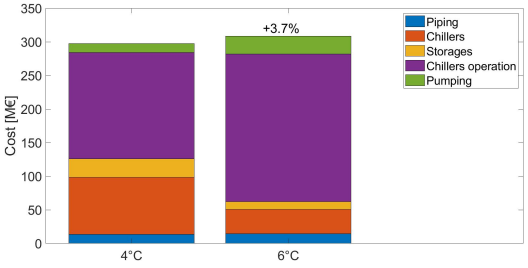

(g) Scenario 7: $c_{el,peak}$=0.4 SGD/kWh

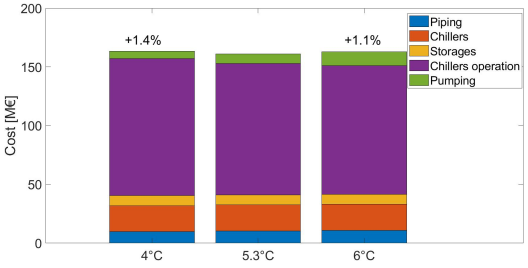

(h) Scenario 8: Space occupancy cost increasing 5% every year

Fig. 7.12 Optimal supply temperature in different scenarios

7.5 Discussion and concluding remarks

The developed hierarchical method proved to effectively optimize different aspects regarding the design and operation of district cooling systems. The results obtained by applying the model to a Singapore neighbourhood case study not only highlighted

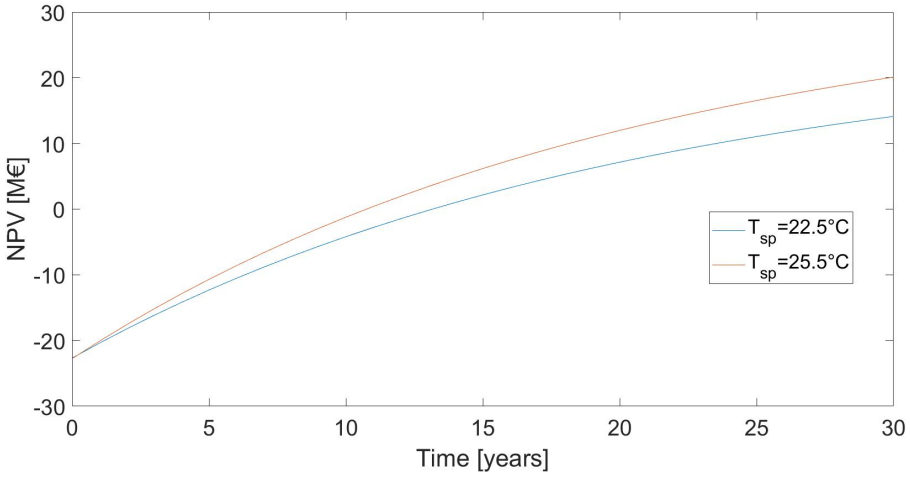

Fig. 7.13 Impact of indoor temperature set-point on the net present value and payback time

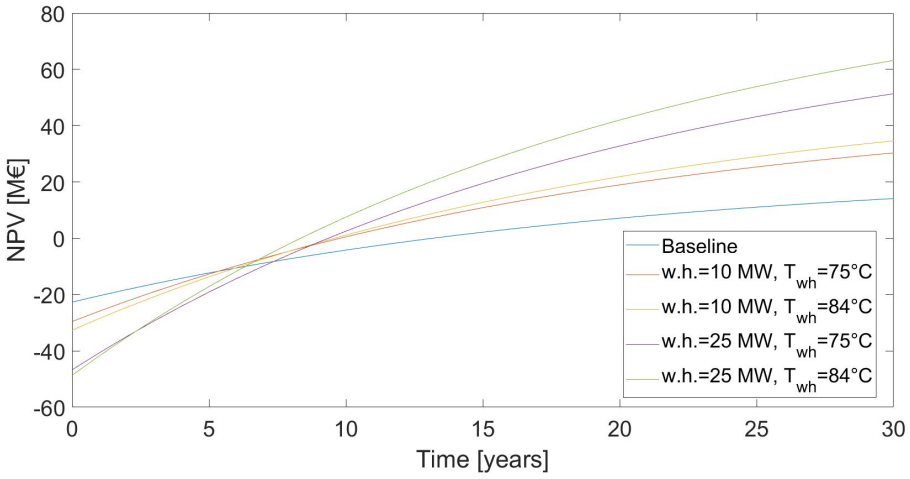

Fig. 7.14 Impact of waste heat availability on the net present value and payback time

the benefits of optimizing these parameters, but also showed how the optimal strategies could change in different scenarios and how further savings can be achieved with little changes in the everyday operation.

In particular, it was shown that sensible thermal storage is not feasible in Singapore due to the extremely large cost of space occupancy. Phase change materials or ice thermal storages should instead be selected for their larger volumetric capacity, although they require lower temperatures to be charged. Moreover, if occupancy cost increases every year, ice thermal storage results being up to 3.6% more cost-effective than commercial PCM with operating temperatures.

In addition, the operation strategy shall be properly optimized with the design, since it allows to sensibly reduce chiller operation and capital costs, compared to heuristic assumptions which use fixed strategies. It was also showed that, in case the difference between off-peak and peak electricity price increases, the storage strategy would change drastically, as it would be more convenient to install larger chillers and storages in order to produce most of the daily cooling demand in the off-peak hours. Moreover, higher electricity costs tend to influence also the topology of the network, due to the larger weight of pumping costs.

It was shown that optimizing the network supply temperature allows to further reduce the total costs, since there is a trade-off between pumping costs and chiller operation costs. The results indeed show that by increasing the network supply temperature, the chiller efficiency increases, but also the pumping costs, due to a lower temperature difference between supply and return line.

The results also highlighted how the availability of waste-heat can significantly increase the potential of district cooling within a certain area, reducing the total costs, and lowering the payback time compared to the baseline scenario. Moreover, the use of waste heat would allow the further reduction of district cooling costs, making it a feasible option also for the buildings with low individual cooling costs.

Chapter 8

Conclusions

In this thesis different models for the optimization of district cooling networks have been presented and applied to real and realistic case studies. The results showed that optimization models significantly increase the advantages of district cooling networks, unlocking their full potential.

The whole work is characterised by the gradual evolution of optimization models, with the goal of carrying out more complex and broader analysis and to provide detailed design guidelines in different urban contexts.

The first model has the aim of optimizing the topology and set of buildings to connect to a district cooling network by means of Mixed Integer Linear Programming. Although the problem is initially formulated as non-linear due to pressure drops and pumping cost terms, it was transformed into a linear by using the reformulation linearization technique and the cutting plane method. However, linearizing these terms causes an increase in dimensionality, due to the additional variables needed to reformulate the problem. In addition, the cutting plane method requires to solve the problem iteratively and to add new constraints after each iteration, further increasing the computational cost. As a consequence, the problem becomes untreatable for more complex networks and when considering more time steps.

The large computational cost led to the implementation of a genetic algorithm. In addition, the search space was reduced, by considering only minimum spanning trees as candidate network layouts. This assumption allowed to consider as decision variables only the buildings to be connected. Although reaching of global optimum is not guaranteed, compared to the MILP model, the solution is only about 1%

more expensive, while the computational time is more than 90% lower. The results therefore suggest using the genetic algorithm for more complex case studies, that could not be handled by the MILP in reasonable times. In addition, the number of variables can be further reduced, easing the convergence to the optimum, by coupling the model with a clustering approach that groups the buildings on the base of their position.

These two models constituted the starting point for the implementation of other models that allowed to solve more complex problems and carry out more general analysis. The improvements made to these models mainly followed two directions.

One of these directions consisted in taking into account the uncertainty of different parameters when optimizing the design of district cooling networks. With this regard, a two-stage stochastic programming algorithm for the optimization of the initial design and the future network expansions was implemented, while considering the uncertainty of the cost parameters and the possible evolution of cooling demand during the years. The results suggest to realize smaller networks initially and eventually expand them in a second stage, in order to mitigate the investment risks. In addition, compared to deterministic solutions based on a single scenario, the stochastic approach allows to save up to 5% in terms of total expected cost. The uncertainties with the highest impact on the results are the ones relative to the cooling demand and the cost of electricity. These indeed are the parameters that affect the most the profitability of district cooling and its potential compared to other technologies.

The second direction of improvements had the final goal of developing a more general framework able to optimize a wider set of design and operation variables. The first step towards this direction consisted in improving the heuristic approach developed in *chapter 3* in order to determine also the optimal position of chillers and storages in district cooling networks. The application of this model to an Italian case study showed that it can be more convenient to install separate independent networks in the areas with largest cooling demand, instead of a unique wider network, as this solution allows to minimize piping and pumping costs, avoiding the connection of areas with lower energy demands. In addition, it was found that the threshold value of linear energy density for the economic feasibility of district cooling is around 700 kWh/m for two different Italian case studies. This parameter could be therefore used to preliminary estimate the feasibility of district cooling in an urban area.

The second step regarded the study of the impact of the simultaneous optimization of design and operation of district cooling networks. It was investigated by implementing a Mixed Integer Quadratic Programming model and comparing the results obtained under different scenario conditions with the ones obtained by the heuristic algorithm that optimizes only the design. Optimizing simultaneously both aspects is more computationally expensive and the results showed that it does not bring significant cost savings if cooling demand is seasonal. As a consequence, in a European context, optimizing only the design assuming an operation strategy is reasonable. In particular, a general rule of thumb that can be used is to dimension chillers and storages based on the average cooling demand and to operate the chillers with a constant load. On the other hand, if the demand is not seasonal and there is a large difference between peak and off-peak electricity prices, optimizing simultaneously the design and operation allows to save up to 4% more in terms of total life cycle costs.

In *Chapter 7*, further modifications have been made to the heuristic algorithm, which led to the implementation of a hierarchical framework for the optimization of design and operation of district cooling networks. This model optimizes also the network supply temperature, the storage technology to be installed and the operation strategy, while taking into account also the costs related to surface occupancy. The application of the model to a Singaporean case study showed that ice thermal storage is the most profitable technology, due to the large occupancy cost of the Asian metropolis that makes cold water tanks unfeasible due to their lower volumetric capacities. The higher chiller operation costs for the ice production are therefore compensated by the lower space occupancy expenditures.

The analysis also showed the impact of optimizing the network supply temperature and the possible savings that can be achieved by slightly increasing the indoor set-point temperature, while respecting the thermal comfort constraints and the dehumidification requirements. The results highlighted the clear existence of a trade-off in the network supply temperature, as it influences both chiller operation costs and pumping in opposite directions. If on one hand, a higher value of supply temperature allows to operate the chillers with higher efficiencies, on the other hand pumping costs are larger due to a lower temperature difference between supply and return. However, increasing the indoor set-point temperature, where possible, allows to increase both supply and return temperatures, lowering chiller operation costs without a significant rise of pumping costs. In particular, the results showed that with

an increase of 3°C the NPV can rise by 43% and the payback time can be reduced by up to three years thanks to the lower operating costs.

In addition, the analysis revealed that electricity tariff structure has a significant impact on the optimal network topology and on the storage strategy. Indeed, with larger electricity costs it is more convenient to install separate independent networks in order to minimize pumping costs, while if there is a large disparity between off peak and peak electricity prices the optimal storage strategy consists in operating the chillers only during the night hours and relying on the storages during daytime.

Furthermore, the Singaporean case study showed that the feasibility of connecting a district cooling network is highly dependent on two main parameters: the cost of alternative cooling technologies and the distance from the chiller plant. As a consequence, using only the linear energy density parameter may be inappropriate for contexts similar to the one of Singapore, characterised by buildings with very large cooling demand.

8.1 Design guidelines

The continuous improvements made to the models allowed to progressively address more complex problems and to identify and recommend different guidelines tailored to various urban contexts, which can be summarised as follows.

Topology and connections optimization

The results demonstrated that without an optimal design, district cooling networks may not be economically feasible. Indeed, these systems are characterised by large investment costs and relatively long payback times, due to the installation of the piping system and the energy transfer stations. Optimizing the network design and set of buildings to connect is therefore crucial for the feasibility of district cooling networks. In particular, the linear energy density represents a significant parameter to consider when designing a district cooling network, as below a certain threshold it is not economically feasible. As a consequence, rules of thumbs can be used in this context to preliminary asses the feasibility of district cooling in an urban context. On the other hand, the profitability of a district cooling network depends also on other parameters, such as the cost of other cooling technologies and the

distance between buildings and the cooling sources. Indeed, it was shown that it may not be convenient connecting buildings to a district cooling network, if they have a very large and constant cooling demand, as other technologies can be installed individually to provide cooling efficiently. The feasibility of connecting a specific building to a district cooling network therefore depends on a wide range of variables, including the distance from the cooling source, the cooling demand, the alternative cooling cost and the availability of free sources within the district cooling network. Exploiting a waste heat source by means of absorption chillers can increase district cooling potential thanks to a reduction of operating costs, which can lead to the profitability of wider networks.

When optimizing the topology of district cooling networks, the adoption of multiple smaller networks, instead of a unique larger one shall also be considered. Indeed, it would allow to reduce the total pipe length, the pumping costs and avoid the connection of urban areas with lower energy density that are in between areas with larger demand.

Model selection

Regarding the modeling approaches, MILP and MIQCP guarantee more accuracy in the optimum search and therefore major savings, but they are more computationally expensive than heuristic algorithms. Hence, in case of more complex problems, the latter shall be preferred, especially if coupled with clustering approaches that allow to reduce the dimension of the problem and ease the convergence to the optimum.

Stochastic programming models allow to handle the risks related with the initial investments of a district cooling networks. In addition, they offer the possibility to divide the design in more phases. Indeed, it is more convenient to start by installing an initial smaller network and eventually expand it in the future stages, if proper conditions arise.

Simultaneous optimization of design and operation

Concerning the trade-off between optimal design and operation, different guidelines have been provided in this work for heating-dominated regions and cooling dominated ones. Indeed, if cooling demand is seasonal, as in the European context, the

most cost effective choice is to select the size of chillers and storages, so that the chillers can operate at constant load and the storages are used only for peak-shaving and valley filling. On the other hand, if cooling demand is present all year round, as in tropical climates, the design and operation should be optimized simultaneously, in order to maximise the profitability, especially if it is expected a rise of the electricity cost. Indeed, in that case the potential savings from power-to-cool strategies would be higher.

Storage technology selection

Regarding the choice the cold storage technology, it shall be carefully studied in the design phases. On one hand, cold water tanks allow to operate chillers at higher efficiencies compared to ice storages, but on the other hand they have low volumetric capacities. Especially, in the case of metropolis, where the space is limited and its occupation is expensive, ice thermal storage represents the optimal choice, although it leads to lower chillers performances.

Utilization of free sources

The results showed that the availability of waste heat significantly increases the potential of district cooling networks and influences the optimal network topology. When waste heat or other free sources are exploited, a higher number of buildings can be connected, thanks to the higher competitiveness of district cooling compared to individual technologies. As a consequence, when planning a district cooling system, particular attention shall be placed on the possible availability of free sources and the network should be built in function of these.

8.2 Future developments

The implemented models can be effectively used to help decision makers in the design phases of district cooling networks and to evaluate their potential in different urban contexts. Next studies shall focus on the optimal integration of district cooling with other energy systems, including district heating networks, especially in the context of smart energy systems and for the development of fourth generation of district

heating and cooling. In particular, the implemented models can be used to study the feasibility of realizing a unique network that provides heating during the winter and cooling during the summer. In addition, as this thesis showed how thermal storage is fundamental for the economic feasibility of district cooling networks, future model improvements should take into account for possible long-term storage strategies, especially when considering case studies characterised by a seasonal demand of cooling. Moreover, since it was highlighted the impact of optimizing the network supply temperature, networks with multiple sources operating at different temperature levels shall also be investigated, in particular in the case of districts characterised by buildings with different dehumidification constraints.

Furthermore, the thesis has focused on the design optimization of district cooling networks, addressing also few aspects regarding the optimal operation. More effort is therefore necessary in the development of optimization models for the operation of district cooling networks in real-time conditions deviating from the design ones. The impact of optimizing dynamically the supply temperature should be also studied. In this context, the impact of operation optimization on the low-delta T syndrome shall be further investigated in the future.

References

[1] A. Mastrucci, E. Byers, S. Pachauri, and N. D. Rao. Improving the sdg energy poverty targets: Residential cooling needs in the global south. *Energy and Buildings*, 186:405–415, 3 2019.

[2] International Energy Agency. The Future of Cooling. IEA. Paris. 2018.

[3] International Energy Agency. Cooling. IEA. 2021.

[4] M. Santamouris. Cooling the buildings – past, present and future. *Energy and Buildings*, 128:617–638, 9 2016.

[5] M. Santamouris and D. Kolokotsa. On the impact of urban overheating and extreme climatic conditions on housing, energy, comfort and environmental quality of vulnerable population in europe. *Energy and Buildings*, 98:125–133, 7 2015.

[6] S. Attia, R. Levinson, E. Ndongo, et al. Resilient cooling of buildings to protect against heat waves and power outages: Key concepts and definition. *Energy and Buildings*, 239:110869, 5 2021.

[7] C. Zhang, O. B. Kazanci, R. Levinson, et al. Resilient cooling strategies – a critical review and qualitative assessment. *Energy and Buildings*, 251:111312, 11 2021.

[8] V. Eveloy and D. S. Ayou. Sustainable district cooling systems: Status, challenges, and future opportunities, with emphasis on cooling-dominated regions. *Energies*, 12:235, 2019.

[9] M. Calderoni, B. B. Sreekumar, S. Dourlens-Qaranta, et al. Sustainable district cooling guidelines, 2019.

[10] T. T. Chow, W. H. Au, R. Yau, et al. Applying district-cooling technology in hong kong. *Applied Energy*, 79, 2004.

[11] A. L. Chan, T. T. Chow, S. K. Fong, and J. Z. Lin. Performance evaluation of district cooling plant with ice storage. *Energy*, 31:2750–2762, 2006.

[12] E. Guelpa and V. Verda. Thermal energy storage in district heating and cooling systems: A review. *Applied Energy*, 252:113474, 10 2019.

[13] P. A. Østergaard, S. Werner, A. Dyrelund, et al. The four generations of district cooling - a categorization of the development in district cooling from origin to future prospect. *Energy*, 253:124098, 8 2022.

[14] A. M. Hawks. The colorado automatic refrigerator system at denver, colo. *Transactions of the American Society of Civil Engineers*, 24:389–392, 1 1891.

[15] Gansevoort Market Historic District: Designation Report. New York Landmarks Preservation Commission. 2003.

[16] Derek Rudd. Written Testimony of Hartford Steam Company. Energy and Technology Committee. 2024.

[17] A. D. Bank. District cooling in the people's republic of china status and development potential, 2017.

[18] District Energy Award. Integrated district cooling plant. https://www.districtenergyaward.org/integrated-district-cooling-plant-idcp/. Accessed: 29-06-2024.

[19] C. Butters, A. Nordin, and D. T. H. Khai. District cooling: A key solution for hot climate cities. *Palgrave Series in Asia and Pacific Studies*, pages 151–171, 2018.

[20] United Nations Environment Programme (UNEP) Ozone Secretariat. Montreal protocol on substances that deplete the ozone layer, 1987.

[21] D. Térouanne, V. Gaschignard, F. Yann, and J. P. Veerapen. Climespace - city of paris: A district cooling system to control impact of air-conditioning in paris, 2011.

[22] C. D. Munck, G. Pigeon, V. Masson, et al. How much can air conditioning increase air temperatures for a city like paris, france? *International Journal of Climatology*, 33:210–227, 1 2013.

[23] G. Fermbaeck. District cooling in stockholm using sea water. *Annual International District Energy Association conference*, 1995.

[24] H. Averfalk, P. Ingvarsson, U. Persson, et al. Large heat pumps in swedish district heating systems. *Renewable and Sustainable Energy Reviews*, 79:1275–1284, 11 2017.

[25] A. David, B. V. Mathiesen, H. Averfalk, et al. Heat roadmap europe: Large-scale electric heat pumps in district heating systems. *Energies 2017, Vol. 10, Page 578*, 10:578, 4 2017.

[26] N. Jung, M. E. Moula, T. Fang, et al. Social acceptance of renewable energy technologies for buildings in the helsinki metropolitan area of finland. *Renewable Energy*, 99:813–824, 12 2016.

[27] H. Lund, P. A. Østergaard, T. B. Nielsen, et al. Perspectives on fourth and fifth generation district heating. *Energy*, 227:120520, 7 2021.

[28] T. Yang, W. Liu, G. J. Kramer, and Q. Sun. Seasonal thermal energy storage: A techno-economic literature review. *Renewable and Sustainable Energy Reviews*, 139:110732, 4 2021.

[29] S. Buffa, M. Cozzini, M. D'Antoni, et al. 5th generation district heating and cooling systems: A review of existing cases in europe, 2019.

[30] P. Gabrielli, A. Acquilino, S. Siri, et al. Optimization of low-carbon multi-energy systems with seasonal geothermal energy storage: The anergy grid of eth zurich. *Energy Conversion and Management: X*, 8, 2020.

[31] ETH Zurich Real Estate Management. The energy of tomorrow. ETH Zurich. Zurich. 2018.

[32] M. G. Fernández, C. Roger-Lacan, U. Gährs, and V. Aumaitre. Efficient district heating and cooling systems in the eu: Case studies analysis, replicable key success factors and potential policy implications, 2016.

[33] M. G. Fernandez, A. Bacquet, S. Bensadi, et al. Integrating renewable and waste heat and cold sources into district heating and cooling systems, 2021.

[34] A. Volkova, A. Hlebnikov, A. Ledvanov, et al. District cooling network planning. a case study of tallinn. *International Journal of Sustainable Energy Planning and Management*, 34:63–78, 5 2022.

[35] M. Jangsten, T. Lindholm, and J. O. Dalenbäck. Analysis of operational data from a district cooling system and its connected buildings. *Energy*, 203:117844, 7 2020.

[36] P. Dalin. Free cooling: natural cooling is crucial for a successfuldistrict cooling development. *Euroheat and Power Annual Conference*, 2012.

[37] S. A. Kalogirou and G. A. Florides. Solar space heating and cooling systems. *Comprehensive Renewable Energy*, pages 449–480, 1 2012.

[38] N. Perez-Mora, F. Bava, M. Andersen, et al. Solar district heating and cooling: A review. *International Journal of Energy Research*, 42:1419–1441, 3 2018.

[39] B. Radowitz. Munich taps into geothermal power to widen district cooling grid. *Recharge News*, 2020.

[40] A. Inayat and M. Raza. District cooling system via renewable energy sources: A review. *Renewable and Sustainable Energy Reviews*, 107, 2019.

[41] UN Global Compact and Sustainia and DNV. Global Opportunity Report. UN Global Compact. 2018.

[42] E. Guelpa, M. Capone, A. Sciacovelli, et al. Reduction of supply temperature in existing district heating: A review of strategies and implementations. *Energy*, 262:125363, 1 2023.

[43] M. Jangsten, T. Lindholm, and J. O. Dalenbäck. Analysis of operational data from a district cooling system and its connected buildings. *Energy*, 203:117844, 7 2020.

[44] American Society of Heating Refrigeration and Air-Conditioning Engineers. *District Cooling Guide*. ASHRAE, second edition edition, 2019.

[45] G. Coccia, A. Mugnini, F. Polonara, and A. Arteconi. Artificial-neural-network-based model predictive control to exploit energy flexibility in multi-energy systems comprising district cooling. *Energy*, 222:119958, 5 2021.

[46] Y. Li, Y. Rezgui, and H. Zhu. District heating and cooling optimization and enhancement-towards integration of renewables, storage and smart grid. 2017.

[47] K. Zhao, X. H. Liu, T. Zhang, and Y. Jiang. Performance of temperature and humidity independent control air-conditioning system in an office building. *Energy and Buildings*, 43:1895–1903, 8 2011.

[48] M. Jangsten, P. Filipsson, T. Lindholm, and J. O. Dalenbäck. High temperature district cooling: Challenges and possibilities based on an existing district cooling system and its connected buildings. *Energy*, 199:117407, 5 2020.

[49] D. P. Fiorino. Achieving high chilled-water delta ts. *ASHRAE Journal*, 41:24–30, 11 1999.

[50] W. J. Coad. A fundamental perspective on chilled water systems. *HPAC Heating, Piping, Air Conditioning*, 70:59–66, 8 1998.

[51] E. Guelpa, A. Sciacovelli, and V. Verda. Thermo-fluid dynamic model of large district heating networks for the analysis of primary energy savings. *Energy*, 184, 2019.

[52] A. Sciacovelli, V. Verda, and R. Borchiellini. *Numerical design of thermal systems*. CLUT, 2013.

[53] M. Capone, E. Guelpa, and V. Verda. Accounting for pipeline thermal capacity in district heating simulations. *Energy*, 219, 2021.

[54] E. Guelpa, L. Marincioni, M. Capone, et al. Thermal load prediction in district heating systems. *Energy*, 176, 2019.

[55] E. Guelpa, L. Marincioni, S. Deputato, et al. Demand side management in district heating networks: A real application. *Energy*, 182, 2019.

[56] E. Guelpa. Impact of network modelling in the analysis of district heating systems. *Energy*, 213:118393, 12 2020.

[57] B. van der Heijde, M. Fuchs, C. R. Tugores, et al. Dynamic equation-based thermo-hydraulic pipe model for district heating and cooling systems. *Energy Conversion and Management*, 151:158–169, 11 2017.

[58] B. van der Heijde, A. Aertgeerts, and L. Helsen. Modelling steady-state thermal behaviour of double thermal network pipes. *International Journal of Thermal Sciences*, 117:316–327, 7 2017.

[59] K. Hinkelman, J. Wang, W. Zuo, et al. Modelica-based modeling and simulation of district cooling systems: A case study. *Applied Energy*, 311:118654, 4 2022.

[60] A. Dénarié, M. Aprile, and M. Motta. Dynamical modelling and experimental validation of a fast and accurate district heating thermo-hydraulic modular simulation tool. *Energy*, 282:128397, 11 2023.

[61] A. Brown, A. Foley, D. Laverty, et al. Heating and cooling networks: A comprehensive review of modelling approaches to map future directions. *Energy*, 261:125060, 12 2022.

[62] M. Jiang, M. Speetjens, C. Rindt, and D. Smeulders. A data-based reduced-order model for dynamic simulation and control of district-heating networks. *Applied Energy*, 340:121038, 6 2023.

[63] T. Oppelt, T. Urbaneck, U. Gross, and B. Platzer. Dynamic thermo-hydraulic model of district cooling networks. *Applied Thermal Engineering*, 102:336–345, 6 2016.

[64] E. Guelpa, C. Toro, A. Sciacovelli, et al. Optimal operation of large district heating networks through fast fluid-dynamic simulation. *Energy*, 102:586–595, 5 2016.

[65] S. J. Cox, D. Kim, H. Cho, and P. Mago. Real time optimal control of district cooling system with thermal energy storage using neural networks. *Applied Energy*, 238:466–480, 3 2019.

[66] M. Sameti and F. Haghighat. Optimization approaches in district heating and cooling thermal network, 2017.

[67] M. Neri, E. Guelpa, and V. Verda. Design and connection optimization of a district cooling network: Mixed integer programming and heuristic approach. *Applied Energy*, 306, 2022.

[68] A. C. Lo, P. Jones, and F. W. Yik. Effects of pumping station configuration on the energy performance of district cooling systems. *Building Services Engineering Research and Technology*, 38:287–308, 5 2017.

[69] E. Guelpa, L. Bellando, A. Giordano, and V. Verda. Optimal configuration of power-to-cool technology in district cooling systems. *Proceedings of the IEEE*, 108:1612–1622, 9 2020.

[70] J. Zeng, Q. Xu, Y. Ning, and X. Zhang. Pipe network optimization in district cooling/heating system: A review. *Proceedings - 2019 International Conference on Robots and Intelligent System, ICRIS 2019*, pages 133–136, 6 2019.

[71] A. L. Chan, V. I. Hanby, and T. T. Chow. Optimization of distribution piping network in district cooling system using genetic algorithm with local search. *Energy Conversion and Management*, 48:2622–2629, 10 2007.

[72] D. Dobersek and D. Goricanec. Optimisation of tree path pipe network with nonlinear optimisation method. *Applied Thermal Engineering*, 29, 2009.

[73] F. Al-Noaimi, R. Khir, and M. Haouari. Optimal design of a district cooling grid: structure, technology integration, and operation. *Engineering Optimization*, 51, 2019.

[74] R. Khir and M. Haouari. Optimization models for a single-plant district cooling system. *European Journal of Operational Research*, 247:648–658, 2015.

[75] J. Söderman. Optimisation of structure and operation of district cooling networks in urban regions. *Applied Thermal Engineering*, 27:2665–2676, 2007.

[76] A. Allen, G. Henze, K. Baker, et al. A topology optimization framework to facilitate adoption of advanced district thermal energy systems. *IOP Conference Series: Earth and Environmental Science*, 588:022054, 11 2020.

[77] A. Allen, G. Henze, K. Baker, and G. Pavlak. Evaluation of low-exergy heating and cooling systems and topology optimization for deep energy savings at the urban district level. *Energy Conversion and Management*, 222:113106, 10 2020.

[78] L. L. Jensen, D. Trier, M. Brennenstuhl, et al. Analysis of network layouts in selected urban contexts, 2016.

[79] R. Yan, J. Wang, S. Zhu, et al. Novel planning methodology for energy stations and networks in regional integrated energy systems. *Energy Conversion and Management*, 205:112441, 2 2020.

[80] M. Wirtz, M. Heleno, H. Romberg, et al. Multi-period design optimization for a 5th generation district heating and cooling network. *Energy and Buildings*, 284:112858, 4 2023.

[81] K. M. Powell, W. J. Cole, U. F. Ekarika, and T. F. Edgar. Optimal chiller loading in a district cooling system with thermal energy storage. *Energy*, 50:445–453, 2 2013.

[82] K. Zaw, Z. Z. Kwik, W. Q. Chang, et al. A techno-commercial decision support framework for optimal district cooling system design in tropical regions. *Applied Thermal Engineering*, 220, 2 2023.

[83] L. Wang, E. W. Lee, and R. K. Yuen. A practical approach to chiller plants' optimisation. *Energy and Buildings*, 169:332–343, 6 2018.

[84] W. Zhang, X. Jin, L. Zhang, and W. Hong. Performance of the variable-temperature multi-cold source district cooling system: A case study. *Applied Thermal Engineering*, 213, 8 2022.

[85] E. Guelpa and V. Verda. Model for optimal malfunction management in extended district heating networks. *Applied Energy*, 230:519–530, 11 2018.

[86] Z. Chiam, A. Easwaran, D. Mouquet, et al. A hierarchical framework for holistic optimization of the operations of district cooling systems. *Applied Energy*, 239:23–40, 4 2019.

[87] W. Gang, S. Wang, G. Augenbroe, and F. Xiao. Robust optimal design of district cooling systems and the impacts of uncertainty and reliability. *Energy and Buildings*, 122:11–22, 6 2016.

[88] G. Mavromatidis, K. Orehounig, and J. Carmeliet. Design of distributed energy systems under uncertainty: A two-stage stochastic programming approach. *Applied Energy*, 222:932–950, 7 2018.

[89] R. S. Lambert, S. Maier, J. W. Polak, and N. Shah. Optimal phasing of district heating network investments using multi-stage stochastic programming. *International Journal of Sustainable Energy Planning and Management*, 9:57–74, 3 2016.

[90] Z. Zhou, J. Zhang, P. Liu, et al. A two-stage stochastic programming model for the optimal design of distributed energy systems. *Applied Energy*, 103:135–144, 3 2013.

[91] R. Egging-Bratseth, H. Kauko, B. R. Knudsen, et al. Seasonal storage and demand side management in district heating systems with demand uncertainty. *Applied Energy*, 285:116392, 3 2021.

[92] E. Silvennoinen, K. Juslin, M. Hänninen, et al. The apros software for process simulation and model development, 1989.

[93] M. Wirtz. npro: A web-based planning tool for designing district energy systems and thermal networks. *Energy*, 268:126575, 4 2023.

[94] J. E. Kelley. The cutting-plane method for solving convex programs. *Journal of the Society for Industrial and Applied Mathematics*, 8:703–712, 12 1960.

[95] O. Grygorash, Z. Yan, and Z. Jorgensen. Minimum spanning tree based clustering algorithms. 2006.

[96] S. J. Oh, K. C. Ng, K. Thu, et al. Forecasting long-term electricity demand for cooling of singapore's buildings incorporating an innovative air-conditioning technology. *Energy and Buildings*, 127, 2016.

[97] M. Neri, E. Guelpa, and V. Verda. Two-stage stochastic programming for the design optimization of district cooling networks under demand and cost uncertainty. *Applied Thermal Engineering*, 236:121594, 1 2024.

[98] J. R. Birge and F. Louveaux. Introduction to stochastic programming. 2011.

[99] L. M. Pastore, G. L. Basso, and L. de Santoli. Can the renewable energy share increase in electricity and gas grids takes out the competitiveness of gas-driven chp plants for distributed generation? *Energy*, 256:124659, 10 2022.

[100] GME. Esiti mgp. https://www.mercatoelettrico.org/It/Tools/Accessodati.aspx?ReturnUrl=%2fit%2fdownload%2fDatiStorici.aspx. Accessed: 06-09-2022.

[101] M. Swedblom, P. Mattson, A. Tvärne, et al. District cooling and the customers' alternative cost, 2014.

[102] M. F. Jentsch, P. A. James, L. Bourikas, and A. B. S. Bahaj. Transforming existing weather data for worldwide locations to enable energy and building performance simulation under future climates. *Renewable Energy*, 55:514–524, 7 2013.

[103] M. Neri, E. Guelpa, and V. Verda. Trade-off between optimal design and operation in district cooling networks. *Smart Energy*, 13, 2024.

[104] Andreas Hauer. Thermal Energy Storage. IEA-ETSAP and IRENA. 2013.

[105] A. Martin-Candilejo, D. Santillán, and L. Garrote. Pump efficiency analysis for proper energy assessment in optimization of water supply systems. *Water 2020, Vol. 12, Page 132*, 12:132, 12 2019.

[106] U. E. I. 52016-1. Energy performance of buildings - energy needs for heating and cooling, internal temperatures and sensible and latent heat loads - part 1: Calculation procedures, 2018.

[107] Gurobi Optimization. *Gurobi Reference Manual*. 2023.

[108] S. Goel, M. Rosemberg, and C. Eley. Ansi/ashrae/ies standard 90.1-2016 performance rating method reference manual, 2017.

[109] Singapore energy market authority. www.ema.gov.sg. Accessed: 01-07-2023.

[110] S. Mazzoni, B. Nastasi, S. Ooi, et al. The adoption of a planning tool software platform for optimized polygeneration design and operation – a district cooling application in south-east asia. *Applied Thermal Engineering*, 199, 11 2021.

[111] Singaporean Building and Construction Authority. Code on environmental sustainability measures for existing buildings, 2016.

[112] N. Yamtraipat, J. Khedari, J. Hirunlabh, and J. Kunchornrat. Assessment of thailand indoor set-point impact on energy consumption and environment. *Energy Policy*, 34:765–770, 5 2006.

[113] US Department of Energy. Absorption Chillers for CHP Systems. US Department of Energy. 2017.